*Journal of Chromatography A*, 656 (1993) 135–196
Elsevier Science Publishers B.V., Amsterdam

CHROM. 25 339

# Review

# Lattice models for the description of partitioning/adsorption and retention in reversed-phase liquid chromatography, including surface and shape effects

Robert Tijssen* and Peter J. Schoenmakers

*Koninklijke/Shell-Laboratorium, Amsterdam, Badhuisweg 3, 1031 CM Amsterdam (Netherlands)*

Marcel R. Böhmer☆ and Luuk K. Koopal

*Department of Physical and Colloid Chemistry, Agricultural University, Dreyenplein 6, 6703 HB Wageningen (Netherlands)*

Hugo A.H. Billiet

*Faculty of Chemistry, Technical University Delft, De Vries van Heystplantsoen 2, 2628 BC Delft (Netherlands)*

ABSTRACT

The retention mechanism in reversed-phase liquid chromatography (RPLC) with silica particles modified with surface-grafted alkyl chains cannot be fully understood unless the specific properties of the surface layers, such as the configurational constraints of terminally attached chains, are taken into account. The commonly accepted view that the main factor governing RPLC retention behaviour is constituted by solute–solvent interactions in the bulk mobile phase is supported by useful but simplified theories based on solvation as in bulk liquids. Solvation in bulk liquids depends on the free energy to create "cavities" for solute molecules in mobile and stationary phases.

This paper first reviews possibilities and shortcomings of regular solution theories, where the partition coefficient is expressed in terms of the Flory–Huggins (FH) interaction parameters for the solute. Where enthalpic effects dominate, these parameters can be obtained from experimental data or from generalized thermodynamic functions expressed as Hildebrand's solubility parameter, $\delta$, representing the square root of the cohesive energy density.

In RPLC with terminally attached chains on the support, entropy effects arising from the molecular organization of chains are also important, and entropic expulsion of solute molecules from the stationary phase is expected to take place. RPLC practice indicates that the nature of the grafted layer [*e.g.*, flexibility of grafted chains and "phase transitions", geometrical effects, chain length effects, chain branching and surface effects (coverage and hydroxyls)] indeed influences the "adsorptive" and retentive capacity of the bonded stationary layer. Theories specially designed for grafted layers are reviewed starting with (oversimplified) rod-like chain models, followed by several, more recent, lattice theories, which are based on extensions of the Flory–Huggins lattice theory for polymers in solution. These theories, when applied to the RPLC retention mechanism, take into account some aspects of the molecular organization in the grafted layer, but are still subject to simplifying assumptions.

A more general approach is based on the self-consistent field theory for adsorption (SCFA) originally developed by Scheutjens

* Corresponding author.
☆ Present address: Philips Natuurkundig Laboratorium, PO Box 80000, 5600 JA Eindhoven, Netherlands.

0021-9673/93/$24.00 

and Fleer to describe polymer adsorption, where in essence the segment density distribution is found resulting from minimization of free energy. Extending the SCFA theory to allow for RPLC conditions provides insight into the effects of the solvent quality (modifier content), collapse of the chain phase, the grafted and solute's chain lengths and the grafting density (surface coverage) on the segment density profile. Both aliphatic and amphiphilic solute molecules appear to be distributed non-uniformly in the grafted layer and are accumulated in the boundary region near the interface between chain phase and bulk solvent. Using the related theory by Leermakers and Scheutjens [self-consistent anisotropic field (SCAF) theory], shape selectivity is shown for flexible chain, star- and rod-like solutes, chain length effects and alignment also being found. In the presence of a specific affinity for the silica surface, due to residual hydroxyls, for both polar solvent molecules and solute molecules with polar groups, both the SCFA and the SCAF theories predict an accumulation of polar segments near the silica surface which is fairly pronounced, displacing most of the (unattached) non-polar segments more towards the chain phase surface.

CONTENTS

## 1. INTRODUCTION

Currently, the main HPLC technique used is reversed-phase liquid chromatography (RPLC). Because of its flexibility towards a wide variety of solutes and mobile phase systems, RPLC is carried out almost exclusively with chemically bonded stationary phases. Most applications are achieved on silica support particles modified with alkyl chains (1–18 carbons long) grafted to the support surface by a monomeric reaction scheme, where a single group reacts with the silica surface to form a siloxane bridge. Typical surface coverages obtained with these monomeric phases are in the range 2.5–4.4 $\mu$mol/m$^2$, *i.e.*, 20–60% of the expected maximum coverage of about 8 $\mu$mol/m$^2$ {limited to that value by either available hydroxyl sites on activated silicas [1] or the maximum packing density of (alkane-type) chains in crystals}. In this paper we do not consider "polymeric" and "resin-type" phases, where multi-functional reaction schemes are used. Chain branching will be treated for the solute, but not for the stationary chain phase. The potential influence of residual adsorption at non-bonded surface hydroxyl sites also receives some attention.

Knowledge of the mechanism of the retention of solutes in separation columns packed with such chemically modified or "hairy" surfaces is of the utmost importance for the control of separation performance and analysis time. This mechanism is as yet not fully understood, and it is still a matter of debate in the chromatographic literature [2–18] whether solutes show an adsorptive behaviour on the chemically bonded phases, or a sorptive "bulk-like" partitioning mechanism, by which solutes are embedded within the chemically bonded phase.

To shed light on this issue and the mechanisms of retention in general, we need a theory that describes both the mobile and the stationary phases, and which pays due attention to conformational aspects of retention in a grafted layer. Further, this theory should provide insight into aspects such as the extent to which alkyl-modified surfaces can be swollen by solvent penetration, the dependence on alkyl chain length and the nature of the mobile phase solvent. It is speculated that solvents compatible with alkanes tend to swell the surface layer, extending the bonded chains perpendicular to the solid surface far into the solvent phase, whereas incompatible solvents tend to collapse the chains upon each other and on to the solid surface, thereby minimizing the contacts with the "hostile" solvent. In the former situation the chain phase may be regarded as "brush"-like, with the extended chains oriented more or less perpendicular to the solid surface and allowing maximum penetration by the solvent and solutes. In the latter instance, with polar solvents, limited solvent penetration can be envisaged, and solute penetration in the liquid-like layer of collapsed chains is still possible. Martire and Boehm [17,18] referred to this qualitative picture as to a "breathing" surface, which adjusts itself to maintain its non-polar character. This picture is consistent with Monte Carlo computer simulations [19–22], scaling theories [23,24] and self-consistent-field theories [16,20,25–34], to be discussed in the following. Summarizing, the required theory should account for the stationary phase structure and composition, which in turn depend on the grafted chain length, its surface coverage, the intrinsic stiffness of the bonded chains and the nature of the mobile phase solvent. We shall discuss the last-mentioned aspect first because, as stated, its importance is well recognized in chromatographic science and becomes apparent directly from the close relationship between partitioning and retention parameters.

As commonly accepted, a practically useful partition coefficient $K^c$ can be based on average molar concentrations $\bar{c} = n/V$, $n$ being the number of moles of compounds present in a (phase) volume $V$. For very dilute solutions $\bar{c}_i = \bar{x}_i/v_p$, where $\bar{x}_i$ is the (average) mole fraction of solute $i$ in phase $p$, and $v_p = M_p/\rho_p$ is the molar volume of the phase, $M$ being the molecular mass and $\rho$ the density of the (liquid) phase. As a result,

$$K_i^c = \bar{c}_{is}/\bar{c}_{im} = K_i^x(v_m/v_s) \quad (1)$$

where $K_i^x = \bar{x}_{is}/\bar{x}_{im}$ is the mole-fraction-based partition coefficient. This form of the partition

coefficient, being based on concentrations, is of particular interest; because of the dynamic nature of the partitioning process, it is $K^c$ that can be related to the residence ("retention") time, which is expressed as

$$(t_i/t_0) = 1 + k'_i; \quad k'_i = (t_i - t_0)/t_0 \tag{2}$$

where

$$k'_i = \bar{c}_{is}V_s/\bar{c}_{im}V_m = K^c_i(V_s/V_m) = K^x_i(n_s/n_m) \tag{3}$$

is the capacity factor, representing the extent to which a partitioning solute $i$ is retarded with respect to the mobile phase itself, which remains in the separation system during the time $t_0$, to be measured with a non-partitioning solute. (In the following we omit the overbar for average concentrations for simplicity.) From these elementary relationships it is clear that the role of the mobile phase is as important as that of the stationary phase. As the latter can in practice only be influenced indirectly by varying the mobile phase or conditions such as temperature, the mobile phase parameters are the ones to change in order to find effective retention and separation.

## 2. REGULAR SOLUTION THEORIES

It is commonly accepted that solute–solvent interactions in the bulk mobile phase constitute one of the main factors governing RPLC retention behaviour, and useful but simplified theories (Schoenmakers and co-workers [2–6], Jandera *et al.* [7]) have been designed on the basis of this premise. These theories are well suited for the description of distribution processes in bulk liquids, where retention is assumed to depend on the free energy to create cavities for solvation of solute molecules in mobile and stationary phases.

At thermodynamic equilibrium, the chemical potentials (or the activities) of the solute in the mobile and stationary phases are equal. From regular solution theory [35,36], in the limit of infinite dilution, it follows that the partition coefficient $K^x_i$ for molecule $i$ in terms of mole fractions, $x_i$, in the mobile (m) and stationary (s) phases, is given by

$$\ln K^x_i = \ln (x_{is}/x_{im}) = \chi_{im} - \chi_{is} = (\mu^0_{im} - \mu^0_{is})/RT \tag{4}$$

where $\chi_{ip}$ is the Flory–Huggins interaction parameter [36,37] for solute $i$ in phase $p$ ($p$ = m, s). $\chi_{ip}$ is the work (*i.e.*, a standard free energy $\Delta\mu_{ip}/RT$, consisting of entropic and enthalpic contributions) required to transfer solute $i$ from pure $i$ to a solution in pure phase $p$. In the limit of infinite dilution, $\chi_{ip}$ is equal to ln $\gamma_{ip}$, $\gamma_{ip}$ being the activity coefficient of $i$ in $p$. In the case where enthalpic effects in simple liquid mixtures dominate, $\chi$ values can be obtained from vaporization energy data or from generalized thermodynamic functions [2]. This requires the assumption that the binary interactions involved can be obtained as the geometric mean of the pure-substance interactions, the basis for the solubility parameter $\delta$ [2,35]. In this and related "cavity" theories [2–7,13–15], which can be seen as extensions of the regular solution theory [35,36], partitioning is assumed to depend on the free energy to create cavities for solvation of solute molecules in the mobile and stationary phases. The Flory–Huggins parameter $\chi_{ip}$ is related to the solubility parameters of $i$ and $p$ in a binary mixture at infinite dilution:

$$\chi_{ip} = \Delta\mu_{ip}/RT = (v_i/RT)(\delta_i - \delta_p)^2 \tag{5}$$

where $\delta$ represents the square root of the cohesive energy density, after Hildebrand *et al.* [35], and $v_i$ is the molar volume of solute $i$. For dealing with polar compounds, it is necessary to divide the total solubility parameter into partial contributions, as discussed elsewhere [2–6,38–41]. We stress the fact that the "cavity" theories are reasonably successful in describing true partitioning phenomena, even in multi-component bulk phases with local ordering from, *e.g.*, hydrogen bonding [2–7,13–15].

For instance, for a binary mobile phase (in RPLC use is often made of aqueous mixtures with an organic "modifier" such as alcohols, acetonitrile or tetrahydrofuran) these theories successfully predict the quadratic dependence of ln $K^c$ *vs.* $\varphi_m$, $\varphi_m$ representing the volume fraction of modifier in water [3–5,41]:

$$\ln K^c_i = A(\varphi_m)^2 + B\varphi_m + C \tag{6}$$

where $C$ is the value of ln $K_i^c$ in pure water. The coefficients $A$, $B$ and $C$ can be expressed in Flory–Huggins $\chi$ parameters [8–12,16], solubility parameters [2–6,41] or interaction "indices" [7], very similar to the Flory–Huggins parameter $\chi$ (eqn. 5). It appears that, owing to all the simplifications and assumptions made, eqn. 6 indeed describes the observed experimental trend, but is not suited for *a priori* predictions of retention *vs.* composition.

However, the application of cavity theories to RPLC is usually convenient because of the often observed correlation between liquid–liquid partitioning and retention in RPLC. Although not suitable for predictive purposes, partitioning data can be readily used to determine interaction parameters [2–12], *e.g.*, with eqn. 6. In spite of its shortcomings, the relative success of the cavity theory, especially when formulated in readily accessible solubility parameters, justifies its treatment with selected applications in the next section.

The solvophobic theory after Horváth and coworkers [13,14], although more elaborate and complex than the former "cavity" theories, still underestimates effects of cavity formation in the stationary phase [8–12]. In fact, in this theory, it is only the mobile phase that "drives" solutes towards the stationary phase, and no account is taken of possible solute–stationary phase interactions. Solvophobic theories thus neglect the experimentally supported fact that retention actually depends on the nature of the chain phase. Consequently, the solvophobic theory is not suitable for predictive purposes either.

The main conclusion is that the "cavity" theories do a good job in bulk phase partitioning, but that they neglect the specific properties of grafted layers such as the configurational constraints of terminally attached chains. In a more satisfactory approach, entropy effects should be incorporated in the theory. Owing to the partial ordering of the grafted alkyl chains, entropic expulsion of solute molecules from the stationary phase is expected to take place. Although it is thus foreseen that *a priori* predictions of absolute data on partitioning especially in grafted systems are impossible using regular solution theory (RST), we shall show that on a relative basis, following Rohrschneider's (originally gas chromatographic) method [42,43] and using well defined calibrating solutes, a very useful practical characterization of the system can be obtained. In liquid–liquid partitioning we shall once more stress the surprising success of RST, especially if use is made of an extended solubility parameter model, to be discussed next.

### 2.1. Potentials and shortcomings of an extended solubility parameter model

To allow an efficacious choice of partitioning systems, a large number of approaches have been chosen over the years in the literature. The resulting models range from theoretical models based on molecular interactions and thermodynamics, to group solution models and semi-empirical models (such as the Hansch $P_{OW}$ system [44,45]). Purely empirical data are largely collected by the manual shake-flask method [44–47] and to an increasing extent by instrumental techniques such as liquid chromatography and flow-injection analysis (FIA) [48].

In this section we review a model for partitioning in chromatographic systems that is capable of predicting trends [such as pressure ($p$), temperature ($T$) and compositional dependences], and which makes it possible to choose optimum separation conditions for specific separation problems. Based on the observation that many liquid–liquid partitioning data are readily correlated with RPLC retention data, it is also thought that the model should cover chromatographic methods that use as the stationary phase grafted layers, instead of a bulk liquid, as with both GC and RPLC.

It is proposed to adapt the multi-dimensional solubility parameter approach as developed earlier by us [2–6] and others [38,39] to characterize partitioning behaviour in analytical separation techniques such as gas, liquid and more recently supercritical chromatography. In essence, the concept of solubility parameters provides a means for a quick estimate of the mutual solubility of two liquids, in the sense that solubility (= miscibility) will be better when the solubility parameters are closer to each other ("like dissolves like"). Although the concept is

very simple, it is yet widely employed and an exhaustive overview can be found in Barton's handbook [48].

It is well known that the solubility parameter approach, being based on the cohesive energy density (CED), rather than on the free energy which is the ruling factor in partitioning (see next section), has its limitations, but prediction of the required trends is surprisingly successful. At the same time, in view of the broad variety of conditions in separation columns (*e.g.*, gas pressures, varying mobile phase compositions, temperature gradients), it is of little use to try to make the predictive model as extended as possible. It is more fruitful to give satisfactory reflections of trends in partitioning behaviour, with empirical data, where possible, helping to guide the choices.

In the authors' opinion, this goal could be reached with the extended solubility parameter (ESP) model, successful in many respects in chromatographic [2–6,38–41,49–51], and chemical engineering sciences [48,52–54]. Based on this experience, it is expected that the ESP model holds considerable promise as the basis of optimization systems for the selection of partitioning systems and the prediction of residence times of solutes.

As, moreover, the numerical values of the CED can be found from reliable data which are based on available and modern equations of state, the use of the solubility parameter model is very convenient. It will be shown in the next section that this approach indeed leads to useful predictions of trends, but not always to correct prediction of $K$ values themselves. In order to overcome this limitation, a semi-empirical model, also based on the solubility parameter concept, will be introduced, where experimental data for selected standard solutes in standard phase systems serve as calibration data for the characterization of partitioning of arbitrary solutes.

### 2.2. Thermodynamic background of partitioning

The main purpose of this section is to serve as a reference for the further discussion. It is by no means exhaustive, but considers the concepts necessary for obtaining a feel for the subject.

In general, the thermodynamics of a system [35,36,55] are fully described by its *fundamental equation*. For a system with a fixed composition, this fundamental equation describes the internal energy $U$ of the system in terms of entropy $S$ and volume $V$: $U = U(S,V)$. From the combined first and second laws of thermodynamics it then follows that $U$ is related to both temperature $T$ and pressure $p$ via $dU = T\,dS - p\,dV$, where $T = (\partial U/\partial S)_V$ and $p = -(\partial U/\partial V)_S$.

Thermodynamics postulate that the equilibrium state (for given $S$ and $V$) corresponds to a minimum of the internal energy $U$, and likewise for given $U$ and $V$ to a maximum entropy $S$. For the purpose of liquid–liquid equilibria, $S$ and $V$ are inconvenient variables and the equation for the *(Gibbs) free energy* is more useful, being expressed in the practical variables $p$ and $T$: $G = G(p,T) = U + pV - TS = H - TS$ with $dG = -S\,dT + V\,dp$; $H = U + pV$ represents the enthalpy. Now, thermodynamic equilibrium at specified $p$ and $T$ is reached for a minimum in $G$, *i.e.*, $(dG)_{p,T} = 0$. For chromatography, mixtures of compounds $i$ are important, so that the number of molecules, $n_i$, of the individual species are also variables: $G = {}_i\Sigma\, n_i\mu_i$ and $dG = -S\,dT + V\,dp + {}_i\Sigma\, \mu_i\,dn_i$, where $\mu$ is the *chemical potential* (or partial molar free energy), defined as $\mu_i = (\partial G/\partial n_i)_{p,T,n_j}$ [the subscript $p$, $T$, $n_j$ indicates that $p$, $T$ and $n_j$ $(i \neq j)$ are kept constant].

Thus the chemical potential of component $i$ describes how the total free energy $G$ of the system changes when one of these molecules $i$ is added to the system, which is otherwise kept constant. An important consequence is that, for constant $p$ and $T$, the chemical potential of the components $i$ cannot be varied independently, *i.e.*, they mutually influence each other: ${}_i\Sigma\, n_i\,d\mu_i = 0$ (Gibbs–Duhem equation). The total free energy $G$ is an *extensive quantity* whose value scales linearly with the size of the system, *i.e.*, with such quantities as total number of molecules $N = {}_i\Sigma\, n_i$, total volume $V = {}_i\Sigma\, n_i v_i$ or total mass or weight $W = {}_i\Sigma\, n_i m_i$. Differentiation of $G$ with respect to one of the quantities $N$, $V$ or $W$ gives an *intensive quantity* that depends only

on the composition, *i.e.*, on either the mole fractions $x_i = n_i/N$, the volume fractions $\varphi_i = n_i v_i/V$ or the mass fraction $w_i = n_i m_i/W$. In the derivations below we shall often use the volume fraction $\varphi$.

For the calculation of phase and partition equilibria [35,36,55,56], the general starting point is the thermodynamic equilibrium condition, $dG = 0$, which in the case of equilibrium between two phases s and m reads: $dG = (\mu_{is} - \mu_{im})\, dn_i = \Delta\mu\, dn_i = 0$. One may thus find the thermodynamic equilibrium state either by minimizing the free energy $G$ or by equalizing the chemical potentials of each component in each phase. For perfect solutions (Raoult type) of solute $i$ in some liquid solvent, the chemical potential can be represented by a common two-factor expression: $\mu_i = \mu_i^0 + RT \ln x_i$, where $R$ is the gas constant and $\mu_i^0$ is the chemical potential valid for a standard state with $i$ in unit concentration [*i.e.*, pure solute $i$ ($x_i = 1$)]. The value of $\mu_i^0$ depends strongly on the molecular interactions and so depends on the phase in which $i$ is present. The value is generally lowest for strong intermolecular interactions, *i.e.*, high affinity between solute and solvent. The second term, $RT \ln x_i$, arises because of the extent of dilution, and is of entropic origin.

If the expression for $\mu_i$ is substituted into the equilibrium condition $\Delta\mu = 0$, the equilibrium ratio, *i.e.*, the partition coefficient, is obtained generally as represented in eqn. 1. Alternatively, we may write

$$K_i^x = (x_{is}/x_{im}) = \exp[(\mu_{im}^0 - \mu_{is}^0)/RT] = \exp[\Delta\mu_i^0/RT] \quad (7)$$

If the deviation from perfect Raoult behaviour is described by the activity $a_i = \gamma_i x_i$, where $\gamma_i$ is the activity coefficient, we have $\mu_i = \mu_i^0 + RT \ln \gamma_i x_i$. When activity coefficients depart from unity, the equilibrium ratio should be expressed in terms of activities and then, in equilibrium, the activities of the solute in both phases are equal, $a_s = a_m$, hence $\gamma_{is} x_{is} = \gamma_{im} x_{im}$ and so (with $\Delta\mu_i^0 = 0$ for pure $i$ as the standard state):

$$K_i^x = (x_{is}/x_{im}) = (\gamma_{im}/\gamma_{is}) \exp[\Delta\mu_i^0/RT] = (\gamma_{im}/\gamma_{is}) \quad (8)$$

It should be realised that the chemical potential is a function of both temperature $T$ and pressure $p$, as a result of which $\gamma = \gamma(p,T)$ and likewise $K = K(p,T)$. Each activity coefficient is a measure of the chemical potential $\mu$, which consists of an enthalpic and an entropic part. Expressed as excess functions [*i.e.*, actual minus perfect (Raoult-type), *e.g.*, $\mu^e = \mu - \mu^{perf} = \mu - \mu^0$ $RT \ln x$], we have

$$\mu^e = h^e - Ts^e = RT \ln \gamma \quad (9)$$

where $h$ is the partial molar enthalpy and $s$ the partial molar entropy.

As mentioned above, $\mu = \mu(p,T)$ and the more important temperature dependence can be obtained from eqn. 9. This expression also describes how the activity coefficient depends on the partial molar excess enthalpy and entropy of mixing. Provided that these quantities are independent of temperature, which is commonly the case especially for the entropic contribution, a plot of $\ln \gamma$ *vs.* $1/T$, and for that matter of $\ln K$ *vs.* $1/T$, often yields in practice a straight line from which both quantities can easily be obtained ($h^e$ and $\Delta h^e$ from the slope, $s^e$ and $\Delta s^e$ from the vertical axis intercept).

This behaviour makes it possible to interpret eqn. 9 such that the activity coefficient consists of two parts, one connected to the enthalpic function (the thermal, residual or regular activity coefficient, $\gamma^h$), the other to the entropic function (the athermal or combinatorial activity coefficient, $\gamma^s$):

$$\ln \gamma = \ln \gamma^h + \ln \gamma^s \quad \text{or} \quad \gamma = \gamma^h \gamma^s \quad (10)$$

Now, as in Hildebrand's RST [35], it is assumed that enthalpic and entropic contributions are independent of each other. This permits the construction of the total activity coefficient from two independent models, one describing the entropic and the other the enthalpic part. The enthalpic part $\ln \gamma^h$ is also known as the enthalpic part of the Flory–Huggins interaction ($\chi$) parameter (see below).

Formally, $\mu^e$ and thus $\gamma$ and $K$ are also functions of pressure, but the resulting pressure dependence, which for $K$ can be written as

$$RT[(\partial/\partial p)(\ln K_i^x(p,T)]_T = (v_i^m - v_i^s) \quad (11)$$

rarely exceeds *ca.* 10 ml/mol in LC, *i.e.*, only pressures in excess of say 500–1000 bar would yield appreciable pressure influences. It is concluded that for all practical purposes the expression for $K^x$ remains eqns. 4 and 8, provided that true (incompressible) liquid–liquid equilibrium is considered. The situation changes, however, as soon as compressibility must be considered, as in GC and SFC [57].

### 2.3. Introduction to lattices: Flory–Huggins

For simple, monomeric, liquids the entropic mixing contribution can be approximated by the well known athermal mixing entropy expression after Flory and Huggins [37]. Assuming that the liquid molecules can be represented by points in a lattice, where the $N$ available lattice sites are occupied by both solute $i$ and phase $p$, $N = n_i + n_p$, the total number of arrangements of the particles is given by $\Omega = N!/(N - n_p)!n_i!$ such that after using the Stirling approximation for factorials and the Boltzmann relationship for the configurational entropy ($k \ln \Omega$), the entropy of mixing ($\Delta S^{mix} = S^{conf} - S^{unmix}$) becomes

$$\Delta S^{mix} = S^{conf} = -k(n_i \ln x_i + n_p \ln x_p) \qquad (12)$$

where $x = n/N$ and $S^{unmix} = 0$ because there is only one way to fill the lattice with indistinguishable molecules of pure species in available sites.

It is often convenient to express the effect of mixing in mixing functions per unit volume and in terms of volume fractions of the components. To this end we attribute a volume $V_L$ to each lattice site such that the total lattice volume equals $V = V_{L\,i}\Sigma\, n_i = V_L(n_i + n_p)$ and mole fractions $x$ are replaced with volume fractions $\varphi$, *i.e.*, the fractions of the total number of lattice sites occupied by $i$ and $p$ segments, respectively. For $i$ being a monomeric molecule occupying only one site and $p$ being a linear polymer chain molecule of $r$ segments each of the same volume of the $i$ sites, $r$ also equals the ratio of molar volumes, $r = v_p/v_i = \varphi_p x_i/\varphi_i x_p$. Hence, after placing $n_i + n_p$ molecules on the available $N$ sites the volume fractions are $\varphi_i = n_i/(n_i + rn_p)$ and $\varphi_p = rn_p/(n_i + rn_p)$ respectively.

Now the enumeration of the number of distinguishable ways $\Omega$ of placing the differently sized molecules in the lattice is not as simple as for small, equally sized molecules, because in oligomers and polymers the positions of consecutive segments are highly correlated as a result of their connectivity. However, as has demonstrated first by Staverman in 1941 [58] and later by Flory and Huggins, the result is surprisingly simple, provided that some approximations are allowed.

Following Flory [37], we start filling a lattice with coordination number $Z$ (the number of bonds per site) with polymer chains, the sites being connected in a random way. Each new molecule can be placed in a smaller number of ways than its predecessor and we start when $j$ polymers have been added. Then there are $N - jr$ positions available to the first segment of the $(j+1)$st molecule. Its second segment, being connected to the first, has at most $Z$ sites available, from which on the average only a fraction $(N - jr)/N$ will be unoccupied. Similarly, for the third and higher segments on the average $(Z-1)(N - jr)/N$ sites are available. After placing all $n_p$ polymer molecules, the remaining $N - n_p r$ sites are thought to be filled with solute $i$ molecules, each occupying one site and the important approximation of a uniform segment density has been introduced. This approximation does not happen for dilute polymer solutions, where polymer coils are present as isolated coils, *i.e.*, segment densities of other polymers will be smaller in the neighbourhood of polymer $j+1$ than assumed above. Although the local segment density of other polymers has been overestimated, that of the same polymer $(j+1)$ has been underestimated, as these segments are not smeared out over the whole volume, but are concentrated around the centre of gravity of the molecule. This counteracts the overestimation of segment densities of the other polymers to some, yet unknown, extent.

Thus, accepting this uncertainty, the number of configurations available for the $(j+1)$st molecule is on average: $\omega_{j+1} = (N - jr)Z(Z-1)^{r-2} \cdot [(N - jr)/N]^{r-1}$. This expression is only quantitative for large $Z$ values [37], but accepting that, we proceed to find the total number of ways to fill the lattice, $\Omega$, from the product $\Omega = (1/$

$n_p!)_j \Pi\omega_{j+1}$ ($j$ ranging from 0 to $n_p$). Once this has been evaluated, the combinatorial entropy change is found from the Boltzmann relationship and we give the result for the entropy of mixing $\Delta S^{mix} = S^{conf} - S^{unmix}$ (with $S^{unmix} = S^{conf}$ for pure polymer, *i.e.*, for $n_i = 0$) without further computational details: $\Delta S^{mix} = -k(n_i \ln x_i + n_p \ln rx_p) = -k(n_i \ln \varphi_i + n_p \ln \varphi_p)$, or

$$\Delta S^{mix} = -k(\varphi_i \ln \varphi_i + \varphi_p \ln \varphi_p)N \quad (13)$$

This is the well known (Staverman) Flory–Huggins entropy-of-mixing expression. Note the close resemblance with the small molecule result (eqn. 12), despite the polymeric intricacies. Differentiation of the excess function with respect to $n_i$ to find the partial molar excess entropy of mixing $s^{e,mix}$ of solute $i$ in the phase $p$ and from that the entropic part of the activity coefficient yields $\ln \gamma_i^s = -s^{e,mix}/k = \ln [(1 - \varphi_p)/x_i] + [1 - (1/r)]\varphi_p$, *i.e.*, for the common chromatographic condition of infinite dilution ($x_i \rightarrow 0$, $\varphi_p \rightarrow 1$), $\ln \gamma_i^s = \ln (1/r) + [1 - (1/r)]$, or, expressed in the more practical terms of molar volumes,

$$\ln \gamma_i^s = \ln (v_i/v_p) + [1 - (v_i/v_p)] \quad (14)$$

It has been argued by Hildebrand [59] that the Flory–Huggins (FH) lattice model overestimates the excess entropy, and modifications have been proposed [58,60–63]. The Prausnitz approach [61–63] and the subsequent UNIFAC/UNIQUAC model [64–67] for this combinatorial contribution certainly lead to better results, using Van der Waals-related volumes rather than molar volumes. However, the required additional information on external molecular surfaces can be obtained only through a complicated procedure involving bond lengths and angles, and in complex multi-component fluids this information is not very easy to obtain. The same applies to the empirical correction of eqn. 14 [54]: the terms in $(v_i/v_p)$ are provided with an exponent to be fitted as an adjustable parameter to experimental data.

As a result, we prefer eqn. 14 in practice, except for aqueous solutions where the associative structure of water clearly contributes to both enthalpic and entropic processes (see, *e.g.*, Moroi *et al.* [68]). For aqueous solutions we have no other alternative than the use of estimation methods [56] or the experimental determination of activities, *e.g.*, by GLC or FIA [48,69].

### 2.4. The residual activity: molecular interactions

The other part of the activity coefficient, the enthalpic (or residual) part, has its origin in the relatively large intermolecular interactions, which are responsible for the cohesion of liquids. In a mixture of $i$ and $p$ there are three types of contacts: $i$–$i$, $p$–$p$ and $i$–$p$, with interaction energies $u_{ii}$, $u_{pp}$ and $u_{ip}$, respectively. If we again assume that in a random mixture each particle is surrounded by $Z$ nearest neighbours (which are the only ones with which interaction can take place), each molecule is surrounded, on average, by $Zx_i$ particles of type $i$. Hence by simply counting the number of (like) contacts that have to be broken in the pure components to form the number of (unlike) contacts in the mixture, the enthalpy (heat) of mixing

$$\begin{aligned}\Delta H_{ip}^{mix} &= H_{ip} - (H_i + H_p) \\ &= NZx_i x_p\{[(u_{ii} + u_{pp})/2] - u_{ip}\} \\ &= NZx_i x_p \, \Delta u^{ex}\end{aligned}$$

where $\Delta u^{ex}$ the exchange energy. Interaction energies of the type related to London–Van der Waals dispersion forces can be calculated from the pure component values by the geometric mean rule $u_{ip} = (u_{ii}u_{pp})^{1/2}$ because of the properties of electrostatic interactions and polarizability. If this were true for all interaction energies, we could write for the exchange energy

$$\Delta u^{ex} = \tfrac{1}{2}(u_{ii} + u_{pp}) - u_{ip} = \tfrac{1}{2}(u_{ii}^{1/2} - u_{pp}^{1/2})^2$$

The Gibbs free energy of mixing now becomes:

$$\begin{aligned}\Delta G^{mix} &= \Delta H^{mix} - T\,\Delta S^{mix} = \Delta H^{mix} - TS^{conf} \\ &= NZx_i x_p \, \Delta u^{ex} + kT(n_i \ln x_i + n_p \ln x_p)\,.\end{aligned}$$

In terms of volume fractions with total volume $V = (n_i + n_p)V_L$, this can be rewritten as

$$\begin{aligned}\Delta G^{mix}/V = kT[&(Z\,\Delta u^{ex}/V_L kT)\varphi_i\varphi_p \\ &+ (\varphi_i \ln \varphi_i + \varphi_p \ln \varphi_p)/V_L]\,.\end{aligned}$$

The first term is usually simplified by introducing the Van Laar *interaction parameter*, $\chi_{ip} = Z\,\Delta u^{ex}/kT$, which is nothing but the predecessor of the (identical) Flory–Huggins (FH) parameter.

In this case $p$ is taken to be a polymer of $r$ segments so that, as before, when we place $j$ polymers in the lattice, the volume fraction equals $\varphi_p = jr/N$. Proceeding along the same lines as for monomer segments, now taking polymer segments as the basic elements, we arrive at a similar expression for the heat of mixing, now expressed in volume fractions: $\Delta H^{mix} = NZ\varphi_i\varphi_p\,\Delta u^{ex}$. This is not exactly correct because one should count the number of interactions rather than the number of segments (*cf.*, Flory [37] or Koningsveld and Kleintjens [70]), but for either $Z$ or $r \to \infty$ the limiting result is still given by the above expression. It was again Staverman in 1937 [58] who gave a more important correction to the present expression by arguing that energetic interactions are proportional to the surface area per segment (rather than the volume) and that chemically different segments may have different interaction surfaces. A significant improvement might be obtained by this approach, using, *e.g.*, Bondi's [71] group contribution scheme for these interaction surfaces, but we refrain from that because of the loss of simplicity. Similarly, we do not take into account the corrections that arise from non-random (rather than the assumed random) mixing. The latter arises naturally in cases where the exchange energy is negative, *i.e.*, when *ip* interactions are energetically more favourable than *ii* and *pp* interactions; as a result, the total energy of the system is further lowered by allowing local ordering such that an *i*-segment will be surrounded by *p*-segments in a higher fraction than based on the random mole fraction of *p*-segments, at the expense of some decrease in entropy [72].

Thus, proceeding with the common FH approach, the free energy of mixing for polymeric phase equilibria is

$$\Delta G^{mix} = \Delta H^{mix} - T\,\Delta S^{mix}$$
$$= NZ\varphi_i\varphi_p\,\Delta u^{ex} + kT(n_i \ln \varphi_i + n_p \ln \varphi_p)$$

or, alternatively, and commonly found in the literature,

$$\Delta G^{mix}/NkT = \chi\varphi_i\varphi_p + (\varphi_i/r_i)\ln\varphi_i + (\varphi_p/r_p)\ln\varphi_p \quad (15)$$

where the monomeric compound $i$ has been extended to a polymer with $r_i$ segments such that $N = n_i r_i + n_p r_p$ and $\varphi_i = n_i r_i/N$; $r_p$ replaces the earlier $r$. From this, for completeness, we find the chemical potentials by taking the appropriate derivative of $\Delta G^{mix}$ with respect to $n_i$ or $n_p$. For the solute molecule $i$ we find

$$\Delta\mu_i = \mu_i - \mu_i^0 = (\partial\Delta\mu_i/\partial n_i)$$
$$= NkT\{\ln\varphi_i + [1 - (r_i/r_p)]\varphi_p + r_i\chi_{ip}\varphi_p^2\} \quad (16)$$

where $\chi_{ip}$ is now the Flory–Huggins interaction parameter: $\chi_{ip} = Z\,\Delta u^{ex}/kT$.

If the geometric mean rule applies for the exchange energy, we have

$$\chi_{ip}kT/V_L = Z\,\Delta u^{ex}/V_L$$
$$= [(Zu_{ii}/2V_L)^{1/2} - (Zu_{pp}/2V_L)^{1/2}]^2$$

The quantities within the square roots represent the amount of binding energy that is stored in one lattice cell volume of the pure component, *i.e.*, the same as the energy required to "evaporate" one unit volume of material. This "*cohesive energy density*" is the basis for the "*solubility parameter*", $\delta$, being the square root function, *e.g.*, for solute $i$, $\delta_i = (Zu_{ii}/2V_L)^{1/2}$ and so

$$\chi_{ip} = (V_L/kT)(\delta_i - \delta_p)^2 = (v_i/RT)(\delta_i - \delta_p)^2$$

Interaction parameters or alternatively solubility parameters play an important role in the thermodynamics of mixtures, as can be expected from the above discussion. For example, the enthalpic part of the activity coefficient, required for the determination of partition coefficients, can be expressed in terms of these parameters: $\ln\gamma_i^h = \chi_{ip} = (v_i/RT)(\delta_i - \delta_p)^2$ (see below).

## 3. EXTENDED SOLUBILITY PARAMETER CONCEPT FOR THE RESIDUAL ACTIVITY

The UNIFAC approach also offers a solution of groups concept (ASOG) for the estimation of the residual part of the activity coefficient, which

has recently been shown to be fairly successful (an accuracy of 6% has been reported [73], probably slightly optimistic in view of the 21% reported for a large data set [54]). Price and Dent [74] obtained predicted partition coefficients with this method for GLC which differ from experimental data by 20–50% for non-polar and >50% for polar stationary phases. Also, as stated earlier, the procedure to obtain the group interaction parameters is not very attractive for the present purposes. Moreover, Thomas and Eckert [54] and more recently Park and Carr [51] have shown that the modified separation of cohesive energy density (MOSCED) model, based on extensions of the RST, is at least as successful as the UNIFAC approach (accuracies of 9% for the same large data set and 18% for a limited set).

The equations used in the MOSCED model are based on the extensions to the RST put forward by Karger and co-workers [38,39] and Schoenmakers and co-workers [2,3,5,6] in their ESP models. These were designed in order to permit a description of the behaviour of polar and associating compounds in addition to non-polar and slightly dipolar solutions for which the RST had been designed originally. The only basic difference between MOSCED and ESP is that the former computes interaction parameters as adjustable, minimizing residuals between experimental and calculated $\gamma$'s, whereas the ESP models use pure-component parameters as initial input data. Although it might be true that the correlational procedure for parameter estimation in MOSCED leads to better predictions, owing to a lack of experimental data in many practical RPLC conditions this cannot be considered as a practical proposition.

### 3.1. Solubility parameters

Being essentially the same basic model, the ESP model is advocated here as a promising starting point for the prediction of partitioning behaviour in RPLC (and also in other cases). The model is based on the Scatchard–Hildebrand mixing rule [35]:

$$\Delta u_{12}^{\mathrm{mix}} = (x_1 v_1 + x_2 v_2)(c_{11} + c_{22} - 2c_{12})\varphi_1\varphi_2 \quad (17)$$

where $u_{12}^{\mathrm{min}}$ is the mixing energy associated with substances 1 and 2, present in the respective mole fractions $x$, with the volume fractions $\varphi$ and the (cohesive) interaction energy densities $c = -(u/v)$. Eqn. 17 is an alternative expression for the energetic part derived above on the assumption that $v^{\mathrm{e}} = s^{\mathrm{e}} = 0$ (*i.e.*, a regular solution). The basis of this regular mixing rule has been consolidated by later derivations via integration of all intermolecular interactions between pairs of molecules throughout the bulk of the solution [36]. If now the rule of the geometric mean cohesive energy densities, $c_{12} = (c_{11}c_{22})^{1/2} = \delta_1\delta_2$ is introduced, where $\delta = c^{1/2}$, the solubility parameter, then eqn. 17 simplifies to

$$\Delta u_{12}^{\mathrm{mix}} = (x_1 v_1 + x_2 v_2)(\delta_1 - \delta_2)^2\varphi_1\varphi_2 \quad (18)$$

The geometric mean rule for the cohesive energy density is basically correct only for interaction energies that are randomly distributed, symmetric and distance-only functions, such as dispersion interaction (London–Van der Waals) and dipolar interactions (Keesom). It is known, however, that for polar interactions (induction, association) the geometric mean assumption fails [35,36,75]. To correct for this deviation from the geometric mean rule in the MOSCED model asymmetry parameters were introduced as adjustable parameters for improving the predictive accuracy of the model. Other empirical correction parameters can be found in the work by Prausnitz and co-workers [35,36] in the form $c_{12} = (1 - l_{12})(c_{11}c_{22})^{1/2}$ such that eqn. (18) is modified to

$$\Delta u_{12}^{\mathrm{mix}} = (x_1 v_1 + x_2 v_2)[(\delta_1 - \delta_2)^2 + 2l_{12}\delta_1\delta_2]\varphi_1\varphi_2$$

For simplicity, we choose to make no use of these empirical $l_{12}$ parameters. As a result, we find the thermal part of the activity coefficient (eqns. 9 and 10) from the partial molar excess enthalpy $h^{\mathrm{e}} = u^{\mathrm{e}} + pv^{\mathrm{e}}$, which for regular solutions equals $u^{\mathrm{e}}$ because by definition $v^{\mathrm{e}} = 0$. Consequently, with eqn. 18 for the mixing energy, $h_i^{\mathrm{e}} = u_i^{\mathrm{e}} = \partial(\Delta u_{ip}^{\mathrm{mix}})/\partial n_i = RT \ln \gamma_i^{\mathrm{h}}$, so at infinite dilution

$$\ln \gamma_i^{\mathrm{h}} = \chi_{ip} = (v_i/RT)(\delta_i - \delta_p)^2 \quad (19)$$

Because of the exponential nature of this rela-

tionship, highly accurate values for the solubility parameters in eqn. 19 are needed (insofar as the approximate nature of eqn. 19 itself is disregarded). Values for the solubility parameter are usually determined from its definition as the square root of the cohesive energy density (CED), $c$. For saturated liquids the internal potential energy equals the sum of the molar energy (heat) of vaporization, (not to be confused with the latent heat of vaporization), $\Delta u^v$, and the energy needed to expand the saturated vapour to the ideal gas state (zero pressure or alternatively infinite volume):

$$-u = \Delta u^v + \int_v^\infty (\partial u/\partial v)_T \, dv \tag{20}$$

or in terms of the common latent heat (enthalpy) of vaporization:

$$\begin{aligned} -u &= \Delta h^v - pv_{gas} + \Delta h_{gas} + pv_{liq} \\ &= \Delta h^v - RT + \Delta h_{gas} + pv_{liq} \end{aligned} \tag{21}$$

Provided that pressure and temperature are far removed from critical conditions, $\Delta h_{gas}$ and $pv_{liq}$ can be ignored in comparison with the other two terms and one arrives at the commonly used expression for the solubility parameter:

$$\delta^2 = (\Delta h^v - RT)/v_{liq} \tag{22}$$

from which $\delta$ values are often estimated, if sufficiently accurate vapour pressure data are available or otherwise by applying Clausius–Clapeyron or Antoine equations with known coefficients. For GLC purposes (low pressures) this is often a good procedure, optionally corrected for gas imperfection by the compressibility factor $Z = pv/RT$:

$$\delta^2 = (\Delta h^v - RT)Z/v_{liq} \tag{23}$$

The well known tables after Hoy [53] are based on this procedure. For the present purposes, especially at high pressure and temperature conditions, this procedure may lead to appreciable errors because of the omission of the additional terms in eqn. 21.

### 3.2. The role of the internal pressure

Internal pressure is defined as the pressure associated with the internal energy. A first approximate correction can be based on the use of the Van der Waals equation to find the ignored expansion terms in eqn. 21. This yields an identity of the internal pressure $\mathcal{P}$ and the CED [for the liquid phase $\mathcal{P} = c = a/(v_{liq})^2$ and for the gas phase $\mathcal{P} = a/(v_{gas})^2$]. Hence eqn. 20 becomes $-u = \Delta u^v + a/v_{gas} = \Delta u^v[1 + (v_{liq}/v_{gas})]$, which leads to the correction term $1 - (v_{liq}/v_{gas})^2$ for the right-hand side of eqn. 23. The validity of this correction term, being based on the uncertain Van der Waals equation, is doubtful especially in view of our goal to obtain quantitative results.

It has been argued by Bagley and co-workers [76–79] and Dack [80,81] that in the regular mixing rule (eqn. 17) the differential quantity $\mathcal{P} = (\partial u/\partial v)_T$, the internal pressure, rather than the integral quantity $c = -u/v$, the CED, should be used. This has been largely neglected as, especially for non-polar substances, the internal pressure and the CED are not very different (although systematic differences of up to about 22% have been measured by Allen and co-workers [82,83]). Also, as stated above, the Van der Waals equation yields an identity of $\mathcal{P}$ and $c$. For polar substances, however, the CED is always larger than the internal pressure as the CED accounts for all contributions to the internal energy and the internal pressure only for those which are volume dependent. As we recall that the mixing rule has been strictly derived for symmetrical potential energy contributions, there is much sense in Bagley and co-workers' proposition of using $\mathcal{P}$ instead of $c$ in the mixing rule. Indeed, it is $\mathcal{P}$ that covers the strongly distance-dependent classical dispersion interaction and the dipolar (orientation) interaction, so

$$\mathcal{P} = -(u_d + u_o)/v \tag{24}$$

The CED, on the other hand covers the whole of $\Delta u^v$, and all of the energy changes involved in the phase change from the liquid into the gas, and thus contains even kinetic energy terms associated with changes in translation, vibration

and rotation between liquid and gas states, in addition to the dispersion interaction. Thus, for non-polar (np) substances:

$$\Delta u^{v}_{np} = -(u_d + u_o) + \Delta u^{kin} = \mathcal{P}v + \Delta u^{kin} \quad (25)$$

Depending on the change in the number of degrees of freedom, $\Delta f$, this results in a kinetic term in eqn. 25 of $\Delta u^{kin} = \Delta f(RT/2)$, with the ideal value of $-(3/2)RT$ based on $\Delta f = 0 + 3 - 6 = -3$. With eqn. 25 it then appears that for non-polar compounds the CED $c$ is slightly but systematically smaller than the internal pressure, in accordance with a large number of observations [82,83]:

$$c_{np} = (\Delta u^{v}_{np})/v = \delta^2_{np} = \mathcal{P} - (3/2)(RT/v) \quad (26)$$

Bagley and co-workers [76–79] determined from experimental $\mathcal{P}$ and $c$ data a large number of $\Delta f$ values and often obtained absolute values larger than 3, up to about 6, possibly because not strictly non-polar compounds such as alkenes, aromatics and chloroalkanes were used. Here we adopt eqn. 26 as the general but idealized relationship between CED and internal pressure for non-polar compounds. As it is $\mathcal{P}$ rather than the CED that appears in the mixing rule, the quantity called $\delta$ in eqn. 19 should be based on internal pressure ($\delta^2_v = \mathcal{P}$) rather than on vaporization data ($\delta^2 = c$), and is larger than the $\delta$ values that appear in most tables:

$$(\delta^2_v)_{np} = \mathcal{P} = c_{np} + (3RT/2v)$$
$$= \delta^2_{np} + (3RT/2v) \quad (27)$$

Numerical values of the correction term $(3RT/2v)$ are always small in comparison with the vaporization energy term, say 8–10%, but vary widely for different compounds. The occurrence of the only small difference of two $\delta$ values is another reason why Bagley and co-workers' treatment has been overlooked for so long. As we are in need of very accurate numerical values we shall use the correct and slightly higher $\delta$ values. In the general case of polar compounds, the CED is always larger than the internal pressure. This is caused by the fact that $\mathcal{P}$, reflecting the classical symmetrical interactions, is still given by eqn. 24, but the now possible asymmetric proton/electron transfer (acid–base) interactions with energy $u_{ab}$ is taken into account by the CED parameter $\delta^2$ as determined from vaporization data. Analogously to eqns. 25 and 26, we have

$$\Delta u^{v} = -(u_d + u_o + u_{ab}) - (3RT/2)$$
$$= \mathcal{P}v - u_{ab} - (3RT/2)$$

and so

$$\delta^2 = \delta^2_v + \delta^2_H - (3RT/2v) \quad (28)$$

where $\delta^2_H = -u_{ab}/v$, the acid–base (often hydrogen bond) contribution. Rearranging eqn. 28 yields the total solubility parameter:

$$\delta^2_T = \delta^2 + (3RT/2v) = \delta^2_v + \delta^2_H \quad (29)$$

where, as in the case of non-polar compounds, the square of the total solubility parameter, $\delta_T$ as defined by eqn. 29, is larger than the CED by the amount $3RT/2v$, by analogy with eqn. 27. Again, the total solubility parameter to be used is slightly higher than those which appear in the literature.

### 3.3. The multi-component ESP model

In a natural way we arrived at a two-parameter model as expressed by eqn. 29. This shows some resemblance with the model developed by Hildebrand *et al.* [35], which applies the qualitative and complex homomorph concept. Eqn. 29 separates the solubility parameter into two parts, one covering the symmetrical interactions ($\delta_v$) the other the chemical acid–base interactions ($\delta_H$) in a unified and elegant way, and is to be preferred, whenever possible.

In general, it cannot be expected that a two-parameter model will be conclusive in describing the effects of the many possible types of interaction: dispersion, permanent dipole orientation, induction of dipoles, multipoles and transfer (chemical) interactions. Indeed, an additional empirical parameter was adopted by Hildebrand *et al.* [35] to account for the additional but unknown contributions. Dispersion, orientation and chemical interactions have been included in the above already and it is believed that these are the main factors to be taken into account.

Although possibilities exist to account for induced dipoles [38] and "hard" and "soft" transfer interactions [84–87], this is not recommended because an estimation of errors reveals that each additional parameter increases the uncertainty in the resulting activity coefficient drastically. For this reason we propose that the extended solubility parameter model be used only with the mentioned three types of interaction, for which accurate methods can be developed to estimate numerical values.

As in eqn. 29 $\delta_v^2 = \mathcal{P} = -(u_d/v) - (u_o/v)$, this can be interpreted as the sum of the squares of two individual partial solubility parameters, one for each type of interaction. Eqn. 29 then reveals its structure as a three-parameter model:

$$\delta_T^2 = \delta_d^2 + \delta_o^2 + \delta_H^2 \tag{30}$$

In this form, Hansen and co-workers [52] were the first to define a three-parameter ESP model to account for acid–base interactions. The only difference from the present treatment is the difference in numerical values for $\delta_T^2$ and $\delta_H^2$, which in our case contain the kinetic energy contributions. If now Hansen and co-workers' suggestion is followed and individual interaction energy contributions $c_j = \delta_j^2$ ($j$ = d, o, H) are treated independently in the derivations following the regular mixing rule, eqn. 17, and additive after eqn. 30, we find

$$\Delta u_{j,12}^{mix} = (x_1 v_1 + x_2 v_2)(c_{j,11} + c_{j,22} - 2c_{j,12})\varphi_1\varphi_2$$

and with

$$c_{j,12} = (c_{j,11}c_{j,22})^{1/2} = \delta_{j,1}\delta_{j,2}$$

we have eqn. 31.

At first sight this new mixing rule is an improvement over the classical Hildebrand rule, eqn. 17. For instance, two substances with equal CEDs do not yield a mixing-energy effect according to Hildebrand, but they may do so according to Hansen if, by way of example, they have different dipole moments as well as different dispersion interactions. However, the acid–base term in eqn. 31 is open to criticism, because this quadratic term is always positive, which means an endothermic mixing energy. However, is well known that transfer reactions are often exothermic, which corresponds to a negative mixing-energy contribution that is impossible from eqn. 31. This situation is to be logically remedied by defining separate partial parameters for the asymmetrical acceptor and donor functions in transfer interactions as has been initially proposed by Small [88] and later by Drago and co-workers [84–87]. Karger *et al.* [38] performed the important task of reformulating the mixing rule for this kind of asymmetric transfer interaction. Defining the separate acid and base parameters, $\delta_a$ and $\delta_b$, such that for the pure substance

$$\delta_H^2 = 2\delta_a\delta_b = -u_{ab}/v \tag{32}$$

and replacing eqn. 30 with

$$\delta_T^2 = \delta_d^2 + \delta_o^2 + 2\delta_a\delta_b \tag{33}$$

reveals the now four-parameter structure of the ESP model. Eqn. 31, which was only valid for the two classical interactions ($j$ = d, o) is thus extended to the transfer interaction from eqn. 32: $c_{ab,11} = \delta_{h,1}^2$; $c_{ab,22} = \delta_{h,2}^2$; $c_{ab,12} = \delta_{a,1}\delta_{b,2} + \delta_{a,2}\delta_{b,1}$. As a result, the revised and total mixing

---

$$\Delta u_{12}^{mix} = {}_j\sum \Delta u_{j,12}^{mix} = (x_1 v_1 + x_2 v_2)\varphi_1\varphi_2[(\delta_{d,1} - \delta_{d,2})^2 + (\delta_{o,1} - \delta_{o,2})^2 + (\delta_{H,1} - \delta_{H,2})^2] \tag{31}$$

$$\Delta u_{12}^{mix} = {}_j\sum \Delta u_{j,12}^{mix} = (x_1 v_1 + x_2 v_2)\varphi_1\varphi_2[(\delta_{d,1} - \delta_{d,2})^2 + (\delta_{o,1} - \delta_{o,2})^2 + 2(\delta_{a,1} - \delta_{a,2})(\delta_{b,1} - \delta_{b,2})] \tag{34}$$

rule including the asymmetrical interactions is eqn. 34.
This expression, which replaces eqn. 31, indeed shows the possibility of producing an exothermic energy effect from the acid–base interactions. In the limiting case of infinite dilution for $i$, eqn. 35 applies.

The activity coefficient that corresponds with this interaction for substance $i$ in phase $p$ is now found from

$$h_i^{e,\infty} = u_i^{e,\infty} = \partial(\Delta u_{i,p}^{mix,\infty})/\partial n_i = RT \ln \gamma_i^{h,\infty}$$

and so

$$\ln \gamma_{ab,i}^{h,\infty} = (2v_i/RT)(\delta_{a,i} - \delta_{a,p})(\delta_{b,i} - \delta_{b,p}) \quad (36)$$

which extends eqn. 19 that applied only for the classical interactions.

The total equation for the activity coefficient at infinite dilution as found from our four-parameter ESP model, including the entropic contribution of eqn. 14, now appears as eqn. 37.
From eqn. 37 the partition coefficient based on mole fractions, $K^x$ according to eqn. 8, is shown as eqn. 38.

From eqn. 38, together with eqn. 1, the partition coefficient based on concentrations, and with eqn. 3 the capacity factor can be obtained as $\ln K_i^c = \ln K_i^x + \ln (v_m/v_s)$ and $\ln k_i' = \ln K_i^x + \ln (n_s/n_m)$, respectively.

### 3.4. Chromatographic selectivity

Another useful expression is that for the relative net residence times of two partitioning solutes, *i.e.*, the ratio $\alpha_{j,i} = k_j'/k_i'$ (such that $\alpha > 1$): eqn. 39.
For $v_i = v_j = v$, which is often the case for common small molecules, eqn. 39 takes an interesting and very tractable form:

$$\begin{aligned}(RT/2v) \ln \alpha_{j,i}^{v} = {} & (\delta_{d,j} - \delta_{d,i})(\delta_{d,s} - \delta_{d,m}) \\ & + (\delta_{o,j} - \delta_{o,i})(\delta_{o,s} - \delta_{o,m}) \\ & + (\delta_{a,j} - \delta_{a,i})(\delta_{b,s} - \delta_{b,m}) \\ & + (\delta_{b,j} - \delta_{b,i})(\delta_{a,s} - \delta_{a,m})\end{aligned}$$

---

$$h_{ab}^{e,\infty} = \Delta h_{ab,12}^{mix,\infty} = \Delta u_{ab,12}^{mix,\infty} = 2v_1(\delta_{a,1} - \delta_{a,2})(\delta_{b,1} - \delta_{b,2}) \quad (35)$$

$$\begin{aligned}\ln \gamma_i^{\infty} &= (v_i/RT)[(\delta_{d,i} - \delta_{d,p})^2 + (\delta_{o,i} - \delta_{o,p})^2 + 2(\delta_{a,i} - \delta_{a,p})(\delta_{b,i} - \delta_{b,p})] + \ln (v_i/v_p) + [1 - (v_i/v_p)] \\ &= (v_i/RT)[(\delta_{T,i}^2 + \delta_{T,p}^2) - 2(\delta_{d,i}\delta_{d,p} + \delta_{o,i}\delta_{o,p} + \delta_{a,i}\delta_{b,p} + \delta_{b,i}\delta_{a,p})] + \ln (v_i/v_p) + [1 - (v_i/v_p)] \quad (37)\end{aligned}$$

$$\begin{aligned}\ln K_i^x = {} & -(v_i/RT)\{(\delta_{T,s}^2 - \delta_{T,m}^2) - 2[\delta_{d,i}(\delta_{d,s} - \delta_{d,m}) + \delta_{o,i}(\delta_{o,s} - \delta_{o,m}) + \delta_{a,i}(\delta_{b,s} - \delta_{b,m}) + \delta_{b,i}(\delta_{a,s} - \delta_{a,m})]\} \\ & + \ln (v_s/v_m) + v_i[(v_s)^{-1} - (v_m)^{-1}] \quad (38)\end{aligned}$$

$$\begin{aligned}\ln \alpha_{j,i} = {} & -(1/RT)\{(v_j - v_i)(\delta_{T,s}^2 - \delta_{T,m}^2) - 2[(v_j\delta_{d,j} - v_i\delta_{d,i})(\delta_{d,s} - \delta_{d,m}) \\ & + (v_j\delta_{o,j} - v_i\delta_{o,i})(\delta_{o,s} - \delta_{o,m}) + (v_j\delta_{a,j} - v_i\delta_{a,i})(\delta_{b,s} - \delta_{b,m}) + (v_j\delta_{b,j} - v_i\delta_{b,i})(\delta_{a,s} - \delta_{a,m})]\} \\ & + (v_j - v_i)[(v_s)^{-1} - (v_m)^{-1}] \quad (39)\end{aligned}$$

or, more concisely,

$$(RT/2v)\ln\alpha^{v}_{j,i} = (\bar{x}_j - \bar{x}_i)\bar{y} \qquad (40)$$

where $\bar{x}$ and $\bar{y}$ are the vectors in a four-dimensional space with coordinates:

$x_1 = \delta_d$ $x_2 = \delta_o$ $x_3 = \delta_a$ $x_4 = \delta_b$
$y_1 = \delta_{d,s} - \delta_{d,m}$ $y_2 = \delta_{o,s} - \delta_{o,m}$ $y_3 = \delta_{b,s} - \delta_{b,m}$ $y_4 = \delta_{a,s} - \delta_{a,m}$

The importance of this formulation becomes especially clear from partial differentiation of eqn. 40:

$$(RT/2v)(1/\alpha^{v}_{j,i})[\partial(\alpha^{v}_{j,i})/\partial y_n] = x_{n,j} - x_{n,i} \qquad (41)$$

which shows that the relative change in $\alpha$ arising from a change in the $n$th coordinate ($x_n$) is directly proportional to that difference in this $n$th parameter for both solutes. This is of great importance for our insight into ways of controlling (relative) residence times and hence controlling and maximizing selective separation in chromatographic techniques. Alternatively, it gives us a tool to characterize phase systems on a relative basis with respect to a standard phase system with the aid of chosen calibration compounds. This is analogous to the commonly used retention index system in GLC (*e.g.*, ref. 39). Such a standardized phase system might well be the octanol–water (OW) system [44,45], already mentioned and often used to correlate partition data with chromatographic studies.

Indeed, the solubility parameter model outlined above suggests that the partitioning information stored in the $P_{OW}$ values and listed by Hansch and co-workers [44,45] can be recalculated into those for any other phase system, especially those which also contain water as one of the phases. This can be seen from the expression for $K^c$, following from eqn. 38 when applied to two two-phase systems, the variable phase ($p$)–W and the (octanol) (O)–W system: eqn. 42.

This shows that the partition coefficient for the solute in the new phase system $p$–W can be recalculated to O–W even without knowing the partial solubility parameters of water.

### 3.5. Estimation of the individual parameters

The usefulness of the above depends first on the extent to which the underlying assumptions can be justified. Second, as has been mentioned before, owing to the exponential relationship between partition quantities and the partial parameters, the usefulness of the ESP model depends heavily on the accuracy and precision with which the individual parameters can be obtained. By way of example, in the case of the dispersion parameter $\delta_d$, eqn. 37 for the activity coefficient yields after partial differentiation that an error ($\Delta\delta_d$) gives the following error in the activity coefficient:

$$\Delta\gamma^{\infty}_i/\gamma^{\infty}_i = (2v_i\delta_{d,i}/RT)(\delta_{d,p} - \delta_{d,i})(\Delta\delta_{d,i}/\delta_{d,i})$$

Comparable error expressions exist for the other partial parameters and it appears that errors of about 1% in $\delta$ values may already result in errors of *ca.* 3–10% in the activity coefficient. Each parameter in addition to the four we have finally chosen contributes to the overall error, and the contribution of parameters such as the asymmetric induction as described by Karger and co-workers [38,39] in particular to the error is larger than the improvement in the accuracy of the predictions.

Although of basic interest and sometimes referred to as of relative importance, we cannot obtain sufficiently reliable estimates via the avail-

$$\begin{aligned}\ln K^c_{Op} &= \ln K^c_{OW} - \ln K^c_{pW} = \ln P_{OW} - \ln K^c_{pW} \\ &= (v_i/RT)\{(\delta^2_{T,p} - \delta^2_{T,O}) - 2[\delta_{d,i}(\delta_{d,p} - \delta_{d,O}) + \delta_{o,i}(\delta_{o,p} - \delta_{o,O}) + \delta_{a,i}(\delta_{b,p} - \delta_{b,O}) \\ &\quad + \delta_{b,i}(\delta_{a,p} - \delta_{a,O})]\} - v_i[(v_p)^{-1} - (v_O)^{-1}] \end{aligned} \qquad (42)$$

able methods to account for the induction effect as well. This is not a large drawback as it appears that the expressions for partitioning including induction forces contain cross-terms $(\delta_{ind,i} - \delta_{ind,p})(\delta_{d,i} - \delta_{d,p})$, which are always small. The corrections obtained for these terms are often smaller than the error introduced by the estimation of the induction parameters, so that we do not recommend the addition of a separate induction parameter.

We shall not describe here in detail the determination of the four main parameters, as this procedure has been outlined before [2] and has remained basically unchanged since then. We maintain the view that the procedure based on generalized thermodynamic properties is by far the best way to proceed, provided that reliable equations of state can be found. We still prefer the use of the three-parameter Lee and Kesler [89] equation because it provides very reliable heats of evaporation [56]. This also has the advantage that both temperature and pressure dependences of the solubility parameters are found, which is especially useful in GC and SFC [57]. For example, in accordance with the linearity of the relationship ln $K$ *vs.* $1/T$, the square of the total solubility parameter shows a strictly linear temperature dependence: $\delta_T^2 = AT + B$. We note interesting developments in estimating multi-dimensional solubility parameters by molecular mechanics and dynamics (MD) methods, which were recently applied [90] to such complex molecules as alkyl phenol ethoxylates for which no EOS is available.

For many small molecules the EOS approach is fairly straightforward, but of course in the case of polymer chain molecules it is not a practical proposition. In that case there is hardly any possibility other than to determine partial solubility parameters either from group contribution schemes according to Small, Hoy, Fedors and others (see Barton [48] for a review) or from experimental data using, *e.g.*, chromatographic techniques themselves as the characterization method, using known solutes (see later). Regarding the group contribution methods, we find that the uncertainty in the values obtained, is too large (up to about 15%) to be of any use for the required quantitative predictions.

## 4. RESULTS OBTAINED WITH THE ESP MODEL, DISCUSSION

Tables were prepared for *ca.* 200 organic compounds [91] for the partial parameters of the proposed four-parameter model, as obtained by the above procedures, extending the list we published previously [2]. Application of these values to different forms of analytical separation methods, in particular to the prediction of residence times in gas–liquid (GLC) and reversed-phase liquid chromatography (RPLC), has been discussed elsewhere [2–6,40,49,50,51]. From those experiences it can be concluded that this ESP model is very capable of predicting trends in retention behaviour.

In this work we are mainly interested in the general case of the prediction of liquid–liquid partition equilibria, including polymeric grafted phases and mobile phase effects from, *e.g.*, mixed solvents. Being so closely related, predictions in organic compound–aqueous systems are of interest for these analytical separation methods and *vice versa*. Moreover, chromatographic techniques can be fruitfully used to obtain experimental data on partitioning in these systems. With the aid of the obtained partial ESP parameters it is possible to find *a priori* predictions of partition coefficients in liquid–liquid systems, based on eqn. 38. The widely accepted octanol–water data according to Hansch and co-workers [44,45] are good test data for the predictive ability of the proposed ESP model. Apart from liquid–liquid partitioning data of solutes in octanol–water and solvent–water systems, Hansch and co-workers also presented a method for deriving partition data from those measured in, *e.g.*, octanol–water to an arbitrary solvent–water system.

We tested the ability of the present ESP model to perform the same task. The results are shown in Table 1, an extension of a table presented in earlier work [2]. The table indicates, in agreement with the observations by Park and Carr [51], that *a priori* prediction of partition data by the ESP model leads to errors up to about 20%. Especially for such polar substances as used here, including water, this is considered to be an encouraging result, taking into account the rela-

TABLE 1

PARTITION COEFFICIENTS OF SOLUTES IN SOLVENT–WATER SYSTEMS AS PREDICTED WITH ESP AND THE HANSCH METHOD

| Solute *i* | Solvent *p* | Log $K_{pw}$ | | Log $K_{ow}$ | | Log $P_{ow}$ | |
|---|---|---|---|---|---|---|---|
| | | ESP prediction | Exptl.[a] | ESP prediction | Recalc., eqn. 42 | Recalc., Hansch | Exptl.[a] |
| Ethanol | Carbon | −1.51 | −1.61 | −0.16 | 0.18 | 0.47 | −0.32 |
| Phenol | tetrachloride | −0.42 | −0.42 | 1.50 | 1.46 | 1.55 | 1.46 |
| Aniline | | 0.22 | 0.25 | 1.23 | 1.83 | 1.11 | 0.94 |
| Methanol | Chloroform | −1.63 | −1.63 | −0.70 | −1.47 | −0.66 | −0.66 |
| Ethanol | | −0.80 | −0.85 | −0.34 | −0.42 | −0.18 | −0.32 |
| Phenol | | 0.42 | 0.35 | 1.43 | 0.97 | 1.53 | 1.46 |
| Aniline | | 1.44 | 1.32 | 0.97 | 1.0 | 0.90 | 0.94 |
| Ethanol | Benzene | −1.60 | −1.54 | −0.24 | 0.36 | −0.13 | −0.32 |
| Aniline | | 0.93 | 1.00 | 0.55 | −0.50 | 1.24 | 0.90 |
| Acetonitrile | Diethyl ether | −0.11 | −0.22 | −0.19 | 1.12 | −0.08 | −0.34 |
| Acetone | | −0.14 | −0.21 | −0.09 | 1.03 | −0.06 | −0.24 |
| Pyridine | | 0.02 | 0.08 | 0.75 | 2.05 | 0.92 | 0.64 |

[a] Experimental data from refs. 44 and 45.

tive ease with which the partial parameters have been obtained. Also, it shows that the ESP model is equally suited to recalculate data obtained in one particular phase system to another as the widely used Hansch method. It shows clearly that large deviations may sometimes occur, but none worse than those in the Hansch method.

Another example of the reliability of ESP predictions for liquid–liquid partitioning is given in Table 2, where experimental partition coefficients of alkanes in glycols obtained by FIA are reported, as obtained at low pressures and room temperature for the systems heptane–diethylene glycol (hd) and heptane–triethylene glycol (ht). Again, the *a priori* prediction of the ESP model is seen to be acceptable, but deviations up to about 20% occur, just as when Pierotti *et al.*'s correlations [92] are used. Published results [2–6,38–40,49,50] demonstrate that

TABLE 2

COMPARISON OF MEASURED (BY FIA) AND PREDICTED PARTITION COEFFICIENTS IN HEPTANE–GLYCOL SYSTEMS AT LOW PRESSURES AND 25°C

| Solute | $K_{x,hd}$ | | | $K_{x,ht}$ | | |
|---|---|---|---|---|---|---|
| | Calc. [92] | Predicted, ESP | Exptl., FIA | Calc. [92] | Predicted, ESP | Exptl., FIA |
| Benzene | 0.221 | 0.21 | 0.23 | 0.323 | 0.37 | 0.39 |
| Butylbenzene | 0.033 | 0.03 | 0.03 | 0.052 | 0.05 | 0.05 |
| Cyclohexane | 0.033 | 0.03 | 0.02 | 0.038 | 0.03 | 0.03 |
| Decalin | 0.013 | 0.01 | 0.01 | 0.022 | 0.02 | 0.02 |
| Naphthalene | 0.263 | 0.27 | 0.29 | 0.667 | 0.65 | 0.67 |
| Terphenyl | 0.236 | 0.23 | 0.26 | 0.608 | 0.68 | 0.71 |
| Tetralin | 0.096 | 0.11 | 0.10 | 0.182 | 0.17 | 0.15 |
| Toluene | 0.112 | 0.12 | 0.13 | | 0.16 | 0.18 |

our four-parameter ESP model is consistent and that no important molecular interactions (*e.g.*, induction) are left out. This is further sustained by the observation that retention times of solutes not contained in a linear regression procedure to find the partial parameters [2] show good agreement between experiment and prediction (see below).

For instance, in GLC with dinonyl phthalate (DNP) as the stationary phase, the experimental retention times and activity coefficients are in good agreement (deviation $\ll$20%) with those predicted from the above characterization of DNP, also at different temperatures. As another example, in liquid–liquid chromatography (LLC) we found that the actual partition coefficients determined from retention times, eqns. 2 and 3, using *n*-hexadecane as the stationary and water as the mobile phase and alcohols and ketones as the solutes, the predicted $K$ values are again within 10% of the measured values.

Concerning RPLC, we show here the results of the ESP characterization method on a series of laboratory-made phases chemically bonded to the surface of 10-$\mu$m porous silica particles and containing a polar group at the non-bonded chain end. These bonded phases do not behave like bulk liquids, so that it is impossible to estimate their solubility parameters by the proposed methods. Measurement of the retention times of 11–22 solutes with known partial solubility parameters and application of linear regression with eqn. 33 gave the partial parameters for these unknown phases reported in Table 3.

Again, the internal consistency of the ESP model is proved by the near equality of the two total $\delta_T$ values, obtained in two different ways, (a) and (b). We believe that this application of the ESP model to characterize unknown or complex liquid (fluid) phases in terms of partial solubility parameters, by calibration with well characterized standard solute compounds, is a very useful tool, especially with complex mixtures and if no universal equation of state can be used to define its physico-chemical behaviour (*e.g.*, in RPLC with grafted substrates).

TABLE 3

CHACTERIZATION OF CHEMICALLY BONDED STATIONARY PHASES BY RPLC WITH WATER AS THE MOBILE PHASE (20°C)

$\delta$ Values in $(cal/ml \cdot mole)^{1/2}$; for $(J/ml)^{1/2}$, multiply by 2.04.

| Chemically bonded phase with polar end-group | $\delta_d$ | $\delta_o$ | $\delta_a$ | $\delta_b$ | $\delta_T$ [a] | |
|---|---|---|---|---|---|---|
| | | | | | (a) | (b) |
| Methoxyphenyl | 6.46 | 1.06 | 0.14 | 2.57 | 6.61 | 6.60 |
| Aminophenyl | 6.66 | 0.81 | 0.18 | 2.32 | 6.77 | 6.77 |
| | 7.21 | 1.41 | 0.19 | 2.23 | 7.88 | 7.40 |
| Triglycine | 8.27 | 0.59 | 0.38 | 1.20 | 9.10 | 8.35 |
| N,N – Dimethylaminophenyl | 7.60 | 1.13 | 0.13 | 2.04 | 8.11 | 7.72 |
| Propylamine | 9.06 | 0.56 | 1.54 | 2.00 | | 10.34 |
| $-(CH_2)_3N{=}C(CH_3)C_6H_4C{\equiv}N$ | 9.08 | 0.85 | 0.69 | 5.10 | | 10.16 |
| $-(CH_2)_3N{=}CHC_6H_4N(CH_3)_2$ | 7.52 | 0.50 | 0.45 | 6.00 | | 8.02 |
| $-(CH_2)_3N{=}C(CH_3)C_6H_4NH_2$ | 8.49 | 0.72 | 0.84 | 2.17 | | 9.32 |
| $-(CH_2)_3N{=}C(CH_3)C_6H_4NO_2$ | 8.43 | 0.87 | 0.67 | 7.09 | | 9.41 |
| $-(CH_2)_3N{=}(CHC_6H_4N{=})_nCHC_6H_4NH_2$ | 9.14 | 0.85 | 0.52 | 3.80 | | 9.87 |

[a] (a) Obtained as independent value from the linear regression; (b) obtained as the sum of all partial parameters, eqn. 33.

### 4.1. Relative characterization of chromatographic systems

Because of the internal consistency of the ESP model with RPLC and for that matter with other liquid–liquid systems, there is in fact no need to use standard calibration compounds with known partial solubility parameters. These can be attributed to the standard compounds in an arbitrary way, as first proposed by Rohrschneider [42,43] for gas–liquid chromatography. Rohrschneider was the first to recognize the property inherent in the RST for partitioning systems that the logarithm of partition coefficients (or their ratios) are described by a binomial function whose terms are composed of two factors, one of which depends on the type of solute only and the other on the nature of the phase system only. This property is clearly shown in eqn. 40, but on closer inspection also in eqn. 38 for the partition coefficient(s) themselves, provided that the entropic terms in the molar volumes are neglected. As a result,

$$\ln K_{ip} = a_{i1}z_{p1} + a_{i2}z_{p2} + \cdots + a_{im}z_{pm} = \sum_{n=1}^{m} a_{in}z_{pn} \quad (43)$$

where $a_{in}$ characterizes the $n$th type of molecular interaction of solute $i$ and $z_{pn}$ that of the phase system $p$. The ESP model prescribes a maximum of $m = 5$ of such interaction terms (including induction), but in practice it is very possible that less than five parameters are sufficient to characterize the whole partitioning system.

The determination of the interaction coefficients $a$ and $z$, in principle to be found from the ESP estimation procedures, may also proceed in a completely experimental way. To do so, we have to measure the partition coefficients of at least $m$ standard solutes on $m$ different phase systems, so for solutes $i$ ranging from 1 to $m$ on each phase system $p$ yields a system of $m$ linear equations:

$$\ln K_{1,p} = a_{11}z_{p1} + a_{12}z_{p2} + \cdots + a_{1m}z_{pm}$$

$$\ln K_{2,p} = a_{21}z_{p1} + a_{22}z_{p2} + \cdots + a_{2m}z_{pm}$$

$$\ln K_{m,p} = a_{m1}z_{p1} + a_{m2}z_{p2} + \cdots + a_{mm}z_{pm}$$

We can solve $z_{p1}$ to $z_{pm}$ once we know the coefficients $a_{11}$ to $a_{mm}$. Each standard solute can now be provided with arbitrarily chosen $a_{ip}$ coefficients (Rohrschneider chose, for instance, 100, 0, 0, 0, 0 for standard solute 1, 0, 100, 0, 0, 0 for solute 2, etc., *i.e.*, $a_{ip} = 100$ for $i = p$, otherwise $a_{ip} = 0$) to obtain the $z$-values for phase $p$, as based on these arbitrary $a$ values. If this is performed on $m$ phase systems with the same $m$ standards, all $z$ values are known for each phase system and each phase system has now been characterized by these $z$ values.

Once this has been done, each new solute that was not chosen as a standard should be partitioned in each of the $m$ phase systems thus characterized, to obtain the $a$ values for that new solute from its measured $K$ value in each phase system. The new solutes thus characterized can subsequently be used to determine the characteristic $z$ values for new phase systems, etc. Because of the already proven consistency of this RST-based model, the arbitrariness of the coefficients is no problem. The choice of the initial values is, however, not optimum in the sense that each product $az$ represents an interaction energy of some type (dispersion, orientation, etc.) and the ratio of those interactions is different in each compound (as reflected by the values of the partial solubility parameters). Assigning arbitrary values to the $a$ and $z$ values conflicts with those ratios, which was the reason why Rohrschneider carefully chose strong representative compounds for each type of interaction as the standards and assigned a maximum value to that particular interaction. Naturally, however, we can find the optimum values of the standard coefficient matrix:

$$|A| = \begin{vmatrix} a_{11} & a_{12} & a_{13} & \cdots & a_{1m} \\ a_{21} & a_{22} & a_{23} & \cdots & a_{2m} \\ a_{31} & a_{32} & a_{33} & \cdots & a_{3m} \\ \cdot & \cdot & \cdot & & \cdot \\ \cdot & \cdot & \cdot & & \cdot \\ \cdot & \cdot & \cdot & & \cdot \\ a_{m1} & a_{m2} & a_{m3} & \cdots & a_{mm} \end{vmatrix}$$

by requiring that the difference between the experimental $K_{ip}$ and that predicted with eqn. 43 for every combination of $m$ standard solutes is minimal, *i.e.* according to the least-squares method:

$$_{ip}\sum\left\{\left[\exp\left(\sum_{n=1}^{m} a_{in}z_{pn}\right)-K_{ip}\right]\Big/K_{ip}\right\}^2=\text{minimum}$$

We tested this concept in an HPLC–FIA study where twenty solutes were analysed in seven phase–water systems, *viz.*, isooctane ($iC_8$)–W, toluene ($C_7H_8$)–W, 1-octene ($C_8H_{16}$)–W, octane ($C_8$)–W, heptane ($C_7$)–W, octadecane ($C_{18}$)–W and cyclohexane ($cC_6$)–W. Together with the tabulated octanol (*O*)–W data from Hansch [44,45], we have a set of $8 \times 20$ partition coefficients, some of which were checked by static shake-flask measurements. For a two-parameter characterization of the partitioning systems, eqn. 43 yields (on a decimal logarithm basis): $\log K_{1,p} = a_{11}z_{p1} + a_{12}z_{p2}$ and $\log K_{2,p} = a_{21}z_{p1} + a_{22}z_{p2}$, *i.e.*, we need to choose two standard systems. If we take rather arbitrarily $iC_8$–W and *O*–W as being characterized with coefficients $(z_{p1},z_{p2}) = (1,0)$ and (0,1), respectively, all coefficients for the solutes $a_{i1},a_{i2}$ are known as $a_{i1} = \log K_{i,iC_8}$ and $a_{i2} = \log K_{i,O}$. Multiple linear regression yields the best match coefficients for other phase systems, *e.g.*, ($C_7H_8$–W) = (0.70, 0.09), ($C_8H_{16}$–W) = (0.84, 0.13), ($C_8$–W) = 1.01, 0.01) and ($cC_6$–W) = (1.35, 0.44). Not surprisingly, it becomes clear that isooctane and *n*-octane are very much alike.

This result is now to be used to predict partition coefficients in any of the characterized phase systems for all solutes included. For instance, in $C_8H_{16}$–W we expect $\log K_{i,C_8H_{16}} = 0.84a_{i1} + 0.13a_{i2}$, and find that these predicted values deviate by ±0.08 units from the experimental results, *i.e.*, a 12% error in *K* is obtained. The same applies for the $C_8$–W system but for the $C_7H_8$–W system the deviation increases to ±0.15 units, *i.e.*, 40% in K. The latter is obviously caused by the fact that two parameters are not adequate to cover all types of interaction, *e.g.*, in the case of $C_7H_8$–W the aromatic properties are not well described by the choice of two non-aromatic standard systems.

We found that for $m = 3$ and including aromaticity in one of the standard compounds the error to reproduce the experimental *K* values was reduced to 10%, or ±0.04 units. *De facto* a fourth main coefficient is expected to reduce the error further, but currently too few data are available to verify this.

## 5. THEORIES FOR GRAFTED LAYERS

In the foregoing we observed that the ESP model is well able to characterize partitioning phase systems, but only for simple molecules that lend themselves to treatment via an EOS. For other cases, which include the grafted phases in use for RPLC, characterization is only possible in a relative way (with respect to arbitrarily chosen standard systems or standard solutes).

Theories specifically designed for *a priori* predictions and absolute characterization of grafted layers were reviewed by Dorsey and Dill [11]. In older views the grafted chains are seen as closely packed rigid rods, or slightly better, as "furry" (or "bristle, stacked, brush" type) rod-like chains. They overestimate the ordering of the alkyl chains and do not treat the solvent penetration in the grafted layer adequately. These oversimplified rod-like chain models, which do not agree with experimental findings, can serve qualitative purposes at best, the more so as there is experimental evidence that grafted alkyl chains are flexible [93,94].

In the last decade several lattice theories, based on extensions of the Flory–Huggins lattice theory for polymers in solution [37] have been applied to the RPLC retention mechanism. These theories do take some aspects of the molecular organization in the grafted layer into account. Martire and Boehm [17,18], in an extension of a mean field statistical thermodynamic adsorption theory for liquid adsorption chromatography, allowed for chain flexibility, but assumed a uniform composition and density in the grafted layer, resembling the case of a liquid crystalline phase organization. In their theory the first segment of the grafted chain is fixed to the solid surface, while the last segment is fixed in the layer adjacent to the mobile phase. Also, to evaluate the configurational free energy contribution, they allow chain segments to be oriented independently in all directions, not preventing backtracking of one segment upon its predecessor, and do not take into account variation of chain density with distance from the

surface. Hence here again the ordering in the stationary phase is substantially overestimated. However, the Martire–Boehm theory qualitatively describes several effects much better than rod-like models. Martire and Boehm also found a strong correlation between liquid–liquid partitioning and retention in RPLC.

Dill and co-workers [8–12] described the grafted layer as small flexible chain molecules in different conformations, forming a layer of constant density. Unlike Martire and Boehm, their description of chain conformations is more detailed (they correctly preclude backfolding of segments in a chain), but they do not include the interaction between grafted chains and solvent, while assuming that solvent is absent in the grafted layer. Artificially, they treat adsorption separately from partitioning by assuming a planar interface between chain phase and mobile phase, thus allowing solute molecules to have interface surface contacts only, not being embedded in the chain phase. However, Dill and coworkers also found a strong correlation between liquid–liquid partitioning and RPLC retention.

### 5.1. *Introduction to conformational aspects of chain molecules*

The physics dealing with the size and shape of polymer molecules has undergone a tremendous development, and we refer to the pertinent literature for reviews [23,37,95–105], including some particularly recommendable accounts [95,97,98,100,104,105]. The essential feature of a polymeric chain molecule is its connectivity. The simplest possible model of a macromolecule is a linear long sequence of $(M/M_0)$ monomer segments of molecular mass $M_0$ each. Because of the rotational freedom of the chemical bonds between the monomer units, the chain can assume a huge number of different spatial arrangements and the "shape" of the whole chain-like structure is continuously changing. The final shape of the macromolecule is a statistically weighted average of the shapes of these conformations. A picture often used to represent such a real chain is that of the "freely jointed equivalent chain" (according to Kuhn), consisting of a sequence of identical and rigid segments, with bond angles that can assume any value. The length of a segment ($a$) and the number of segments ($N$) are adjusted so as to mimic the length ($L = Na$) and flexibility of the real chain, *i.e.*, with increasing flexibility of the real chain $N$ increases and $a$ decreases. Typically each segment represents two to five (maximally nine) monomer units.

As each segment has a characteristic length ($a$) and a (bond) direction, a convenient and simple idealization of flexible polymer chains is found in simulating it by a random walk, consisting of $N$ steps of length $a$, starting at the origin (the first segment of the chain) and reaching out ("diffuse" or random fly away) to an arbitrary endpoint, where the last segment of the chain is supposedly located. The analogy between the two processes (diffusion and the formation of a random coil) is obvious, if we imagine that a diffusing particle leaves a trace of its movements in time: a perfect picture of a random coil chain emerges, with the associated density distribution of segments being Gaussian. From this the average (mean square) distance $\langle r^2 \rangle$ is obtained as $\langle r^2 \rangle = Na^2$. The quantity $\langle r^2 \rangle$ has a prominent status among polymer properties, being related to experimental characteristics such as viscosity, diffusion, sedimentation and light scattering. Of course, the average end-to-end distance $l$ is now obtained as the root of the mean square end-to-end distance: $l = \langle r^2 \rangle^{1/2}$.

Volkenstein [101] proved mathematically that the mean-square end-to-end distance ($Na^2$), on average, is the largest square distance between any pair of segments in the chain, and represents as such a good parameter for the characterization of the "length" of the chain. The fact that $\langle r^2 \rangle = Na^2$ is a factor $1/N$ smaller than the squared stretched chain length $(Na)^2$ indicates that for not too small a number of segments $N$, the chain is strongly coiled. We recall that $l = \langle r^2 \rangle^{1/2}$ and stress the fact that this is not identical with the (linear) mean end-to-end distance $\langle r \rangle$. The most probable end-to-end separation of this spring-like chain can be envisaged to result from the tendency of the chain ends to equilibrate between two opposing actions, *i.e.*, either to diffuse away from one another by the three-dimensional (thermal motion) random walk or to

contract according to an entropic spring force. The latter is readily found from using the perception of macromolecular chains being modelled according to Hookean springs. Later this spring-like picture, also used in polymer kinetics literature [106,107], will be of use in the discussion of stretching of grafted chains.

However valuable this idealized model is, its intrinsic artificiality is very clear: an obvious difference between a diffusing particle and a polymeric chain is that the particle is free to cross its own path, while the chain is not capable of self-intersection, *i.e.*, segments are not allowed to occupy the same space at the same time (so-called long-range interactions). Also, when two segments are in close contact, (short-range) interactions (attraction or repulsion) may occur. For the description of volume exclusion of polymer chains, we shall follow the early and comparatively simple approach of Flory [37,96,100], which yields very good results. This expansion due to excluded volume effects makes itself apparent through experiments, *e.g.*, viscosity measurements [108]. On this we base the notion of the *Flory radius*, $R_F = aN^{3/5}$, also used by De Gennes and co-workers in their successful scaling theory [23,24,109–113], to represent a realistic polymer size parameter. We recall that in good solvents the polymer coils are swollen and contract with diminishing solvent quality. For instance, in a $\theta$ solvent the radius of free linear chains is $aN^{1/2}$, whereas in poor solvents the chains further collapse strongly (via a phase transition) and result in a radius of $aN^{1/3}$ [23,37,97,113].

We recently reviewed the case of chain molecules near a solid surface and in pore spaces [105] for application in size separation chromatography [*i.e.*, in size-exclusion (SEC) and hydrodynamic chromatography (HDC)]. Using the theory of De Gennes and co-workers [23,109–111], it is possible to picture a confined and wriggling chain in a pore as a train of contacting segments or "blobs" forming a pearl necklace. Successive blobs act as hard spheres, which on the scale of the pore size are each allowed to behave as in the unrestricted free solution, *i.e.*, the blobs show a knotted and partially swollen structure as described by the Flory statistics as in free solution. Thus the chain is represented by a succession of $N_b$ blobs of $g$ segments each and size $D_b = 2R_c = 2R_p$. Particle (= blob) size equals the channel size as the chain is being squeezed into the pore confinement. In view of the supposed analogy with the Flory case, we have that each blob shows the same relationship between size and number of segments as in free solution. Hence $D_b$ takes over the role of $R_F$ (omitting numerical factors such as 2, as is customary in De Gennes' scaling theory), and $g$ the role of $N$.

### 5.2. Conformations of grafted chains

For the present discussion, terminally attached grafted chains (if closely packed also called polymer brushes) are of interest. It is not unexpected that the size of polymers attached to interfaces shows a similar behaviour towards changing solvent quality to the behaviour of free coils, *viz.*, a collapse of chains is predicted as the solvent quality diminishes, although the differences in configuration between grafted chains and those in free solution will lead to corresponding differences in collapse behaviour.

De Gennes [24], using scaling theory, obtained a semi-quantitative insight in the conformation of these terminally grafted chains on a solid surface, clearly discriminating between cases of different surface coverage, ranging from separated chains to closely packed brushes. In the case of low coverage, such that coiling of the chains can take place in an unobstructed way (except for the presence of the solid surface), each coil can be envisaged to occupy roughly a half-sphere with a radius comparable to the Flory radius for that coil in a good solvent: the "mushroom" regime [113, 114]. Owing to the lack of interactions between coils, the chains behave essentially as free chains in this instance, also with respect to collapse behaviour with diminishing solvent quality: strong collapse occurs in this low grafting density regime.

For example, Auroy *et al.* [114] recently proved experimentally that in good solvents at wide spacing of chains, hemispherical or at least swollen juxtaposed spherical cuts are formed, extending clearly away from the silica surface. In poor solvents, however, very thin films are

formed, spreading flatly on the surface, which are strongly collapsed coils. However, as there are no interactions, no phase changes can occur.

### 5.3. Introduction of the lattice for grafted layers

Introducing a cubic surface lattice with grid size $a$, corresponding to the segment size of the chain molecule, allows an estimation of the conditions needed to obtain these separate coils at the surface: for touching coils which occupy an area of about $R_F^2$ each (omitting numerical factors such as $\pi/4$) the maximum number of chains that can be grafted in the lattice equals the lattice area divided by $R_F^2$, from which we obtain the maximum separated chains fraction $\sigma_{sep}$ of grafted chains as $\sigma_{sep} \approx N^{-6/5}$. For all cases $\sigma < \sigma_{sep}$ and for a random distribution of grafting points it is illustrative to obtain the average chain segment concentration distribution perpendicular to the solid surface, *i.e.*, in the $z$-direction, in the cubic lattice also in units of $a$. In such a lattice the concentration distribution $c(z)$ equals the volume fraction distribution $\varphi(z)$ and so in the lower limit of $z \approx a$ (*i.e.*, in the first layer above the surface) we expect the fraction of grafted volume elements to be $\sigma$, so $\varphi(a) = \sigma$. On the other hand, collecting all segments of all grafted chains in the layers up to $z \approx R_F$, where each chain contains an average chain concentration of $N/R_F^3$, the overall volume fraction is estimated to be $\varphi(R_F) \approx N(R_F^2/R_F^3) = N/R_F = \sigma N^{2/5}$. Interpolating between the two limiting cases with the power fit function $\varphi(z) = \sigma(z/a)^m$, as is customary in scaling theory, it is seen that the unknown exponent $m$ should equal 2/3 in order to match the condition for $\varphi(R_F)$.

This result illustrates that the grafted chain density profile perpendicular to the solid surface is far from constant, starting at $\varphi \approx \sigma$ at the surface layer, going through a maximum ($\approx \sigma N^{2/5}$) at $z \approx R_F$ and then dropping rapidly for distances $> R_F$ from the surface. However, the behaviour is essentially that of free coils, including the strong collapse behaviour. Later we shall refine this semi-quantitative result in a more sophisticated lattice model, but at present we shall proceed with the qualitative treatment of the more practical situation that the grafting density fraction $\sigma$ becomes higher than $\sigma_{sep} \approx N^{-6/5}$, which occurs for separation distances between chains $< R_F$. Coils of the grafted chains tend to overlap in this case and stretch away from the grafting surface to avoid a high segment density.

### 5.4. Grafted layer thickness

The brush height $h$ in the strongly stretched chain phase is (for large enough $N$) readily $\gg R_F$, which can be shown again with simple arguments. Consider a square surface area $A$ consisting of $N_{sites}$ surface elements, which contains $n_{chains}$ attached chains at average distances $D$ from each other. The grafting density $\sigma$ is by definition $n_{chains}/N_{sites}$ and so $\sigma = (A/D^2)/(A/a^2) = (a/D)^2$. By analogy with the case of confined polymer chains, a grafted chain may be envisaged as being subdivided into a string of "blobs", each of size $D$ and each containing $g_D$ monomers, such that $g_D = (D/a)^{5/3}$ by analogy with $N = (R_F/a)^{5/3}$. As $D = a g_D^{3/5}$, we can picture the grafted chain as a cylindrical entity ("cigar") with an effective total length $\mathcal{L}_D = (N/g_D)D = aN(a/D)^{2/3} = aN\sigma^{1/3}$. As $D \ll R_F$ in the overlapping chains regime, $g_D \ll N$ and $\mathcal{L}_D \gg R_F$, *i.e.*, the chains are strongly stretched, mainly perpendicular to the solid surface, such that the "blobs" which act as hard spheres are densely packed into cylindrical "cigars" with volume $\mathcal{L}D^2$. The brush height $h$ equals $\mathcal{L}_D = aN\sigma^{1/3}$, which shows that brush height is proportional to the molecular mass of the grafted chains. It should be stressed that, although the chain consists mainly of a linear string of "blobs" along the normal to the solid surface, there is a certain spread parallel to the wall plane, as neighbouring "blobs" from nearby chains strongly interact (which is why stretching occurs in the first place) and are potentially able to enter, at random, the cylindrical volume of each individual chain.

Summarizing the above, we find depending on the grafted density two extreme regions, one unstretched (for small $\sigma$) and one stretched. It is predicted that the segment density profile in both instances near the wall is depleted [$\varphi(a) = \sigma$],

follows a 2/3 power relation with $z$ in the region $a < z < D$, and for $z > D$ in the case of moderate grafting density the concentration reaches a nearly constant value ($\varphi = g_D a^3/D^3 = \sigma^{2/3}$) up to $z = \mathcal{L}_D$, whereas for $z > \mathcal{L}_D$ the concentration drops off abruptly (as in the case discussed for non-overlapping chains).

The above picture is approximate only and gives a qualitative insight into the behaviour of attached chain phases in the case of good-solvent Flory-type chain statistics. Halperin [113] and Auroy *et al.* [115] have extended the line of reasoning to poor solvents, in which event it appears that the brush height is proportional to $N\sigma$ rather than to $N\sigma^{1/3}$ as in good solvents, experimentally confirmed by SANS experiments [116]. In both instances the layer thickness appears to be a linear function of the molecular mass of the chain, the signature of chain grafting in the brush regime, where lateral interchain interactions tend to stretch the polymer into the solvent phase, irrespective of solvent quality. The latter is indicated by the variation of the layer thickness with the grafting density to the power 1/3, rather than linearly as in a good solvent, whilst repulsive monomer–monomer interactions result in a less dense interfacial layer than in a poor solvent.

The general picture which arises from these (scaling) laws is that the grafted layer is to be seen as a close packing of segments (monomers), while the density or volume fraction of the monomers $\varphi$ inside the layer is fixed by the solvent–polymer interactions. For poor solvents $\varphi$ ranges from *ca.* 0.9 to 0.6, *i.e.*, almost no or little solvent is present and $\varphi$ is roughly equal to the mean volume fraction, which points to a more or less step-function-like behaviour of $\varphi(z)$. Although the chains are collapsed, the resulting layer thickness still increases linearly with increasing molecular mass, *i.e.*, the chains tend to be stretched and are certainly anisotropic in configuration, as predicted by Halperin [113]. This "weak" collapse behaviour contrasts very much with the strong collapse behaviour of free coils and widely spaced sparsely attached chains: although the layer contracts with diminishing solvent quality, the chains remain stretched *i.e.*, $h \approx Na$, even for poor solvents.

In good solvents, on the other hand, it appears that the average volume fraction of monomers drops to *ca.* 0.2 (almost equal to the concentration of the original grafting solution), indicating the presence of much solvent, while the density profile is smoother than a step function, and a parabolic profile would fit the observations better, as has been suggested from theoretical work (Milner *et al.* [32], see later). However, the observed "blob" size is very close to the average distance between grafting sites, offering at least qualitative support to the De Gennes scaling theory.

The insight it offers into the behaviour of grafted layers as used in RPLC is of importance from two points of view: (i) the structure of the layer as a function of solvent quality (mixed solvents, preferential solvation) and (ii) the concentration profiles of both chain segments and solvents towards the solid surface, which largely determine the penetration of solute molecules to be separated.

With regard to the layer structure (i), Auroy and Auvray [116], using SANS experiments, obtained layer thicknesses of grafted polydimethylsiloxanes (PDMS, $M = 166\,500$) on porous silica in mixtures of methanol (MeOH, poor solvent) and dichloromethane (DCM, good solvent). As already naively expected, effects of the preferential solvation of one of the solvent components, DCM, to the PDMS layer occur. Almost pure DCM is trapped preferentially near the solid surface rather than near the solvent interface, a view that is supported to some extent by Monte–Carlo calculations [117].

Unique and very interesting are the experiments reported by Auroy and Auvray [116] in which they brought about the same collapse effects not with the chemical composition of a binary mixture of solvents but with temperature. Using styrene, which is a $\theta$ solvent for PDMS at about 30°C, it appears that all the features are the same, but the total change in layer thickness (which is now linear in $T$) requires a broad temperature range of more than 80°C. Although it is far simpler to change the stretching behaviour of the grafted layer by a relatively small composition change of solvent systems, both temperature and the composition effects are

shown to be of importance, also in connection with RPLC.

### 5.5. Introduction of potential energy fields

Although the present line of thought based on scaling theories has been further extended towards the conditions more appropriate for RPLC, including the presence of free solute chain molecules, which partition between chain phase and solvent phase, it is again stressed that the approach is necessarily approximate only. More recent work, based on more precise self-consistent-field (SCF) methods [20,32–34,118, 119], has shown that the simplified energy-balance or scaling (blob) arguments miss several important features of the brush, which has so far been suggested to consist of a mainly homogeneous layer of considerably stretched overlapping chains with a nearly constant concentration of segments, and only at the peripheries of the layer are rapid changes in concentrations predicted.

A major point of criticism to this simple picture is that chains do not have to behave alike: the conformations of different chains in the brush are not necessarily similar, chains are not uniformly stressed, and the free ends of the chains are not required to lie at the extreme front edge of the brush, as is tacitly assumed in the De Gennes' theory [23,24,120]. Thus, the density profile is not necessarily a step function, and SCF calculations where no *a priori* assumption is made on the monomer density profile indeed show that a density profile is parabolic, going continuously to zero at the outer extremity of the brush [20,32,119]. This is largely confirmed by molecular dynamics [121] and Monte Carlo simulations [21]. Even more convincing is the mathematical proof by Klushin and Skvortsov [122] that in order to obtain stretched chains at all, the density should decrease with the distance $z$ from the grafting plane *a priori*. Milner *et al.* [32] proved also that the Alexander–De Gennes ansatz of a step function profile is unstable.

As many gross features of brushes are somewhat insensitive to the details of the parabolic structure, this non-uniform stretching of chains from the grafting surface towards the brush's extremity has been a useful working hypothesis for a long time; for example, the mean brush height, being defined by the first statistical moment of the monomer density, is qualitatively well described by the step function ansatz. However, properties that depend in detail on the monomer density in the outer fringe of the brush are expected to be sensitive to a non-abrupt decrease in monomer density at the brush–solvent interfacial region. Properties belonging to this class are compression forces required to compress the brush, hydrodynamic penetration of shear flow alongside a brush and non-uniform partitioning of solutes between solvent and brush phases. The latter two aspects are of importance to the chromatographic processes we intend to describe, which is why the parabolic deviation from the step function ansatz in monomer density is necessarily to be discussed in the following. Before going into that, we shall attempt to clarify the situation by way of elementary reasoning. To this end we refer to the previously introduced simple picture of a chain molecule as a Hookean spring, with (entropy-based) force $\mathcal{F}_S = Hz$ ($H$ = force constant), and in unperturbed conditions the resulting mean-square end-to-end distance equals is $\langle r^2 \rangle_{\text{spring}} = 3kT/H$. In the present case of stretched and terminally attached chains, it is obvious that stretching the spring-like chains perpendicular to the grafted surface requires some counterforce equal to $\mathcal{F}_S$ but opposite in sign to be provided by interactions between segments in the brush phase itself.

The criterion for the thermodynamic equilibrium being reached in any system is that the chemical potential be constant throughout the system, so that $d\mu^* = 0$, where $\mu^*$ is the overall chemical potential, consisting of the classical chemical potential $\mu$ and the external field potential $\mu^{\text{ext}}$: $\mu^* = \mu + \mu^{\text{ext}}$; *cf.* Guggenheim [123]. Here $\mu = \mu^\theta + kT \ln c$, which describes intermolecular interactions including entropic contributions and enthalpic contributions from attractive forces such as dispersion, orientation, induction and hydrogen bonding; $c$ is a relevant concentration, which is interpreted as the segment density in the present case of chain mole-

cules; $\mu^{ext}$, on the other hand, includes potential energy to the system from external fields such as electrical and magnetic fields, temperature and composition gradients, and is treated identically with the classical (internal) potential $\mu$ (for a discussion on this, see Giddings [124]). In the present case of spring-like chain molecules, $\mu^{ext}$ may be equated with the potential energy associated with the spring force field, *i.e.*, $\mu^{ext} = U_{spring}$, where the latter is known by virtue of the general relationship between potential energy and driving force in potential theory: $\mathcal{F} = -dU/dz$ (in the one-dimensional case). Thus $F + \mathcal{F}_S = 0$, *i.e.* $-d\mu/dz + Hz = 0$ and so $-kT\, d(\ln c)/dz + Hz = 0$, from which the density profile follows as being exponential, and in a first approximation for small $z$ parabolic in nature $c = C \exp[-Hz^2/2kT] \approx C[1 - Hz^2/2kT]$, where $C$ is a constant equal to the grafted density at $z = 0$. Also, $c = C \exp[-U_{spring}/kT]$, which shows a Boltzmann density profile. This is not unexpected because if we employ the picture of the chain as being a random flight process diffusing away from the grafted anchoring point ($D = a^2/6\tau$) [105] while undergoing an external force or potential, we would have had to solve the steady-state diffusion equation, $-D[(dc/dz) + (c/kT)\, d(U_{ext})/dz] = 0$, whose solution is the Boltzmann distribution for $c(z)$ given above.

In the present light it is not surprising that in more quantitative analytical SCF approaches [32–34,125] both the density profile and the self-consistent potential fields are shown to be parabolic. This has been derived under the *a priori* assumption of strong stretching of the chains with respect to their Gaussian dimension. This assumption is not unrealistic in the moderate density (brush) regime, as discussed above in the work of De Gennes and co-workers, and allows the underlying SCF equations, basically of a diffusion type of equation, to be solved analytically. The self-consistent field theories, where neither the potential field nor the density distribution are known *a priori*, but which result from the requirement of self-consistency in obtaining minimum free energy of the system, *i.e.*, the potential generated by the segment distribution must in its turn generate that same distribution, can be divided into two large groups: mean-field lattice models and continuum space analogues.

The continuum approaches apply to very long chains and utilize the analogy between random walk statistics and diffusion. For example, a continuum analogue of the Scheutjens–Fleer theory has been proposed by Ploehn *et al.* [29], which allows an analytical solution for the concentration profile but, being based on an eigenfunction expansion using the dominating terms only, this result is necessarily less accurate than the Scheutjens–Fleer lattice theory (to be described later). This approach is appealing through its more realistic continuum character and analytical solutions, the prevailing physical picture of the background mechanisms and also the close relationship with other well known diffusion-type theories (Casassa [126–130], De Gennes [23], Doi and Edwards [131,132]). Drawbacks of this approach are the difficult tuning towards a variety of experimental conditions and the necessity of, albeit realistic, limiting *a priori* assumptions.

In lattice treatments, on the other hand, the random walk is constricted to a discretization of space, an artificial approximation that may not accurately reflect the reality of continuous physical space, especially near the solid surface, where details on a length scale comparable to the lattice segment dimensions may be lost. Further, model equations are written in finite difference form to facilitate the numerical treatment, which obscures the underlying physics. However, the easy adaptation to experimental conditions (*e.g.*, the explicit modelling on a segment level basis that allows shorter chains to be considered, of much importance to RPLC) and the absence of approximations (other than the lattice discretization and mean-field assumptions) make the latter approach more attractive for our purposes. Moreover, extensive comparisons between lattice model-based numerical results and analytical approaches [32,133] prove the reliability and exactness of the lattice theory approach.

## 6. SELF-CONSISTENT FIELD LATTICE THEORY

As stated above, the most realistic approach (because of the lack of simplifying assumptions

on segment density distributions) can be based on the self-consistent field theory for adsorption (SCFA) originally developed by Scheutjens and Fleer [25] to describe adsorption of (homo)polymers on solid surfaces. The original theory has been extended to many other cases over the last decade and a generalized treatment of the theory has been given recently by Evers *et al.* [26]. Cosgrove *et al.* [20], Böhmer *et al.* [16] and Wijmans *et al.* [133] treated the case of grafted polymer chains with one of the segments anchored to a solid surface, the case of particular interest in connection with RPLC.

In contrast to all other theories, the SCFA theory relaxes the constraint of a "block" (or any other pre-assumed) concentration profile of the grafted layer and allows inhomogeneity in the direction perpendicular to the solid surface. The equilibrium distribution of each type of segment [solvent (possibly multi-component), chain and solute] is found as the result of the minimization of the free energy of the system. The model is most universal in the sense that it provides a very detailed insight into the spatial distribution and conformation of chain molecules [linear and branched homopolymers and copolymers, including systems with various chain lengths (molecular mass distributions), functionalized molecules such as surfactants] in multi-component solvent systems. The SCFA theory does not make *a priori* assumptions about the conformations of the molecules, and the required physicochemical data for the parameters used are in principle subject to experimental measurement.

To account for interactions between the various segments and to establish the relative occurrence of different chain conformations, a convenient lattice is used. The set of possible configurations of chain molecules in the lattice comprises a representative sample of the very large number of spatial distributions in a real system. The lattice used may be either flat, cylindrical or spherical, depending on the type of problem (*e.g.*, for micellar association of amphiphilic chain molecules a spherical lattice is used [27,28]; in the present case of "sorption" at or in hairy layers, the sphericity of support particles is assumed to be unimportant (the layer thickness for chain lengths <30 Å is much smaller than the particle or pore size) and a flat lattice will be used.

The equilibrium distribution of each type of segment is found as the result of the self-consistent minimization of the free energy of the system, subject to the packing constraint that every lattice layer has to be filled completely with segments of either type: solvent, chain or solute (here we do not consider the potential presence of vacancies, although in principle they could be treated as one of the components). Within each layer crowding neighbour effects between interacting segments are treated with the Flory–Huggins (or Bragg–Williams) mean field theory [37].

In a previous paper [16] we extended the SCFA theory to allow for RPLC conditions, which imply mixtures of different types of molecules near a grafted layer. All components, including the grafted chains, are allowed to adjust their local segment density to local conditions. This is in contrast with Dill and co-workers' theory [8–11], where the segment density profile of the grafted chains is prefixed, and only the distribution of solute in the grafted layer is found from statistical thermodynamics. An additional advantage over Dill's model, where solute and solvent are always monomeric, is that flexible oligomeric solutes (and solvents) are allowed, just as in the model of Martire and Boehm [17]. This allows us to study the retention of flexible chain molecules.

In the next section we shall give the principles of the SCFA theory, followed by a more detailed treatment of the present model and the derivation of an expression for the distribution coefficient and the capacity factor in terms of the SCFA theory. The effects of solvent quality, grafted chain length and surface coverage on the segment density profile and shape effects besides residual adsorption effects are considered. Segment density distributions for monomeric and oligomeric solutes retained at a grafted layer are given. The retention of monomeric and oligomeric solutes is studied as a function of solvent quality, grafted chain length, surface coverage, solute chain length and its composition. Also, a comparison will be made between solute distribution near a liquid–liquid interface and at a

grafted layer in contact with a liquid phase. As in the SCFA theory there is, in principle, no limit to the system composition with respect to the number of different molecules and their chain lengths, we consider in this paper not only monomeric solvents and linear, flexible, solutes, but also mixed and/or non-monomeric solvents and rod-like and branched solutes. The role of residual hydroxyls and associated specific affinity for the solid surface and the case of mixed solvents will also be treated.

### 6.1. General outline of SCFA theory

The theoretical models that describe the (average) configuration of (adsorbed) polymers can be grouped roughly into four categories: (i) single chain theories, (ii) scaling theories, (iii) (self-consistent) mean field theories and (iv) Monte Carlo simulations. The first group, being dedicated to the simple case of isolated chains only, are described in the earliest theories up to the work of Silberberg [134]. Scaling theories, using power law arguments [23], are known to be adequate for weakly overlapping long flexible chains in relatively dilute solutions in good solvents only. The application to block copolymer adsorption by De Gennes [24], resembling our case of terminally attached chains, pre-assigns the shape of the density profile of segments and thus becomes of limited validity (selective solvents and small range of chain compositions only) as compared with the third group of theories, the mean field theories. Although in this group many theories also use specific assumptions on the segment density profile near the grafted surface (*e.g.*, Martire and Boehm [17,18], Gast and Leibler [135], Dill and coworkers [8–12]), DiMarzio and Rubin [136] showed that these additional assumptions are not necessary. For the fourth group, the numerical Monte Carlo methods, Cosgrove *et al.* [20] proved for the case of terminally attached chains that the results are very similar to those obtained in the case of SCF calculations using the Scheutjens–Fleer approach.

This is strong support for the latter SCF method, and in view of the large difference in computational effort the SCF method is the preferred one. Scheutjens and Fleer in their SCFA theory combined the DiMarzio–Rubin concept with the Flory–Huggins mean field lattice theory [37], thereby extending the latter for polymers in solution to systems that are inhomogeneous in one direction, in particular perpendicular to a surface. In the SCFA theory the segmental interactions and the conformations of the molecules are interrelated in a self-consistent way: the distribution of molecules over various conformations depends on the local conditions that the segments experience as a result of all present chains in this particular distribution. Local conditions in this context are, for instance, interactions between the various components in the system such as the local magnitude of intersegmental/wall adsorptive forces or equivalently (as forces are negative gradients of potential energies) the local magnitude of a potential field. This picture of a segment density gradient perpendicular to and near a surface resulting from a potential field present is to some extent comparable to the Boltzmann concentration gradient of gases in our atmosphere which is exponential with height and settles itself as a result of the gravitational potential field perpendicular to the earth's surface. In the same way, every segment experiences a potential depending on the distance to the solid surface and also on the mutual distances between segments. As the segments "feel" each other through the potential field only, a concentration profile of segments results, adjusted to the potential field that the segments themselves partly create. The situation is also analogous to the case of an interacting ensemble of elementary particles that populate the available energy levels. To calculate the population density or the concentration profile if the potential field is known or *vice versa*, statistical mechanical rules (in the present case Boltzmann statistics) are applied.

As said, for convenience, the molecules are placed on a lattice to allow an easy count of molecular conformations. The lattice sites are grouped in layers parallel to the surface, here assumed to be flat, and each layer is completely filled. Each chain-like molecule that consists of a number of, say, $r$ segments fills the same number

of $r$ lattice sites. Usually, but not necessarily, the size of the solvent molecules is assumed to be identical with that of one segment. As is known, polymer molecules that consist of a sometimes large series of segments can have various conformations. For homopolymers, to some extent, the molecules can be described as a sequence of identical and rigid segments with bond angles that can assume almost any value. Typically, each segment represents 2 to *ca.* 5 monomer units. In equilibrium, the molecules are distributed over their various possible conformations in the lattice such that the free energy of the system is at its minimum and in each lattice layer potential and concentration for each type of segment or molecule are mutually consistent.

If we now adopt a mean field approximation within each lattice layer, *i.e.*, density and potential fluctuations within each layer are ignored and only gradients perpendicular to the surface are allowed, we reduce the immensely large number of possible conformations to a conveniently small number of relevant conformations. The only thing needed to characterize the (free) energy of a chain molecule in a certain conformation is the position of the segments in each layer, rather than the exact spatial position of each segment. Therefore, it is sufficient to specify how many segments of a chain molecule are situated in each layer and a (relevant) conformation in the lattice is defined as the sequence of layers in which the subsequent segments of a molecule find themselves [25,26]. Thus, in Fig. 1 the top molecule has the conformation 1–1–2–2–3–4–5–5.

Every segment experiences a potential, depending on the lattice layer the segment is in and the average segmental and solvent environment. The potential field is, of course, different for polymer segments, solvent and solute molecules, owing to the differences in interaction energies. In the lattice layer next to the surface, the potential also depends on the segment–surface interactions. Thus, the four terminally attached molecules depicted in Fig. 1, although having the same length (eight segments), all have different conformations and so different energy levels. The various possible conformations are not equally probable, however, and their frequency

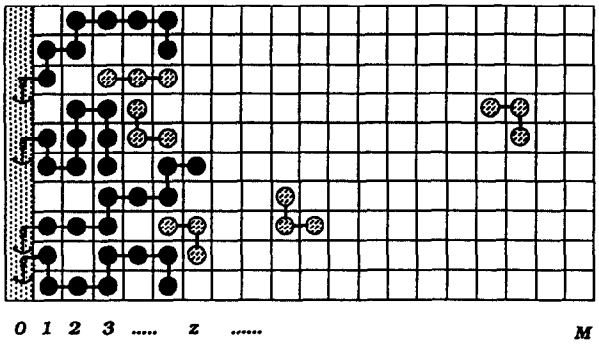


Fig. 1. Schematic two-dimensional representation of the lattice. Some grafted chains and solute molecules are indicated, the remaining lattice sites are filled with solvent. From ref. 16.

depends on the interaction energies, which in turn are a function of the local concentrations of segments. For instance, when a segment is placed in the lattice, a step into a region of high segment density is less probable.

From the potentials, the statistical weights of the segment positions are calculated, which in turn can then be used to calculate the statistical weights of chain conformations. The statistical weight of a chain in a particular conformation consists of two contributions: the chain connectivity and the statistical weights of the individual segments in this sequence of layers. As the potentials determine the local concentrations and the local concentrations in turn affect the potentials, a self-consistent potential field and the corresponding volume fraction profiles for the molecules can only be found iteratively. Thus, the SCFA method does not, in general, lead to analytical solutions but produces a set of equations that can be solved by numerical methods only. The resulting concentration profiles of all types of molecules in the system contain the set of conformations for every type of molecule which gives the lowest free energy of the system in equilibrium with the bulk solution.

Today many extensions of the original theory exist, the polymers that have been treated including grafted polymer chains [20,133], where one of the segments of a chain is anchored to a solid surface, and copolymers [26,27], where the segments in the chain may be of different types. A first-order Markov approximation is used in

the evaluation of chain statistics of polymers. A rotational isomeric state (RIS) scheme (a third-order Markov approximation) has been developed [28] to reduce chain flexibility and to distinguish *gauche* and *trans* conformations (see later). The RIS scheme is especially useful for small chain molecules.

Adsorption at liquid–liquid boundaries has also been studied with the SCFA theory [137]. For liquid–liquid systems the relationship between the Flory theory and the SCFA theory becomes especially clear. The partitioning of a solute over two homogeneous bulk phases follows from the Flory equations. In the SCFA theory the same concentration ratio is found in the homogeneous regions of the two liquid phases, which is far from the liquid–liquid interface. The additional contribution of the SCFA theory is that the structure of the liquid–liquid interface itself is also obtained. In this study we shall use the RIS scheme for grafted chains. This requires a straightforward modification of the original RIS scheme because of the fixed orientation of the first segment of the attached chain. Moreover, we have to formulate quantities measurable in chromatography in terms of the SCFA theory. As we shall also investigate the retention behaviour of amphiphilic molecules, the SCFA extension to copolymers [26,27] is used. Although phase transitions may occur in grafted layers of relatively long alkyl chains at high densities [138], we restrict ourselves in this paper to grafted layers well above the phase transition temperature. Gel to liquid phase transitions can be modelled if the self-consistent anisotropic field theory (SCAF) by Leermakers and Scheutjens [139] is employed. In RPLC, especially with monomeric bonded phases, the coverages are usually too low to generate a phase transition. The presence of vacancies can be investigated by treating them as another component [140,141], but in this work we do not incorporate this feature.

### 6.2. Segment density distribution of molecules on a lattice

The molecules in the system, in our case solvent, solute and grafted chains, are located in M planar lattice layers parallel to the surface. The layers are numbered $z = 1, \ldots, M$. Layer 1 is situated next to the solid, which fills layers $z \leq 0$ (see Fig. 1). Each lattice layer contains L lattice sites. A lattice site has $Z$ neighbouring sites (coordination number) of which a fraction $\lambda_0$ is in the same, $\lambda_{-1}$ is in the previous and $\lambda_1$ is in the next layer. In a hexagonal lattice, for example, $Z = 12$, $\lambda_0 = 6/12$ and $\lambda_1 = \lambda_{-1} = 3/12$, whereas in a cubic lattice $Z = 6$, $\lambda_0 = 4/6$ and $\lambda_1 = \lambda_{-1} = 1/6$.

A monomer is assumed to occupy one lattice site and the type of molecule is denoted by the subscript $i$. A chain molecule, which may consist of different segment types, denoted by the subscripts $x$ and $y$ totalling $r_i$ segments, numbered $s_i = 1, \ldots, r_i$, thus fills $r_i$ lattice sites. In each layer the concentrations of the different segment types are expressed in terms of volume fractions ($\varphi$). We ignore inhomogeneities within a lattice layer and consider only variations in concentration perpendicular to the surface. The volume fraction in layer $z$ of segments $x$ that belong to molecules $i$ is given by $\varphi_{xi}(z)$, molecules of type $i$ having a volume fraction $\varphi_i(z)$ in layer $z$ and the total volume fraction of segments of type $x$ in layer $z$ is being denoted as $\varphi_x(z)$.

In filling the lattice with segments or molecules, a most important requirement during the generation of conformations of chains, is that the volume of the segments be incorporated such that each lattice site is not occupied by more than one segment at a time: all steps into a lattice site already occupied by a segment have to be prohibited. An approximate but effective solution to this problem is the use of a mean field approach, *i.e.*, a volume fraction averaging procedure. The assumption is made then that the probability of an occupied site at distance $z$ from the surface is equal to the average volume fraction $\varphi(z)$ of segments at location $z$. This leads to a weighting factor $[1 - \varphi(z)]$ for each step in or towards layer $z$. Thus a step into a region of high segment density is less probable and the generation of conformations is shifted towards the required self-avoiding walks.

In a mixture of different types of molecules near a surface a concentration gradient for every type of segment is present, as each segment of

type $x$ in layer $z$ is subjected to a potential field $u_x(z)$, where $u_x$ is a function of $z$ only based on the mean field approximation, and not dependent on the exact mutual positions of molecules and segments. An expression for the potential, which can have entropic and energetic origins, *i.e.*, a free energy, normalized with respect to the bulk solution, can be derived from statistical thermodynamics [26], but before going into that we shall illustrate the basic procedure with a simple example.

We assume first that the lattice layers parallel with the solid wall are equipotential planes for the segments. For the reference we take the potential far away from the solid wall, *i.e.*, in the bulk solution, to be zero. On adopting common Boltzmann statistics, segments and molecules will distribute themselves in the $z$ direction according to the potential field $u_x(z)$ and following a Boltzmann distribution. The weighting factor $G_x(z) = \exp[-u_x(z)/kT]$ is a measure of the probability of finding a segment $x$ at position $z$ in the potential field $u_x(z)$. For example, in the bulk, where $u(z \rightarrow \infty) = u^b = 0$, and so $G^b = 1$, there is no concentration gradient, as expected.

In each lattice layer we find for each segment or molecular type a potential and a concentration that are consistent with each other, but as indicated before, the potential field is not identical for different types of segments or solvent molecules because of the differences in energetic interactions. The "energy level" of a molecule equals the sum of the potentials of all its segments, where in general each segment may "feel" a different potential. As a result, each spatial conformation of a molecule may possess a different level of energy, and is consequently more probable or less probable. For example, taking the case of a chain of three segments, of which the first and second are in layer 1, and the third is in layer 2, its conformation being (1,1,2), has an energy level of $u(1,1,2) = 2u(1) + u(2)$, and associated Boltzmann weighting factor $\exp[-u(1,1,2)/kT] = G(1)G(1)G(2)$.

As the chain molecule in the given conformation may be present in many internal configurations, the conformation is degenerated. For instance, in a polymer melt, polymer chains form coil-like structures, based on the number of allowed bond angles, say $\zeta$. For an $r$-mer then, there are $\zeta^{r-1}$ different conformations which are equally probable in the bulk: each conformation has a normalized concentration of $\omega_{conf} = 1/\zeta^{r-1}$. In terms of the present lattice model where bonds allowed are either parallel or perpendicular, an $r$-mer has $Z^{r-1}$ possible arrangements for its segments, *i.e.*, for our trimer $Z^2$. In boundary layers, where chains are deformed by adsorption, grafting, etc., some conformations are more preferred than others. In a lattice model, where each site has $Z$ nearest neighbouring sites, the fractions $\lambda_0$ and $\lambda_1 = \lambda_{-1}$ define the number of neighbours in the same and in the two nearest layers, respectively, such that $\lambda_0 + \lambda_1 + \lambda_{-1} = \lambda_0 + 2\lambda_1 = 1$. Thus, stepping from the first segment of our trimer in layer 1, towards segment 2 in the same layer (parallel bond), is possible only through a fraction $\lambda_0$ of all $Z$ neighbouring directions, while the next step (perpendicular) towards the second layer is possible through a fraction of $\lambda_1$ of all directions $Z$. In all, only a fraction of $\lambda_0\lambda_1$ of all possible internal configurations ($Z^2$) belongs to the specific conformation (1,1,2). The associated statistical weight of this conformation now reads $G(1,1,2) = \lambda_0\lambda_1 \exp[-u(1,1,2)/kT] = \lambda_0\lambda_1 G(1)G(1)G(2)$. As a result, we need to specify the segment weighting factors as a function of the layer number (and not the ranking number in the chain), in combination with the bond weight factors $\lambda_0$ and $\lambda_1$, to obtain the statistical weight (relative concentration) of each conformation via a step-weighted walk over the lattice layers. In general, for an $r$-mer in conformation c, with $r^c(z)$ being the number of segments in layer $z$ and $\omega^c$ being the degeneracy:

$$\omega^c = (\lambda_0)^{q^c}(\lambda_1)^{r^c - 1 - q^c}$$

where $q^c$ is the number of parallel bonds in conformation c, we have that the statistical weight of conformation c is

$$G^c = \omega^c \prod_z G(z)^{r^c(z)} \tag{44}$$

with obviously $\Sigma\, r^c(z) = r$. The fraction of segments of conformation c in layer $z$ is thus $f^c(z) = r^c(z)/r$ [for our trimer $f^{1,1,2}(1) = 2/3$ and

$f^{1,1,2}(2) = 1/3$]. From this it is now possible to obtain the sought volume fraction segment profile as

$$\varphi(z) = \sum_{c} G^{c} = f^{c}(z)\omega^{c} \prod_{z} G(z)^{r^{c}(z)} \qquad (45)$$

For each layer (*i.e.*, any $z$) it is required that $\varphi(z) = 1$ (for one component) or ${}_{i}\Sigma\, \varphi_i(z) = 1$ (multi-component). Through an iterative numerical procedure and for this set of simultaneous equations, it can be found that only one combination of weight factors matches the requirement of unit density in each layer, all this provided that $G(z)$, and so the potential $u(z)$, are known. Hence the above procedure reflects the complete entropic behaviour of a chain molecule near a solid wall, including conformational and translational contributions. Of course, in the present case of grafted chains, polymer chains cannot adopt any possible conformation, but are restricted by the surface condition that the first segment must be in the first layer. Also, translational entropy is necessarily absent for attached chains. We shall return to this, but first we continue to discuss other general aspects of interest, including the background of the potential function $u(z)$ in the light of the Flory–Huggins theory.

### 6.3. *Multi-component systems*

In the multi-component case it is possible to treat a solvent molecule ($s$) as a monomer (polymer with one segment and $r = 1$). We then have $\varphi_s(z) + \varphi_p(z) = 1$, and $\varphi_s(z) = \omega_s(1) \exp[-\Delta u_s(z)]$; because in the bulk $\exp[-\Delta u_s(z)] = \exp[-u_s(z)] = 1$, $\omega_s(1)$ represents the volume fraction of $s$ in the bulk solution. Recall that $G(z)$ is the determining function for the volume fraction profile with respect to the bulk fraction: detached and monomeric segments would have their distribution given by $\varphi_i(z) = \varphi_i^{b} G(z)$. The procedure now covers the segment density profile generated by conformational entropic contributions of both the chain polymer and the solvent, but for the latter also the translational and configurational entropic contributions.

As in the above the treatment applies to athermal solutions only, *i.e.*, for cases where the energy of a segment does not depend on the local concentration of other segments, we should take into account the case of a non-zero mixing energy, $u^{mix}$, where energetic interactions between segments take place. Then, in addition to the Boltzmann factor as obtained above, in each layer the ratio of weighting factors for segments $s$ and $p$ should equal the Boltzmann factor $\exp\{-[u_s(z) - u_p(z)]/kT\}$, which takes into account the energy differences of segments $s$ and $p$ in each layer with respect to the bulk solution. This energy difference can be a difference in interaction energy with the solid wall (adsorption or bonding in layer 1), or a difference in mutual interactions, which can be described for example by a Flory–Huggins parameter. Thus, in the latter case the Boltzmann factor occurs because most compounds feel at home best in their own company. In fact, a polymer segment competes with a solvent molecule for a lattice site, where according to FH the additional interaction energy for a polymer segment, when transferred from pure polymer ($\varphi_s = 0$) to pure solvent ($\varphi_s = 1$), equals $\chi_{ps}kT$, identical with the energy for pure solvent being transferred to pure polymer: $\chi_{ps} = \chi_{sp}$ (by definition $\chi_{xx} = 0$). In this process $Z$ $p$–$s$ contacts are formed and $\frac{1}{2}Z$ $p$–$p$ contacts and $\frac{1}{2}Z$ $s$–$s$ contacts are broken. In general, transfer of one segment $p$ from a position $z_1$ to $z_2$, with associated solvent volume fractions $\varphi_s(z)$, is associated with an energy change of $\chi_{ps}[\varphi_s(z_1) - \varphi_s(z_2)]kT$ and, by analogy, for one solvent molecule, $\chi_{ps}[\varphi_p(z_1) - \varphi_p(z_2)]kT$.

In the present case where segments are transferred between layer $z$ and the bulk solution, the mixing energy for segment $p$ would be $\chi_{ps}[\varphi_s(z) - \varphi_s^{b}]kT$, but because of the concentration gradient we have to consider the segment contacts with the nearest $Z$ neighbours in three lattice layers together: a fraction $\lambda_0$ in layer $z$, and fractions $\lambda_1 = \lambda_{-1}$ in layers $z + 1$ and $z - 1$, respectively. This results in the following interaction energies of the segments:

$$u_p^{mix}(z) = \chi_{ps}[\langle\varphi_s(z)\rangle - \varphi_s^{b}]kT;$$
$$u_s^{mix}(z) = \chi_{ps}[\langle\varphi_p(z)\rangle - \varphi_p^{b}]kT \qquad (46)$$

where $\langle\varphi_i(z)\rangle$ is the average contact fraction of segments around a site at $z$:

$$\langle\varphi_i(z)\rangle = \lambda_{-1}\varphi_i(z-1) + \lambda_0\varphi_i(z) + \lambda_1\varphi_i(z+1) \tag{47}$$

In this way, using the described mean-field approximation, all interactions in a layer are smeared out and the sought segment density profiles are a function of $z$ only. Recall that in the bulk solution the additional interaction energy equals zero as $\langle\varphi_i(z)\rangle = \varphi_i(z) = \varphi_i^b$.

The expressions for $u^{mix}(z)$ in the case of chain molecules consisting of more than one type of segment, say $x$ and $y$, are easily generalized as

$$u_x^{mix}(z) = {}_y\sum \chi_{xy}[\langle\varphi_y(z)\rangle - \varphi_y^b]kT \tag{48}$$

where the summation extends over all segment types $x, y, \ldots$ . Segment type $x$ itself may also be included because by definition $\chi_{xx} = 0$. Although only valid for layers $z > 1$ (because of the assumed mean-field averaging), interactions with the solid wall, located in layer $z = 0$ with segment type S, can also be included. This can be seen illustrated most clearly for a more "soft" adsorptive interaction with the wall with adsorption energy per segment $u_p^{ads}$. As the contact with the surface involves $(\lambda_1 Z)$ $p$–S contacts, the energy involved is $u_p^{ads} = \lambda_1\chi_{pS}kT$. In general, a segment $x$ in the first layer, being also in contact with surface sites S, experiences the total interaction potential:

$$u_x^{int}(1) = u_x^{ads}(1) + u_x^{mix}(1) = \lambda_1\chi_{xS}kT + {}_y\sum \chi_{xy}[\langle\varphi_y(1)\rangle - \varphi_y^b]kT \tag{49}$$

If we now take the step to consider S as a separate component of the system, with $\varphi_S(0) = 1$ and $\varphi_S(z > 0) = \varphi_S^b = 0$, it is seen that the adsorption term in eqn. 49 can be written as $u_x^{ads}(z) = \chi_{xS}[\langle\varphi_S(z)\rangle - \varphi_S^b]kT$, and it can be included in the summation for $u_x^{mix}(z)$ to obtain the total interaction potential for all $z$:

$$u_x^{int}(z) = {}_y\sum \chi_{xy}[\langle\varphi_y(z)\rangle - \varphi_y^b]kT \tag{50}$$

The case of monomer ($m$) adsorption is a particularly simple and illustrative example in this context. For an athermal system of homopolymers (one segment type), $\chi_{xy} = \chi_{yy} = 0$ and $u_x^{int}(z) = u_y^{int}(z) = u'(z)$, except for the first layer, where $u_s(1) = u'(1) + u_s^{ads}$ and $u_m(1) = u'(1) + u_m^{ads}$. Hence with $P = \varphi_m^b/\varphi_s^b$, the well known Langmuir equation is obtained, which for small $P$ transforms into Henry's law: $\varphi_m(1) = k_1 P$. After this excursion into adsorption we could treat the case of polymer adsorption as the next step, but for that we refer to the pertinent literature and proceed with terminally attached chains directly.

### 6.4. The potential field

The entropic change of the polymer molecules has already been taken into account in the earlier lattice-filling and purely (conformational and for the solvent also translational) entropic procedure, which was based on the generation of a self-consistent potential field, that can formally be described by $u'(z)$ and is independent of the type of segment. Evers *et al.* [26] provided explicit expressions for the formal free energy $u'(z)$ associated with this conformational process. The total potential, being the sum of all possible potentials, becomes

$$u_x(z) = u'(z) + u_x^{int}(z) \tag{51}$$

The potentials are defined with respect to the supposedly infinitely large and homogeneous bulk solution ($u'^b = u_x^b = 0$), $u'(z)$ being independent of the type of segments, and the mixing and adsorption contribution $u_x^{int}(z)$ accounting for segment interactions of type $x$. The general expression for the associated statistical weight of a free segment of type $x$ in layer $z$ with respect to the bulk solution is now known from $u_x(z)$:

$$G_x(z) = \exp[-u_x(z)/kT] \tag{52}$$

For the present purposes, it suffices to realise that the potential $u'(z)$ originates from local hard-core interaction potentials in layer $z$ (with respect to the bulk solution) and adjusts itself self-consistently such that the free energy is minimized and the boundary condition of unit space filling (*i.e.*, constant segment density up to the interface) in each layer $z$ is obeyed: ${}_i\Sigma\,\varphi_i(z) = 1$. Indeed, if there is no mixing energy, all $\chi_{xy}$ are zero, *e.g.*, in a polymer melt of one

segment type, and only $u'(z)$ is left to ensure complete occupancy of the lattice. In the polymer melt case it prevents the depletion of the surface region which would occur by entropic restrictions.

Physically, with increasing segment density, this hard-core potential switches from $-\infty$ to $+\infty$ at the moment that ${}_i\Sigma\,\varphi_i(z)$ exceeds 1. Equilibrium values of $u'(z)$ depend strongly on the conditions in the system, but are of the order of $\leqslant kT$. For example, for terminally attached chains, the first segments are constrained to be in layer 1, being anchored $[u'(z) = -\infty]$ in layer $z = 0$. Similar "hard core" potentials also occur in other theories; see, *e.g.*, refs. 8,9 and 142–147. Thus, Marqusee and Dill [8] used the parameter $\ln q(z)$ for the same physical phenomenon as that for $u'(z)$. We feel, however, that they did not correctly make use of this; see our earlier discussion [16].

The above being formal, we may obtain some feeling for the all-important potential field by the application of the well known FH theory, as has been done by several workers [33,133]. The segment potential field $u_p(z)$, being a chemical potential and as such the derivative of the free energy per segment with respect to the segment concentration in layer $z$, $u_p = (\partial g/\partial\varphi)kT$, contains, apart from the above mixing energy term, also entropic contributions. One way to account for the total of energetic and entropic interactions included in this potential field is realized by application of the full FH theory to find the change in free energy when a solvent molecule in layer $z$ is exchanged with a single polymer segment in the bulk solution. The free energy of mixing for the grafted polymer segments using the FH theory with omission of the term representing the absent translational entropy contribution of the attached polymer chain per segment reads, according to eqn. 15,

$$g[\varphi_p(z)]/kT = \varphi_s \ln \varphi_s + \chi_{ps}\varphi_s$$

and appropriate partial differentiation gives the (chemical) segment potential as

$$u_p^{\text{int}}(z)/kT = -\{\ln \varphi_s + 2\chi_{ps}[1 - \varphi_s(z)]\}$$
$$= -\{\ln [1 - \varphi_p(z)] + 2\chi_{ps}\varphi_p(z)\} \qquad (53)$$

This result can also be obtained more intuitively by summing the appropriate changes comprised in the following contributions:

(i) $-\chi_{ps}[\langle\varphi_p(z)\rangle - \varphi_p^b]kT$, resulting from loss of interaction energy by removal of a solvent molecule from layer $z$ plus the gain in energy from interaction of this solvent molecule with the bulk solution; recall that for fully grafted chains, there is in fact no free polymer in the bulk, *i.e.*, $\varphi_p^b = 0$;

(ii) $+\chi_{ps}[\langle\varphi_s(z)\rangle - \varphi_s^b]kT$, resulting from the gain in interaction energy by the insertion of the segment in layer $z$ minus the loss in interaction energy of this segment due to its removal from the bulk solution;

(iii) $-[\ln \varphi_s(z) + \ln \varphi_s^b]kT$, resulting from the change in the translational entropy of the solvent molecule, eqn. 15. As $\varphi_s^b = 1 - \varphi_p^b$ and $\langle\varphi_s(z)\rangle = \langle 1 - \varphi_p(z)\rangle$ and in fact $\varphi_p^b = 0$ from (i) above, $\varphi_s^b = 1$. Thus, summing (i), (ii) and (iii), we arrive again at the above expression for $u_p(z)$. It is stressed that this expression is valid only if no other components such as solutes are present. For later use, we retain the full expression including $\varphi_p^b$ and $\varphi_s^b$ and thus obtain for the energy of mixing the sum of the above contributions (i)–(iii):

$$u_p^{\text{int}}(z)/kT = \chi_{ps}[\langle 1 - 2\varphi_p(z)\rangle - 1 + 2\varphi_p^b]$$
$$- \ln [1 - \varphi_p(z)] + \ln [1 - \varphi_p^b] \qquad (54)$$

The earlier expression eqn. 53 for the interaction energy can also be found as resulting from eqn. 54, both equations being special cases of the shorter but general eqn. 50. Eqns. 53 and 54 show that two types of terms arise, those only in $\varphi(z)$, independent of segment type and entropic in origin, together with those which are segment type dependent because of energetic interactions.

### 6.5. The volume fraction profile

Now that the underlying potentials have been discussed, the statistical weight $G_x(z)$ of a free segment of type $x$ in layer $z$ with respect to the bulk solution is calculated from $u_x(z)$; for each type of molecule $i$ we then have

$$G_{x,i}(z) = \exp\{-[u_{x,i}(z)/kT]\}$$

$$= \exp\{-[u'(z) + u^{\text{int}}_{x,i}(z)]\} \quad (55)$$

where $u'(z)$ is assumed to be the same for all compounds $i$. To calculate the volume fractions of chain molecules from the statistical weights, the connectivity of the segments must be taken into account: in a chain the distribution of a segment is of course also affected by that of all the other segments in the same molecule and may depend on its position in the chain. To this end two different approaches can be followed. The first is after Scheutjens and Fleer [25], who developed a model based on step-weighted random walk statistics, that does not forbid backfolding of segment $s+1$ on segment $s-1$ (first-order Markov chains). This scheme is useful for studying flexible polymers, where one statistical segment corresponds to 2–5 monomeric units [148].

To gain detailed information on the conformational statistics of small chain molecules, for instance the molecules used for surface modification in RPLC and even smaller ones in solutes, every chemical group, such as a $CH_2$ unit, should be treated as one segment. Obviously, this definition of segments will lead to an overestimation of the flexibility if use is made of first-order Markov statistics. To overcome this problem a second approach, developed by Leermakers and Scheutjens [28] and based on a rotational isomeric state (RIS) scheme, is used. This approach leads to reduced flexibility, because backfolding is forbidden for five subsequent segments. Moreover, the energy difference between *gauche* and *trans* configurations can be incorporated.

A detailed derivation of the SCFA theory for first-order Markov statistics has recently been given by Evers *et al.* [26]. The relative occurrence of each conformation must be obtained from adapted statistical weights, $G(z,s)$, taking into account that the segments are connected to each other. $G(z,s)$ equals $G_x(z)$ if segment $s$ is of type $x$ and in layer $z$. For a short discussion on obtaining $G$ values, see our earlier publication [16], section "First-Order Markov Chains". A *chain end segment distribution* function $G_i(z,s_1)$ is introduced for a chain part of molecule $i$ consisting of the segments $1,\ldots,s$. This distribution function gives the average statistical weight of all possible walks along a chain of $s$ segments (*i.e.*, all conformations), starting from segment 1 (being located anywhere in the lattice) and ending after $s-1$ steps at segment $s$ in layer $z$. The subscript 1 in $s_1$ indicates that the walk along the chain starts at segment 1 [28]. For example, for a trimer with $s=1$ in $z=1$ and $s=3$ free, $G(1,1_3) = G(1,1,1) + G(1,1,2) + G(1,2,1) + G(1,2,2) + G(1,2,3)$, *i.e.*, five conformations contribute. However, for instance, in $G(3,1_3)$ there are nine contributing terms, and so nine conformations.

In the general case of $s$-mers, if segment $s$ is in layer $z$, segment $s-1$ must be located in one of the layers $z-1$, $z$ or $z+1$. This implies that $G_i(z,s_1)$ is proportional to the weighted average of statistical weights of $(s-1)$-mers of which the last segment is in one of the layers $z-1$, $z$ or $z+1$. As, further, segment $s$ in layer $z$ contributes a factor $G_i(z,s)$, it is seen that a general recurrence relationship holds:

$$G_i(z,s_1) = \langle G_i(z,s'_1)\rangle G_i(z,s)$$

$$\langle G_i(z,s'_1)\rangle = [\lambda_{-1}G_i(z-1,s'_1) + \lambda_0 G_i(z,s'_1) + \lambda_1 G_i(z+1,s'_1)] \quad (56)$$

Here $s' = s-1$, *i.e.*, the segment to which $s$ is connected. Note that subscript 1 refers to the bond 1 with which the rest of the chain is connected. Through this relationship the end-point distributions can be directly computed from $G(z,s)$ and hence from the potential field $u(z,s)$.

It is easiest to start the recurrence sequence with monomers, each application of the $s$-mer eqn. 56 extending the chain by one segment and by one bond. So we start with [26,133] $G_i(z,1_1) = G_i(z)$, the statistical weight of a free segment $s$ (monomer) in layer $z$, which equals $G_x(z)$ as defined by eqn. 52, if segment $s$ is of type $x$. Extending the chain by one segment [taking into account the segmental weighting factors $G(z-1)$, $G(z)$ and $G(z+1)$] and by one bond (weighting factors $\lambda_{-1}$, $\lambda_0$ and $\lambda_1$) finally results in the building of the required chain of an $r$-mer, if starting point (1) and end-point ($r$) are

free (*i.e.*, not in layer 1). The sought volume fraction $\varphi_i(z,s)$ for segments $s$ in layer $z$ of molecules $i$ is found to be

$$\varphi_i(z,s) = C_i G_i(z,s_1) G_i(z,s_r)/G_i(z,s) \quad (57)$$

$C_i$ is a normalization constant that can be derived from given boundary constraints. For open systems and chains in equilibrium with the bulk, we may express $C_i$ in terms of the bulk concentration $\varphi_i^b$, because in the bulk solution $\varphi_i(z)$ necessarily equals $\varphi_i^b$. As $u(z) = 0$ and all $G$ values are 1 in the bulk, from eqn. 10 it follows that $\varphi_i(z) = \varphi_i^b = {}_s\Sigma\, 1 = r_i C_i$, *i.e.*,

$$C_i = \varphi_i^b / r_i \quad (58)$$

Note that for monomers, $\varphi(z)/\varphi_i^b = G(z)$, as found before.

This expression is not general and is not to be used for grafted chains, where $\varphi_i^b = 0$. Here and also in the case of adsorption of polymers in a closed system where the bulk concentration is not constant, $C_i$ follows from the knowledge of the total amount of polymer present. If we introduce the total amount of molecule $i$ as the sum of $\varphi(z)$ over all layers $z$:

$$\theta_i = {}_z\sum_1^M \varphi_i(z) \quad (59)$$

then $\theta$ is expressed in equivalent monolayers or number of segments per site, *i.e.*, if the number of molecules of type $i$ with $r_i$ segments is $n_i$, $\theta_i = n_i r_i / L$. We finally find [16,26]

$$C_i = (\theta_i / r_i) \cdot {}_z\sum_1^M G_i(z,r_1)$$

$$= (\theta_i^g / r_i^g) \cdot {}_z\sum_1^M G_i^g(z,r_1) \quad (60)$$

where the second equality is valid for terminally attached or grafted chains, since the bulk solution volume fraction of anchored chains is zero and the grafting density $\sigma = \theta^g / r^g$ determines the normalization constant.

### 6.6. Rotational isomeric state scheme

So far chain conformations were generated by a Markov-type approximation, which allows chains to intersect with themselves or other molecules in the lattice. The main advantage of the procedure is the possibility of finding the conformations from handy recurrence relationships. However, the stereochemical structure (steric hindrance) of many polymeric molecules requires that each rotatable skeletal bond is almost restricted to one of a small number of discrete rotational states such that conformations with lower energy ($U$) are preferred by the Boltzmann factor $\exp[-U/kT)$. The conformation of higher alkanes, for instance, can be represented as a random sequence of *trans* ($t$) and *gauche* ($g$) groupings, the relative frequency of these forms being determined by their Boltzmann factors. The *trans* form ("staggered" position of neighbouring building blocks *e.g.*, for $CH_3$ groups in ethane with H atoms farthest apart) is energetically much more preferred than the *cis* form ("eclipsed" position where the building block is rotated with respect to the *trans* form over $\pi/3$ radians such that for ethane the H atoms are all in line) [95,96]. In most chain molecules there are three preferred "staggered" positions located at rotational angles of 0 and $\pm 2\pi/3$, where 0 corresponds with *trans* ($t$) and $\pm 2\pi/3$ with *gauche* groupings ($g^+$ and $g^-$ or sometimes $g$ and $g'$, respectively). In the *gauche* conformations of ethane, *e.g.*, the energy minima are slightly higher (*ca.* $kT$ or 800 cal; 1 cal = 4.14 J) than that in the *trans* conformation, where methyl groups are farthest apart and do not interfere. Hence $t$ conformations prevail but $g$ conformations are still appreciable, even enhanced by their degeneracy of 2. The conformations of higher alkanes can thus be represented as a more or less random sequence of $t$, $g^+$ and $g^-$ groupings, taking into account the restriction that if a sequence $g^+g^-$ is attempted a severe overlap of the first and the fifth methylene group occurs ("pentane effect").

In the rotational isomeric state (RIS) approximation [101], each molecule or bond is treated as occurring in one or another of several of these three rotational states, rather than using the Boltzmann statistics for the complete $U(\varphi)$ function where $\varphi$ is the rotational angle. Fluctuations about the minima are ignored, on the assumption that these fluctuations, being of random

sign, will be mutually compensatory. In order to take into account the interdependence of rotational states, statistical weights are assigned to *pairs of conformations* about adjoining skeletal bonds or, in other words, the third-order Markov process used in RIS to generate the various conformations has a "memory" of the random walk type of two bonds long. A third bond of course, can only have three different directions, which form *trans* or *gauche* configurations with its two predecessors.

The RIS scheme as developed by Leermakers and Scheutjens [28] is based on a tetrahedral (diamond) lattice with $Z = 4$, which is well suited to accommodate the above chain configurations. The extension of the RIS scheme to grafted chains is straightforward and has been described elsewhere [16]. It should be noted that Dill and Cantor [146] used different but similar recurrence relationships to generate the possible conformations on a lattice for micellar aggregates. However, they fixed the head groups in particular layers and allowed all segments only to be in the same layer or in layers closer to the centre of the aggregates. Moreover, no solvent molecules or head groups were allowed in the tail region, therefore ignoring energetic interactions.

## 7. CHROMATOGRAPHIC RETENTION

### 7.1. The capacity factor

In chromatographic experiments the observed retention, expressed as the capacity factor, $k'_i$, is described by eqn. 3. In this relationship $K_i^c$, the concentration-based distribution coefficient of solute $i$ between the stationary and the mobile phase, is directly comparable with the liquid–liquid partition coefficient, $K_{i(\mathrm{LL})}$, as found with the earlier solubility parameter approach. Using the SCFA theory, we obtain a volume fraction profile, rather than a concentration profile, and the distribution coefficient in the SCFA theory is therefore more conveniently expressed in terms of average volume fractions, which are proportional to concentrations:

$$K_i^c = \bar{c}_{is}/\bar{c}_{im} = \bar{\varphi}_{is}/\bar{\varphi}_{im} \tag{61}$$

From this it follows that the average volume fraction, $\bar{\varphi}_{ip}$, in each phase is required. The average bulk volume fraction of solute in the mobile phase, $\bar{\varphi}_{im}$, can be approximated by the bulk solution fraction $\bar{\varphi}_i^b$, whereas the average volume fraction in the stationary phase is calculated from the amount retained per surface site, $\theta_{is}$, and the volume of the stationary phase, $V_s$:

$$\bar{\varphi}_{is} = \theta_{is}/(V_s/V_L) \tag{62}$$

where $V_L$ is the volume of a lattice layer and $\delta_s = V_s/V_L$ the thickness of the stationary phase, expressed in number of layers. The amount $\bar{\varphi}_{is}$ in (or at) the stationary phase is calculated from the total amount of $i$ minus the amount in the mobile phase:

$$\bar{\varphi}_{is} = \theta_i - [\mathrm{M} - (V_s/V_L)]\varphi_i^b \tag{63}$$

The thickness of the stationary phase, $\delta_s$, has to be defined more precisely, because the boundary between mobile and stationary phase is not sharp. Lyklema [147] advocated the use of the *Gibbs dividing plane* for defining the extent of regions where phases have their bulk properties, but here, taking into consideration the chromatographic migration process, we propose to take for it the hydrodynamic layer thickness $\delta_h = \delta_s$. This quantity is an equilibrium property of the grafted layer. The equation for the hydrodynamic layer thickness in terms of the SCFA theory has been given by Scheutjens *et al.* [149] (see the next section). As a result, we write

$$k'_i = K_i^c(V_s/V_m) = K_i^c\delta_h/(\mathrm{M} - \delta_h) = k_i/(\mathrm{M} - \delta_h) \tag{64}$$

where $k_i$ is an alternative capacity factor, equal to $K_i^c\delta_h$. According to eqns. 61 and 62, $k_i$ is obtained from the numerical results as

$$k_i = K_i^c\delta_h = \theta_{is}/\bar{\varphi}_{im} \tag{65}$$

The volume of the mobile phase is usually much larger than that of the stationary phase, therefore the relative changes in the volume of the mobile phase are small and $\mathrm{M} - \delta_h \approx \mathrm{M}$ is approximately constant. Hence the only difference between $k'_i$ and $k_i$ is the nearly constant number of layers $\mathrm{M} - \delta_h$. As results are often represented graphically in terms of the logarithm

of the capacity factor (as a function of the parameters under study), only the intercept differs if we plot ln $k_i$ instead of ln $k'_i$.

### 7.2. The hydrodynamic layer thickness, $\delta_h$

As chromatographic techniques are dynamic and involve flow phenomena, it is of special interest to obtain an insight into the behaviour of polymer brushes when these are subjected to shear forces from flow past the grafted surface. There is little doubt that for isolated chains the latter are squeezed down against the surface, the more strongly as the shear rate becomes higher. For a recent review supported by Brownian dynamics simulations, see Parnas and Cohen [150]. For the relatively short chains of interest in RPLC, it appears that shear rates in excess of 10 $s^{-1}$ are required to observe any reduction in extension of the chain, but at shear rates of 100 $s^{-1}$, typical of modern LC columns, drastic effects are predicted.

This situation is entirely different, however, for the case of polymer brushes, where the chains "support" each other to obtain the highly stretched brushes discussed before. Because of the expected parabolic density profiles, one might expect that flow penetration will be most prominent in the outer bush extremity and vanish somewhere inside the chain phase, where the higher polymer segment density reduces the permeability (note that this would be different in the step function ansatz for the segment density, where the permeability would be constant throughout the grafted layer). Based on the (Debye–)Brinkman equation [151], an empirical modification of Darcy's law for flow in a porous medium, assigning a friction factor to each polymer segment and assuming a linear wedge-like segment density profile at the fringe of the brush, Milner [152] recently obtained for simple shear flow (no pressure gradient and a linear velocity profile) a first guess of the hydrodynamic penetration depth (*i.e.*, the depth in the brush as seen from the outside where the velocity vanishes). The result justifies the view that hydrodynamic penetration of a linear velocity profile is only important in the outer extremity, but solvent flow appears in surprisingly deep layers (roughly half the brush height).

More quantitative results can be based on the Scheutjens–Fleer theory, as has been shown by Cohen Stuart *et al.* [153] and Scheutjens *et al.* [149]. Here the segment density profile (for adsorbed polymer chains) is found as illustrated above, and the use of the relevant hydrodynamic equation according to Brinkman, again assigning permeability or friction factors to each layer, yielding the relationship between pressure drop and flow. The appropriate hydrodynamic layer thickness easily follows from that; for instance, for the flow through a pore of radius $R$, the value of $\delta_h$ may be defined as resulting from the ratio of volumetric flow rates $Q/Q^0$ in the cases of polymer present at the wall of the pore ($Q$) and in the absence of polymer ($Q^0$):

$$\delta_h/R = 1 - (Q/Q^0)^{1/4} \tag{66}$$

Usually, polymeric layers in flow channels are very thin with respect to the width of the channel, where moreover flow profiles (without polymer present) are essentially linear close to the channel walls. Hence the definition of $\delta_h$ may be safely chosen on the basis of a two- rather than a three-dimensional system, as is the case, for example, in slit flow between flat plates. For the latter case the (Debye–)Brinkman equation relates pressure drop and linear flow velocity $v(\zeta)$ ($\zeta$ being the perpendicular coordinate to the wall) along the flat plates in the $x$-direction as

$$-\mathrm{d}p/\mathrm{d}x = \eta[(\mathrm{d}^2v/\mathrm{d}\zeta^2) - v/k^2] \tag{67}$$

where the left-hand side is the transversal pressure gradient in the $x$-direction driving the flow parallel to the wall, $\eta$ the solvent viscosity and the term linear in $v$ represents the friction with $k^2$ being the permeability factor (with dimension (length)$^2$, *e.g.*, for a capillary with radius $R$, $k^2 = R^2/8$ according to Poiseuille).

We take the simplest case of simple shear flow between plates a distance M apart [in terms of our lattice model, each lattice step ($z$) being of length $a$, so $\zeta = za$] such that the grafted layer is at the fixed wall (adjoining $z = 1$) and the other plate (adjacent to $z = M$) moves with a constant

and maximum velocity $v_M$, we obtain a linear velocity profile $v(z) = (z/M)v_M$, and a zero pressure gradient, and so

$$d^2v/dz^2 - v/q^2(z) = 0; \quad q^2(z) = k^2(z)/a^2 \qquad (68)$$

For the permeability we use the semi-empirical expression after Mijnlieff *et al.* [154], $q^2 = c_h\varphi_s/(1-\varphi_s)$, where $\varphi_s$ is the solvent volume fraction present. The constant $c_h$ is of the order of unity [153].

In our case of grafted (or adsorbed) layers the situation is complicated since the solvent content of each layer varies by virtue of the concentration (volume) profile of polymer segments as discussed, and so $\varphi_s$ and $q^2$ are functions of $z$. As only grafted (or adsorbed) chains contribute to the permeability, it is better to express $q^2(z)$ in terms of $\varphi^g(z)$ and write $q^2(z) = c_h[1-\varphi^g(z)]/\varphi^g(z)$. Note that for $\varphi^g(z) = 1$, $q^2(z) = 0$ (*i.e.*, no permeability is left in a completely filled grafted lattice, as should be).

Now, with these values for $q^2(z)$ the reduced Brinkman equation can be solved for each layer for $v(z)$ and, through a numerical iteration procedure, $\delta_h$ can be obtained from the distance the plates must be moved towards each other [153], such that the flows $Q$ and $Q^0$ are equal. Scheutjens *et al.* [149] pointed out that an analytical procedure is equally possible. This procedure is based on the above analytical solution of the Brinkman equation per layer and defining the ratio of velocity $v(z)$ and velocity gradient $v'(z) = dv/dz$ as $\alpha(z) = v(z)/v'(z)$. It turns out that a single recurrence relationship is obtained with hyperbolic functions of the form $\tanh[1/q(z)]$, and containing only $\alpha(z)$, $\alpha(z-1)$ and $q^2(z)$, starting with $\alpha(0) = 0$. For layers close to the surface, with relatively high $\varphi$-values, $q^2(z)$ is small and $\alpha(z)$ increases only very slightly per layer. This implies that $v(z)$ is virtually zero near the solid surface, as expected.

At the other extreme, far out in the bulk solvent and in the absence of (grafted) polymer, $q^2(z) \rightarrow \infty$ and the recurrence relationship reduces simply to $\alpha(z) = \alpha(z-1) + 1$, *i.e.*, each layer behaves the same, the linear velocity profile $v(z) = (z/M)v_M$ is preserved and $\alpha(z) = z$, as should be. Going from the solid surface towards the bulk solvent region, because of the hyperbolic tanh functions, major changes in $\alpha(z)$ via changes in $q^2(z)$ occur only where $\varphi^g(z)$ drops below say 0.01, *i.e.*, in the very fringes of the chain phase. Obviously the tail ends in the outer peripheries of the brush layer screen the liquid flow from the inner parts of the layer very effectively. The analogous situation of limited draining of free polymer coils in solution is well known (see, *e.g.*, ref. 95). Therefore, adsorbed or grafted polymer layers at interfaces produce more or less immobile solvent layers with an effective thickness that is largely determined by the tail extension [153,155]. Indeed, hydrodynamic layer thicknesses are always larger than those determined by other methods such as ellipsometry and SANS (for a review, see ref. 155).

As a consequence, $\delta_h$ is virtually independent of all inner properties such as the difference between adsorption and grafting, and also independent of flow properties such as the velocity itself. Indeed, $\alpha(z)$ is not dependent on velocity, as it is only a function of $q^2(z)$, and represents the number of layers over which a velocity difference $dv(z) \neq 0$ becomes effective. Owing to the polymer present in the grafted layer, the velocity profile is only linear at large $z$ and is shifted in comparison with the absence of polymer over a distance $\delta_h$:

$$\delta_h = M - \alpha(M) \qquad (69)$$

Thus, in eqn. 64 the term $M - \delta_h$ may be replaced by $\alpha(M)$, and hence

$$k_i' = K_i^c(V_s/V_m) = K_i\delta_h/(M-\delta_h) = k_i/(M-\delta_h) = k_i/\alpha(M) \qquad (70)$$

### 7.3. Choice of parameters

As indicated in the Introduction, we shall start by considering simple systems composed of a surface with a grafted layer of chain molecules, a monomeric solvent and linear flexible solutes. When we properly understand these simple systems, we can study more complicated situations, such as mixed solvents. In RPLC the solvent is polar, whereas the grafted chains are mainly aliphatic. The interaction between the mobile and the stationary phase is therefore unfavourable, and a high positive value for $\chi$

between segments of the grafted chains, G, and the monomeric solvent, O, should be chosen. Typically, we use $\chi_{GO} = 2$ and the effect of $\chi_{GO}$ on the properties of the grafted layer will be studied by varying $\chi_{GO}$ between 0 and 2. If the mobile phase is water and the grafted chains are aliphatic, we take $\chi_{GO} = 2$, a value also used in the calculations on non-ionic surfactants [156]. To limit the number of different segment types, we ignore end effects, such as the fact that a terminal $CH_3$ group is more hydrophobic than a $CH_2$ group in an alkane chain [157].

Apart from the solvent–grafted chain segments interaction, we also have to specify solute–solvent and solute–grafted chain segment interactions. The solute may consist of one or more segments which can be of different types. In practical systems, the solubility of the solute in the mobile phase is poor, and therefore positive $\chi$ values are chosen for the interaction between at least one type of solute segment (referred to as the aliphatic segments, type A) and the solvent. The interaction parameter between these A segments and the aliphatic segments of the grafted chains is always taken to be zero, $\chi_{AG} = 0$, and we shall vary both $\chi_{GO}$ and $\chi_{AO}$ between 0 and 2. Potentially, high values of $\chi_{AO}$ may lead to separation of a solution into two phases, one solute-rich and the other solute-poor. Using the extended Flory–Huggins equations [27] we ascertained that phase separation does not occur at the low bulk volume fractions of solute considered in this study.

The interaction of the hydrophilic segments of the solute, if present, with the grafted chains is unfavourable and consequently positive $\chi$-values are chosen for the interaction between the hydrophilic segments and the segments of the grafted chains. To keep the number of variable parameters small, we have only considered the case where the hydrophilic segments, H, of the solute are of the same type as the solvent molecules, *i.e.*, $\chi_{xH} = \chi_{xO}$ and $\chi_{HO} = 0$.

Concerning the solid surface, a value of zero was assigned to all interaction parameters involving the surface (S). This leads to some adsorption of grafted chains on the surface if $\chi_{GO}$ is positive, because unfavourable contacts between aliphatic segments and the solvent can be replaced by more favourable contacts with the surface. The surface densities chosen in the calculations correspond to values commonly reported for practical RPLC systems, which are in the range 2–4 $\mu$mol/m$^2$. In the model we use the surface coverage, $\sigma$, which is the number of grafted molecules per surface site. At the theoretical maximum surface coverage ($\sigma = 1$) the grafted chains are aligned in an all-*trans* conformation. The density of silanol groups on a silica surface is between 7 and 9.5 $\mu$mol/m$^2$ [1], which results in about the same cross-sectional area as the $CH_2$ units. Using 9 $\mu$mol/m$^2$ for the maximum surface density, a surface density between 2 and 4 $\mu$mol/m$^2$ corresponds to a surface coverage between 0.22 and 0.44. In most calculations a typical value of $\sigma = 0.3$ is chosen.

### 7.4. Results for the grafted layer

Here we consider terminally attached $G_{18}$ chains consisting of 18 segments of type G, at a typical surface coverage $\sigma = 0.3$. We start with a solvent consisting of monomers of type O, and Fig. 2 shows volume fraction profiles for three solvent qualities. The volume fraction profiles are extrapolated from layer 1 to layer 0 where $\sigma = 0.3$. It appears that in an athermal solvent, *i.e.*, $\chi_{GO} = 0$, the volume fraction profile is dominated by two entropic factors: the conformational entropy of the grafted chains and the entropy of mixing in every lattice layer. As a result, the chains protrude far into the solution as expected: the Flory radius in a good solvent would amount to $(18)^{3/5} = 5.66$ (layer numbers), whereas the chain for $\chi_{GO} = 0$ extends to about $z = 15$–$18$, depending on the type of statistics (Markov or RIS) used. This confirms the earlier qualitative discussion on the formation of highly extended layers ("brushes") in grafted layers. The profiles do show a nearly constant density region (in accordance with the step function ansatz of De Gennes) only for $\sigma > 0.3$ and more constant with increasing $\chi_{GO}$ values (Fig. 5 in ref. 16).

At these larger values of $\chi_{GO}$, GG interactions are preferred to GO interactions and the grafted layer becomes more compressed and the number of contacts between segments of the grafted chains and the solvent molecules decreases. For $\chi_{GO} = 2$ the grafted layer is strongly compressed,

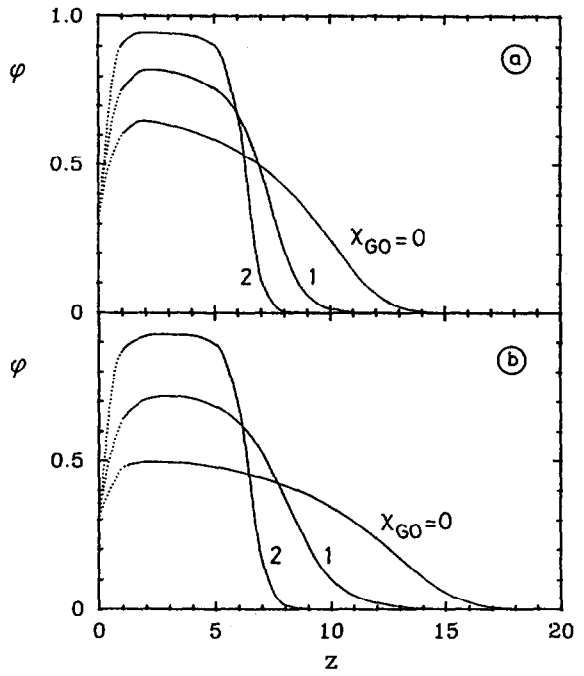


Fig. 2. Volume fraction profiles of terminally attached $G_{18}$ chains for $\chi_{GO} = 0$, 1 and 2. $\sigma = 0.3$. (a) First-order Markov chains; (b) RIS chains (third-order Markov chains). From ref. 16.

the grafted chains have formed a separate phase and the boundary region with the solvent is only a few layers wide. This last situation is typical of RPLC systems.

In all cases a maximum in the segment density distribution is found, occurring for entropic reasons, confirming the results by Cosgrove *et al.* [20], who used first-order Markov statistics with SCFA theory only and longer chains, resulting in more pronounced maxima. At positive $\chi_{GO}$ values, the grafted chains adsorb slightly on the surface, because contacts with the surface are preferred to contacts with the solvent. The shapes of the profiles that are obtained for $\chi_{GO} = 1$ and $\chi_{GO} = 2$ are typical of weakly adsorbing grafted chains. For $\chi_{GO} = 0$ and $\chi_{GO} = 1$ the volume fraction profiles calculated with the use of the RIS scheme differ from the volume fraction profiles calculated with first-order Markov statistics. The "RIS chains" are more stretched, because backfolding is forbidden and *trans* bonds are energetically preferred to *gauche* bonds. If $\chi_{GO} = 2$, however, the profiles with and without the use of the RIS scheme are almost identical. At such high $\chi_{GO}$ values a collapse of the grafted chains occurs; minimization of the number of contacts between segments of the grafted chains and solvent molecules dominates the volume fraction profile.

Generalizing for the moment the above results by considering the $\chi_{GO}$ parameter as an overall characteristic of the solvent with respect to the grafted layer (independent of the precise molecular structure or composition of the solvent), we may say that in good solvents the grafted layer is extended, whereas in poor solvents the grafted layer collapses. Concluding, with and without the use of the RIS scheme, we find the same trends as observed by Martire and Boehm [17]. The difference between the two types of statistics we used is small at the high values of the interaction parameters that are relevant in RPLC. Nevertheless, we prefer the use of the more exact RIS scheme.

If $\chi_{GO} = 0$, the chains extend far into the solution for all coverages, and when $\sigma$ increases the volume fractions become higher and the slopes of the curves near layer 18 become steeper. The hypothetical limiting coverage, $\sigma = 1$, leads to a block profile of the grafted chains: the volume fraction drops from 1 in layer 18 to 0 in layer 19. For $\chi_{GO} = 2$ the layer collapses and the maximum value of the volume fraction (*ca.* 1) depends only weakly on the surface coverage. In contrast to the volume fraction profiles for $\chi_{GO} = 0$, the volume fraction profiles in the boundary region have the same shape for all coverages, except for $\sigma = 1$, which must lead to an exact block profile. We conclude that the high value of $\chi_{GO}$ leads to condensed grafted layers for all coverages, in agreement with experimental findings and the theory of Martire and Boehm [17].

The effect of the chain length of the terminally attached chains on the volume fraction profiles is such that for all $\chi_{GO}$ values longer chains always form thicker layers. For high $\chi_{GO}$ the layers collapse into layers with high segment density (0.85–0.95), where the shape of the volume fraction profiles in the thin boundary region between grafted chains and solvent are more or

less parallel and independent of the chain length (see Fig. 6 in ref. 16). The volume fraction profile of grafted chains is largely determined by the unfavourable chain–solvent interactions, in contrast to the volume fraction profile at $\chi_{GO} = 0$, where conformational aspects dominate and chains protrude into solution as far as their number of segments allow. In these instances the shape of the profiles is far from block-like and, qualitatively, agrees much better with the expected parabolic profiles (except at the extremes for $z = 0$–2 and $z$ large).

We conclude that for the case of practical relevance, *i.e.*, high $\chi_{GO}$ values, the grafted layer is strongly collapsed. The conformational entropy and the energetically favoured formation of *trans* bonds cannot prevent the formation of a separate phase with a thin interfacial region with the mobile phase. For the relatively low-molecular-mass grafted chains used here, experimental verification of the profiles presented above is difficult. For grafted high-molecular-mass polymer layers a maximum in the volume fraction profile has indeed been found using neutron scattering [155,158] and it also agrees with Monte Carlo simulations [155]. The same techniques and also molecular dynamics simulations can probably provide a check on the profiles, and measurement of grafted layer thicknesses seems feasible by hydrodynamic layer thickness determination [155].

### 7.5. Solute distribution

On allowing a monomeric solute A, we note that A could also be interpreted as another solvent and the results apply to mixed solvents also. The total amount of segments of type A, $\theta_A$, in eqn. 60 is chosen to be 1 in 20 layers, being relatively high, but the amount retained in the grafted layer is still proportional to the bulk volume fraction, and the linearity of the adsorption isotherm is ensured (Henry's law limit). Indeed, the resulting shape of the solute distributions does not change if $\theta_A$ is lowered, and therefore the given distributions are relevant to analytical RPLC. The interaction parameters are $\chi_{GO} = 2$, $\chi_{AO} = 2$ and $\chi_{AG} = 0$. These parameters apply, for instance, to an aqueous solvent, apolar grafted chains and apolar solute.

We find (Fig. 7 in ref. 16) that the volume fraction of A in the grafted layer is higher than in solution, *i.e.*, the capacity factor is in excess of 1 and appreciable retention occurs. Comparison with the volume fraction profile of grafted chains in the absence of solute shows that the profile of the grafted chains has changed owing to the uptake of solute: the boundary between the grafted chains and the solvent becomes less thin, being referred to as "a breathing surface" which adjusts itself to local conditions [17]. Although the effect is small, the solute is slightly enriched in the boundary region between grafted layer and solvent. The uptake of solute in the boundary region allows the grafted chains to form more *trans* bonds, *i.e.*, to become more aligned, without an increase in the number of unfavourable GO contacts.

In poor solvents the grafted chains gain conformational entropy if the solute is present in the boundary region, because it allows the grafted chains to protrude further into the solution. On the other hand, there are entropic restrictions: the space already occupied by segments of the grafted chains limits the uptake of solute in the interior of the grafted layer.

At lower $\chi_{AO}$ values, *i.e.*, when O is a better solvent for A, with the other interaction parameters kept unchanged, less A is taken up and the maximum in the volume fraction profile of A is more pronounced than for higher $\chi_{AO}$. By their accumulation in the boundary region, the solute molecules A are capable of reducing the number of GO contacts, which are more unfavourable than AG and AO interactions.

On varying the solute chain length, the extent of partitioning in the grafted layer, and so retention, increase with increasing chain length. For example, in a poor solvent (higher $\chi_{AO}$) the volume fractions of $A_5$ in the interior of the grafted layer are higher than for $A_2$ and A, because the solubility in the solvent decreases with increasing solute chain length. The distribution of solute in the grafted layer becomes less homogeneous with increasing chain length, because conformational constraints make it more difficult to accommodate an $r$-mer in the interior

of the grafted layer than $r$ monomers. In the boundary region, on the other hand, conformational restrictions are less important and the grafted chains even gain entropy by solute uptake, just as in the case of monomeric solutes. This is in contrast with Dill's theory (see the discussion in ref. 16).

Results for the retention of short and amphiphilic molecules, $A_2H$ and $A_5H$ (with interaction parameters $\chi_{HO} = 0$ and $\chi_{AH} = \chi_{HG} = 2$) represent, for instance, the case of an aqueous solution with alcohol molecules and an aliphatic grafted layer. The maximum of $\varphi_H$ is located nearer the solution side than that of the A segments. The presence of hydrophilic head groups obviously decreases the retention as the entire molecule is located more to the outside of the grafted layer. If the chain length of the solute exceeds the length of the grafted chains, the accumulation in the boundary region is even stronger. These long-chain molecules find themselves predominantly at the G–O boundary because the presence of the grafted chains and the solid surface strongly restrict the number of possible conformations of $A_{r>r_g}$ in the interior of the grafted layer. Experimental verification of the discussed profiles is only possible indirectly through retention behaviour, *i.e.*, through the partition coefficient $K_i$ (leaving out the superscript c, for simplicity), eqn. 61.

For a given solute the retention depends on the solvent quality and for a monomer solute A we investigated the effect of $\chi_{AO}$ on the retention of A at $\chi_{AG} = 0$. It appears that for a given value of $\chi_{GO}$ the retention increases with increasing $\chi_{AO}$. Retention also increases with increasing $\chi_{GO}$, except for very low $\chi_{AO}$ values. For all $\chi_{GO}$ values a practically linear relationship between $\chi_{AO}$ and ln $K_A$ appears to exist, as should be the case, and is often reported in experimental observations (see, *e.g.*, Möckel and Freyboldt [159,160]).

As an illustration, we first consider liquid–liquid partitioning of a trace amount of a monomeric solute A between immiscible monomeric liquids O and G. For this system the relationship between ln $K_i$ and the difference in interaction parameters, $\chi_{AG}$ and $\chi_{AO}$, is linear, as is expressed for a regular solution by eqn. 4. For trace amounts of monomeric solutes and non-mixing, non-monomeric solvents this equation holds approximately. As we have chosen $\chi_{AG}$ to be zero, the relationship between ln $K_i$ and $\chi_{AO}$ is linear with a slope of unity and passes through the origin, as $Z$ contacts between A and O are replaced with $Z$ contacts between A and G.

If we now consider the adsorption of isolated monomeric molecules A on a rigid $G$ surface from solvent O, a linear relationship between the volume fractions at the surface and in solution exists with a slope related to the adsorption constant $K_A$ (Henry's law region). For otherwise identical conditions (identical $\chi$) the expected slopes of the ln $K_A$ *vs.* $\chi_{AO}$ curves for liquid–liquid partitioning and for adsorption on a solid surface are not the same, even for regular systems: for liquid–liquid partitioning of monomer A with $\chi_{AG} = 0$ the slope of ln $K_A$ *vs.* $\chi_{AO}$ is unity (see above), whereas for adsorption the slope of ln $K_A$ *vs.* $\chi_{AO}$ is $\lambda_1$, since only a fraction $\lambda_1$ of the $Z$ contacts between A and O are replaced by AG contacts.

For mutually soluble solvents in liquid–liquid partitioning (say, $\chi_{GO} = 2$ with $G$ the other solvent), the precise partitioning coefficient should be calculated with the extended Flory equations [28,37] instead of with eqn. 4, and a slope of ln $K_A$ *vs.* $\chi_{AO}$ equal to 0.87 results. For the RPLC system (Fig. 8 in ref. 16), for the case $\chi_{GO} = 2$, the slope equals 0.83, which is only slightly lower than 0.87. At low $\chi_{GO}$ the number of AO contacts replaced by AG contacts is lower than for $\chi_{GO} = 2$ and the grafted layer is penetrated by a large amount of solvent. Nevertheless, the slope of the ln $K_A$ *vs.* $\chi_{AO}$ curve at $\chi_{GO} = 0$ equals 0.43, much exceeding $\lambda_1$ (0.25), the slope expected for adsorption on a rigid G surface.

From these slopes and from the volume fraction profiles, it is clear that retention in RPLC cannot be modelled as adsorption on a rigid solid surface. The fact that the curves in ln $K_A$ *vs.* $\chi_{AO}$ do not pass through the origin is a result of the arbitrary choice of the thickness of the grafted layer and the inhomogeneous distribution of the solute. For example, the crossing over of the curves at low $\chi_{GO}$ values (Fig. 8 in ref. 16) is an effect of the layer thickness, $\delta_h$. At lower $\chi_{GO}$, $\delta_h$

is larger, leading to an increase in ln $K_i$ although the amount retained (and so $k_i$) becomes smaller.

The effect of $\chi_{AO}$ on the retention is more pronounced than the effect of $\chi_{GO}$ and $\chi_{AG}$, *i.e.*, the retention is to a large extent determined by squeezing the solute out of the solvent, a solvophobic effect. This explains the success of the application of the solvophobic theory [13], where only solute and solvent interactions are considered.

### 7.6. Chain lengths and composition of the solvent

The chain length of the solute strongly affects the retention (much more strongly than the above $\chi_{AO}$ and $\chi_{GO}$ effects), as can be seen from the calculation of distribution coefficients of a homologous series $A_n$ in a $G_{18}$ layer–solvent system as a function of the number $n$ of A segments. Not unexpectedly, more or less linear relationships between the chain length and ln $K_i$ are obtained, in agreement with, *e.g.*, the Martire and Boehm theory [17]. We note, however, that the relationship between the solute chain length and the distribution coefficient is not exactly linear, a fact that becomes easily visible if we extend the calculation over a large range of $n$ values, say from $n = 1$ to 30. The slope of the curve decreases slightly as the chain length increases, which can be attributed to the loss of conformational entropy of the solute on retention. Only for solutes longer than about fifteen segments does the slope become virtually constant.

A more sensitive way of demonstrating non-linearity of retention data for homologous series results when the ratio $K(n+1)/K(n)$ is plotted *versus* $n$. The value of $K(n+1)/K(n)$ then decreases with the number $n$ of A segments instead of being constant according to Martin's rule [6,39,42,43]. This is caused by the decrease in conformational entropy when the solute is dissolved in the grafted layer, which increases with increasing solute chain length. It is illustrative to compare this behaviour with that of the liquid–liquid distribution coefficient. As we are dealing with partly miscible chain molecules, we again choose the extended Flory equations to calculate the distribution equilibria of $A_n$ between O and a liquid consisting of $A_{18}$ chains. The slope obtained for the RPLC system at $\chi_{AO} = 2$ is about 1.06, whereas in the liquid–liquid system a slope of 1.12 is calculated. For $\chi_{AO} = 1.5$ these values are 0.60 and 0.66, respectively, and for $\chi_{AO} = 1$ we find 0.20 and 0.26, respectively. These figures show that in all instances the solute molecules are better "solvated" in the $A_{18}$ liquid than in the $G_{18}$ grafted layer.

To study the effect of the presence of a hydrophilic head group in the solute on the retention of homologous series, calculations were performed for homologous series of $A_nH$ molecules (*e.g.*, alcohols) with interaction parameters $\chi_{AO} = \chi_{GO} = \chi_{HA} = \chi_{HG} = 2$ and $\chi_{HO} = \chi_{AG} = 0$. Comparison of the results with those for $A_n$ shows that the presence of a hydrophilic head group reduces ln $K_i$, especially for small values of $n$. For high $n$ the slope of the (approximately) linear part of the curve ln $K$ *vs.* $n$ is about the same as (slightly less than) in the case of non-polar $A_n$ molecules. Our calculations also show the effect of the grafted chain length on retention of $A_nH$.

The general picture arises that the relationship ln $K_i$ *vs.* $n_i$ is non-linear and even more so for short grafted chains. The distribution coefficient of alcohols depends on the grafted amount and for constant grafted density ($\sigma = 0.3$ in all calculations for all chain lengths) on the chain length of the grafted chains. For short-chain alcohols, ln $K_i$ increases with decreasing grafted chain length, because alcohols tend to accumulate in the boundary region between grafted chains and solvent. In contrast, for long-chain alcohols ln $K_i$ increases with increasing grafted chain length, because for short grafted chains the grafted layer is too thin to accommodate long solutes without a significant decrease in entropy. For the same reason the slope of the curves depends strongly on the grafted chain length up to $G_8$, leading to intersection of the curves ln $K_i$ *vs.* $n$ (for example, the $G_1$ and $G_4$ curves cross over with $G_8$ near $n_i = 4$). The $G_8$ and $G_{18}$ curves are close together, nearly parallel and almost linear with the $G_{18}$ curve slightly below the $G_8$ curve. Expressed in terms of capacity factors, using

eqn. 65, the curves of ln $k$ *vs.* $n$ no longer cross over, because in the capacity factor the changing volume of the stationary phases is accounted for. Hence, for all $n$ the capacity factor increases with increasing grafted chain length, especially for the shorter chains (and provided that $\sigma$ is the same). For grafted chain lengths between 8 and 18, the difference in retention becomes small, which can be attributed to the fact that the alcohols are accumulated preferentially in the boundary region.

Experimentally, linear relationships between ln $k_i'$ and the chain length have been obtained for many homologous series (see, *e.g.*, refs. 159–168). Möckel [160] recently obtained very precise measurements and demonstrated a strong case in the experimental proof of the linear relationship. Karch *et al.* [161] presented measurements for the retention of a series of alcohols on reversed phases of different chain lengths, the slopes of which agree with our calculations. We note that these experiments were not carried out at the same surface densities for all chain lengths studied. The existence of a limiting length of the grafted chains, *i.e.*, a length beyond which no further increase in retention occurs, has also been confirmed by experimental studies [161,162].

The non-linearity of ln $K_i$ *vs.* $n$ as found here for short-chain alcohols was demonstrated experimentally [169–171] for several homologous series in which a wide range of solute chain lengths were included. If we calculate again the value of $K(n+1)/K(n)$ for $A_nH$ molecules, we observe the same behaviour as for non-polar molecules, *viz.*, a decrease with increasing number $n$ of A segments. The deviations from a horizontal line are more evident in the case of polar $A_nH$ molecules than for non-polar $A_n$ molecules, but at long chain lengths ($n > 15$) the curves for $A_n$ and $A_nH$ coincide because the effect of the head group vanishes. Tchapla *et al.* [169] measured the retentions of various homologous series on RPLC columns up to long solute chain lengths. Their results for a "polymeric" bonded phase ($\mu$Bondapak) agree very well with the above and indeed a continuously decreasing curve was obtained for $K(n+1)/K(n)$ *vs.* $n$. For "monomeric" bonded phases, however, they observed that $K(n+1)/K(n)$ slowly decreased only for chain lengths of the solute smaller than the length of the grafted chains. If the solute is about as long as the grafted chains, a sharp break occurs, and for solutes longer than the grafted chains they again found a slowly decreasing ratio $K(n+1)/K(n)$ with increasing $n$. As seen from our discussion above, the sharp break cannot be explained on the basis of our theory.

### *7.7. Retention as a function of the surface coverage*

In the above, we kept the surface coverage constant at $\sigma = 0.3$, this being a typical value for available RPLC packings whose $\sigma$ values range between 0.22 and 0.44. Obviously, however, retention is strongly influenced by the grafting density and, to gain further insight, we calculated distribution and capacity data as a function of $\sigma$, ranging from its minimum value of zero (bare solid surface) towards its maximum of 1 on a surface with grafted chains of 18 segments. To scale the results we divided the calculated distribution data by the liquid–liquid ($C_{18}$–O) partition coefficients for the solutes, as calculated with the extended Flory equations, and denoted as $K_{i(LL)}$. For all molecules a maximum in $k_i/K_{i(LL)}$ as a function of $\sigma$ is found (see Fig. 12 in ref. 16). At $\sigma = 0$, no grafted chains are present and therefore retention is ideally zero, but actually very small as typically some retention by adsorption occurs because of the positive $\chi_{AO}$ value in polar solvents. If $\sigma = 1$, the grafted layer forms a block profile, in which all chains must be perfectly aligned and retention can only occur by adsorption on the outer surface of the grafted layer. This leads to small values for $k_i/K_{i(LL)}$, as absorption is not possible, because all the lattice sites in the first 18 layers next to the surface are occupied by segments of the grafted chains. Thus, between these extremes, two opposing effects cause the maximum in retention: starting with the bare solid surface and increasing $\sigma$, the enlarged volume of the stationary phase results in more retention, but at large values of $\sigma$ the stronger ordering in the grafted layer causes a decrease in retention.

It appears that with increasing solute chain

length the maximum retention occurs at lower coverages: for the monomeric solute A, the maximum in $k_i/K_{i(LL)}$ at a value of 10 is located around $\sigma = 0.65$, whereas for the oligomers $A_2$ and $A_5$ lower maxima of 8 and 6 are near $\sigma = 0.5$ and $\sigma = 0.4$, respectively. In fact, the whole function $k_i/K_{i(LL)}$ decreases with increasing solute chain length at all values of $\sigma$, which supports the earlier observation that the insertion of chain molecules into a grafted layer is entropically less favourable than that of monomers. If a hydrophilic segment is added to the solute chain, the relative retention $k_i/K_{i(LL)}$ increases much faster initially, reaching a high value of 15 at low $\sigma$ (about 0.2) and a maximum of about 18 at $\sigma = 0.45$, but does not change much for the whole range of $\sigma$ from 0.2 to 0.6. This can be explained by the fact that amphiphilic molecules are preferably in the boundary region between grafted chains and solvent, which does not change very much when $\sigma$ is increased, as discussed before: for collapsed layers the boundary region shifts further into the solvent at increasing $\sigma$ without changing its density gradient. This explains why the relative retention remains approximately constant over a wide range of coverages. In practical RPLC systems, coverages above 50% are not available. The maximum in relative retention will therefore be hard to find, but saturation of retention as a function of surface coverage has indeed been reported for a number of systems [163,172,173]. The present results for high surface coverages are probably more relevant for the partitioning of solutes in membranes [8,10].

Not surprisingly, the SCFA theory gives not only a maximum in relative retention $k_i/K_{i(LL)}$ as a function of surface coverage, but also in relative partitioning $K_i/K_{i(LL)}$. For all types of solute molecules, after an initially sharp increase a maximum is found at low $\sigma$ values ($\sigma < 0.2$) above which $K_i/K_{i(LL)}$ decreases gradually with increasing surface coverage to zero at $\sigma = 1$. The decrease in $K_i$ is caused by the increasing volume occupied by the grafted chains, so that less room remains for monomeric A, whose maximum is located near $\sigma = 0.05$. For flexible chain molecules the maximum shifts to higher $\sigma$ as the solute chain length increases. At very low $\sigma$, the effect of the presence of a non-interacting surface gives a reduction in retention caused by the loss of entropy (negative adsorption). As $\sigma$ increases, the effect of the presence of the surface becomes less prominent since the conformational restrictions, imposed by the surface, do not affect the solutes that are accumulated at a certain distance from the surface.

Comparing these results with other theories, Martire and Boehm reported [17] that $k_i$ levels off as the coverage increases, whereas with Dill and co-workers' theory [10,11] a maximum in the distribution coefficient of a monomeric solute is found as a function of the amount of the grafted chains at $\sigma = 0.33$ (see Fig. 17 in ref. 10 and Fig. 13 in ref. 11). This contradicts our findings for monomeric solutes. In Dill and co-workers' theory a parameter $q_i$ describes the conformational aspects of the grafted layer, but the exact meaning of $q_i$ is not clear to us; see our discussion in ref. 16, where we came to the conclusion that the maximum found with Dill and co-workers' theory is probably an artefact, because that theory does not properly describe the conformational statistics at low coverages and the maximum at $\sigma = 0.33$ in Fig. 17 in ref. 10 is probably caused by an inconsistent choice of the stationary phase volume, being the total volume of the grafted chains without intercalated solvent.

Experimentally, Sentell and Dorsey [174] observed a maximum in $K_i$ for naphthalene in RPLC at a surface density of 3 $\mu$mol/m$^2$ and they explained their results using Dill and co-workers' model for the retention of monomers. In view of the above this explanation is questionable and in our opinion a better explanation is that naphthalene is a large molecule. At low surface coverage the presence of the silica surface will restrict the number of possible orientations, leading to the observed initial increase in $K_i$, just as predicted by our model.

### 7.8. *The retention mechanism of RPLC*

From our results for the distribution and retention as a function of interaction parameters and solute chain length, it seems that retention in RPLC resembles liquid–liquid distribution more closely than adsorption on a solid surface,

which is in agreement with the cited theories of Dill [9] and Martire and Boehm [17]. However, the volume fraction profiles we obtained prior to the calculation of the distribution coefficients show that solutes accumulate near the boundary between grafted chains and solvent. This stresses the fact that in order to obtain an accurate description of the retention mechanism in RPLC, the boundary region between grafted chains and solvent cannot be ignored as was done by Martire and Boehm [17] and cannot be treated as a simple planar interface as was done by Dill and co-workers [8–11]. To investigate this issue in more detail we compare our RPLC results with results obtained for liquid–liquid systems, for which the SCFA theory has also been used [137].

In order to compare the solute distribution in the two situations, volume fraction profiles were calculated. Fig. 3a shows the volume fraction profiles of O, $A_5H$ and grafted $G_{18}$ and Fig. 3b those of O, $A_5H$ and a bulk liquid consisting of $C_{18}$ chains, the segments C being identical with the G segments. The bulk volume fraction of $A_5H$ in phase O is the same in both instances. The volume fraction of $A_5H$ in the $C_{18}$ phase (far from the interface) is related to its bulk volume fraction in O through the liquid–liquid partition coefficient. The partition coefficient thus calculated is identical with that calculated with the extended Flory equations.

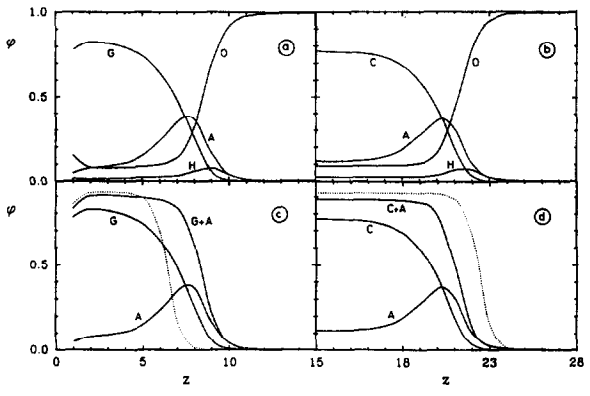


Fig. 3. Retention in RPLC ($G_{18}$, $\sigma = 0.3$) and liquid–liquid ($C_{18}$–O) partitioning for $A_5H$. The total amount of $A_5H$ equals 2 equivalent monolayers; interaction parameters are $\chi_{GO} = \chi_{AO} = \chi_{AH} = 2$, $\chi_{HO} = \chi_{AG} = 0$. Segment type C is identical with segment type G. (a) Volume fraction profiles of $A_5H$, grafted chains $G_{18}$ and solvent O. (b) Volume fraction profiles of $A_5H$, non-polar solvent $C_{18}$ and solvent O. (c) Volume fraction profiles of segments of type A and G (both aliphatic), their sum (G + A) and the volume fraction profile of grafted chains in the absence of solute $A_5H$ (dots). (d) Volume fraction profiles of segments of type A and C (both aliphatic), their sum (C + A) and the volume fraction profile of C at the $C_{18}$–O interface in the absence of solute $A_5H$ (dotted line, arbitrary position). From ref. 16.

It is seen that the volume fraction profiles of the alcohol are very similar in the two systems, both having clear maxima in $\varphi_A$ at the phase boundary. Close to the solid surface the volume fraction of A in the $G_{18}$ phase is, however, lower than that in the liquid $C_{18}$ phase for entropic reasons: the presence of the surface and the grafted layer restrict the conformational freedom of $A_5H$. The boundary region of the grafted layer and the solvent O is just as disordered as the boundary region of the $C_{18}$–O interface. We may conclude that, if the grafted chains are not too short and the surface coverage is moderate, the solute distribution in RPLC is very similar to that in liquid–liquid partitioning. The main difference occurs because of the limited volume of the grafted phase, so that both the region near the solid interface and the boundary with the solution are important and the distribution coefficient is largely determined by the whole segment density profile. In liquid–liquid partitioning the $C_{18}$ phase is a macroscopic phase and the interfacial region has little influence on the liquid–liquid partition coefficient, and the partition coefficient is determined by the bulk concentrations in both phases only.

For both the grafted layer–solvent interface (Fig. 3c) and the liquid–liquid interface (Fig. 3d) we plotted the sum of the volume fractions of the aliphatic segments A + G and A + C, respectively. The resulting profile of aliphatic segments for the modified surface (Fig. 3c) is comparable to the profile of $G_{18}$ chains in the absence of solute (dotted curve), but it is shifted outwards. The total volume fraction of aliphatic segments (A + C) at the $C_{18}$–O interface is shown in Fig. 3d, together with a profile of $C_{18}$ chains in the absence of alcohol, and here, too, the two volume fraction profiles of the aliphatic segments are very similar. With the RPLC system, accumulation of alcohol near the boundary region

changes the volume fraction profile of the grafted chains in such a way that an extension of the hydrophobic phase is established. Consequently, the total number of unfavourable contacts between A and O hardly changes. This explains why a strong correlation between the liquid–liquid distribution coefficient and the retention factor $K_i$ is obtained, even if the solute is not distributed uniformly in the grafted layer. In a non-uniform distribution, the increased number of contacts between solute and grafted chains is compensated for by a decreased number of contacts between segments of grafted chains and solvent. As long as the total volume fraction of grafted chains and hydrophobic solute is constant, their spatial distribution hardly affects the total interaction between the stationary and mobile phases.

### *7.9. Specific effects in partitioning at chemically modified surfaces in RPLC*

In this section, several additional calculations are carried out for (1) solutes with a specific affinity for the surface, (2) mixed solvents and (3) solutes with different shapes.

#### *7.9.1. Specific adsorption of solutes*

In the foregoing solutes accumulate in or near a grafted layer because of an attraction between solute and grafted layer and/or a repulsion between solute and mobile phase. However, in some instances, the solute also accumulates because it has an affinity for the surface sites on which no grafted chains are anchored. This may lead to undesired effects such as "tailing". In practice, such effects are often reduced by end-capping, *i.e.*, methylation of the surface hydroxyls, which renders the surface completely hydrophobic so that the surface–solute and grafted chain–solute interactions become very similar. The following calculated results illustrate the effects of a specific affinity of solute and/or solvent for the surface.

Calculations were carried out for a system consisting of 20 lattice layers partly filled with grafted chains ($G_{18}$) in equilibrium with the bulk solution of an aqueous solvent (monomer W) containing a solute. As before, the surface coverage $\sigma = 0.3$, and consequently $18 \cdot 0.3 = 5.4$ equivalent monolayers of $G_{18}$ are present in the system. The solute is chosen to be a chain molecule consisting of five aliphatic segments of type A (identical with G) and one segment of type B ($A_5B$). The Flory–Huggins interaction parameters ($\chi_{xy}$) are taken as $\chi_{AW} = \chi_{AB} = 2$ and $\chi_{BW} = 0$, *i.e.*, meant to be representative of an alcohol adsorbing from an aqueous solution on a $C_{18}$ bonded phase. Note that with this choice segments B and W are identical. The bulk solution volume fraction of $A_5B$ is taken as $3 \cdot 10^{-3}$. The RIS scheme is used with the energy difference between a *trans* and a *gauche* conformation of $1 \cdot kT$. The surface is represented with an S and the $\chi$ parameters between the various segments and the surface will be specified below.

In Fig. 4a results for $\chi_{WS} = \chi_{BS} = \chi_{AS} = 0$ are displayed, representing the case that there is no specific affinity for the surface, as discussed in the foregoing. In Fig. 4b the B segment of $A_5B$ has been given a specific affinity for the surface: $\chi_{BS} = -10$, simulating a specific interaction between B and silica. In this case segments B and

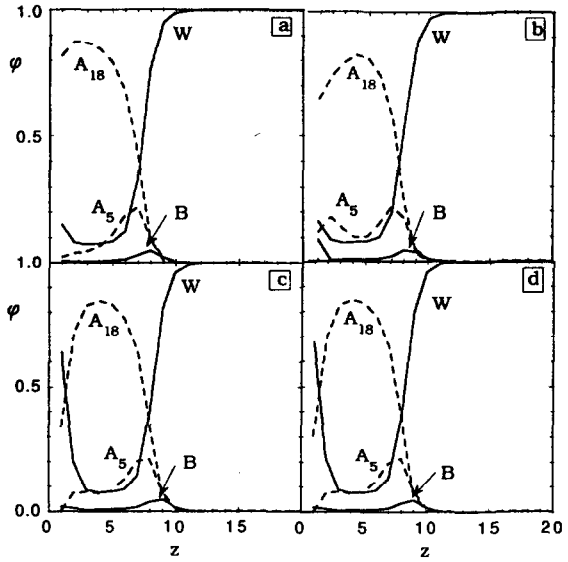


Fig. 4. Volume fraction profiles of $A_5B$, grafted $A_{18}$ and solvent W. $\sigma = 0.3$, $U^{st} = 1$, bulk volume fraction of $A_5B$ is $3 \cdot 10^{-3}$. $\chi$ Parameters: $\chi_{AB} = \chi_{AW} = 2$, $\chi_{BW} = 0$. (a) $\chi_{AS} = \chi_{BS} = \chi_{WS} = 0$; (b) $\chi_{AS} = \chi_{WS} = 0$, $\chi_{BS} = -10$; (c) $\chi_{AS} = 0$, $\chi_{WS} = \chi_{BS} = -10$; (d) $\chi_{AS} = 0$, $\chi_{WS} = \chi_{BS} = -20$.

W are no longer identical. The adsorption energy of B leads to accumulation of $A_5B$ near the solid surface side owing to "head-on" adsorption. As a result, the profile of A segments now shows an additional maximum close to the surface, where some of the A segments of the grafted $G_{18} = A_{18}$ chains have been displaced from the surface by A and B segments belonging to $A_5B$. The solution-side of the volume fraction profiles remains almost unchanged.

Fig. 4c and d give results for the case that not only the B segments, but also the solvent W have an affinity for the surface, so that B and W are identical again. In Fig. 4c $\chi_{WS} = \chi_{BS} = -10$ and in Fig. 4d $\chi_{WS} = \chi_{BS} = -20$. In these cases the accumulation of W in layer 1 is fairly pronounced. It has displaced almost all of the unanchored A segments from the surface and also all possible A segments of the grafted chain, as the volume fraction of $A_{18}$ in layer 1 is close to its minimum value of 0.3. Even though the volume fraction of solvent in layer 1 is so high, additional $A_5B$ is present close to the solid surface in comparison with the situation in Fig. 4a.

The relative presence of W and $A_5B$, where $\chi_{WS} = \chi_{BS}$, near the surface depends on a number of factors. The main factor of importance is that the bulk volume fraction of W is much higher than that of $A_5B$. The latter is a chain molecule and we know already that it is more difficult to make space for it available near the surface. Note that the volume fraction profile of $A_{18}$ in layer 2 in Fig. 4c and d is lower than that in Fig. 4a, mainly to make space available for the $A_5B$ molecules rather than for W molecules. Although sterically it is unfavourable to have much $A_5B$ in the layers near the surface, the contact interactions between the aliphatic part of the $A_5B$ chain with the grafted layer are preferred to the AW contact interactions. Apparently, this is an important contribution because $A_5B$ is accumulated significantly in layers 2 and 3 (as compared with Fig. 4a). The accumulation is, however, considerably less than in Fig. 4b, where the W segments have a low affinity for the surface. As seen, increasing the interaction parameter $\chi_{WS} = \chi_{BS}$ from $-10$ to $-20$ hardly changes the situation. Already for $\chi_{WS} = \chi_{BS} = -10$ almost all unanchored A segments are displaced from layer 1, so that a further simultaneous increase of the affinity of B and W for the surface has no effect.

### 7.9.2. *Mixed solvents*

The retention of a solute can be reduced drastically by adding a co-solvent to W (water), which effectively changes the solvent strength. As stated before, with the SCFA model solvent mixtures and differences in size between various solvent molecules can easily be taken into account. In the following calculations, the solution parameters are the same as in the previous calculations. All interaction parameters with the surface have been set to zero. The bulk volume fraction of $A_5B$, from now on denoted $A_5W$ to stress that the head group segment of the solute is identical with the solvent, has been chosen much lower, *viz.*, $1 \cdot 10^{-8}$, to make sure that the Henry region of the adsorption isotherm is reached.

Results for the retention of $A_5W$ from mixtures of W and AW and from mixtures of W and $A_2W$ are plotted in Fig. 5a. At low volume fractions of co-solvent or modifier ($m$) the effect on the retention ($k$) is already marked; see Fig. 5a and note the logarithmic vertical axis. In the literature [9,175] sometimes a linear relationship between ln $k'$ and the volume fraction of methanol in water has been reported, which does not agree with the results presented in Fig. 5a or with the expected quadratic relationship as predicted by the ESP model. Linear relationships are typically obtained for solvent mixtures for which the components have a low mutual interaction ($\chi$) parameter, which is the case for methanol and water. For example, Dill [9] gives a $\chi$ value of 0.42 between methanol and water.

Apparently the calculated example in Fig. 5 represents a more complicated system as no linear relationship is observed. To analyse the situation in more detail we consider the chemical potential of a solute $i$, $\mu_i$, in a solvent mixture [137,147] as

$$\Delta\mu = \ln \varphi_i + 1 - r_i \cdot \sum_j \varphi_j r_j + \tfrac{1}{2} r_i \cdot \sum_x \sum_y \sum \chi_{xy} (\varphi^0_{xi} - \varphi_x)(\varphi_y - \varphi^0_{yi}) \quad (71)$$

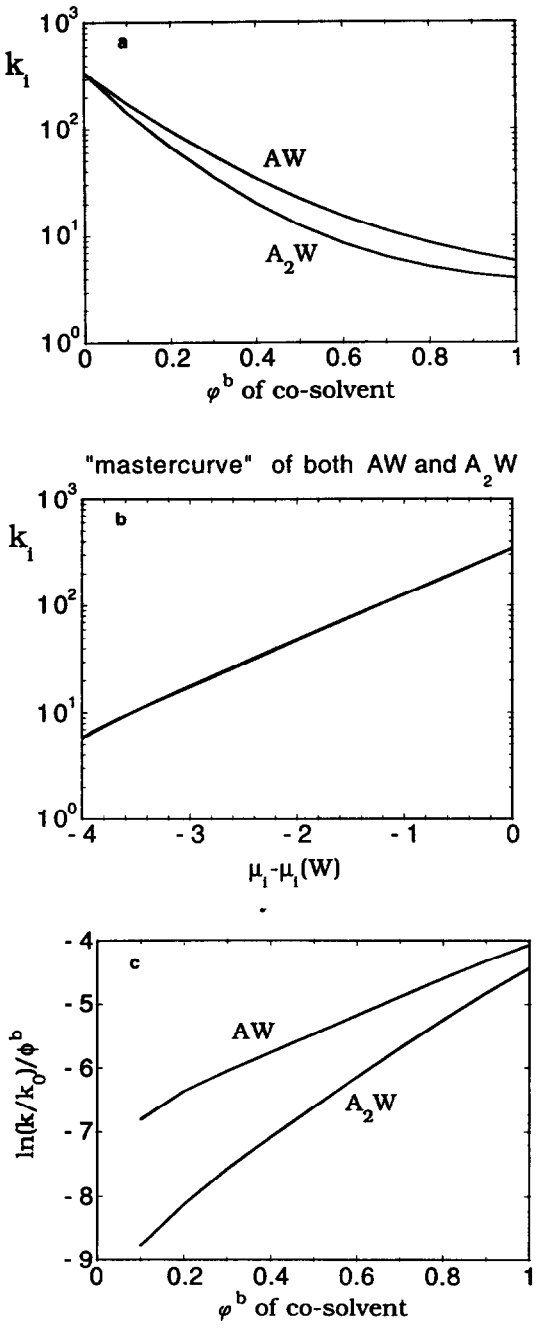


Fig. 5. Retention of $A_5W$ as a function of mobile phase composition; solvent W, modifiers AW and $A_2W$. $A_{18}$ with $\sigma = 0.3$, $U^{gr} = 1$, bulk volume fraction of $A_5W$ is $1 \cdot 10^{-8}$. $\chi_{AW} = 2$. All interaction parameters with the surface are set to zero. (a) Retention as a function of the volume fraction of modifier; (b) retention as a function of the shift in chemical potential of the solute, as calculated with eqn. 71; (c) "Dill" plot, $(1/\varphi_m)$ ln $k$ as a function of $\varphi_m$.

where $\Delta\mu = \mu_i - \mu_i^0$ and the term $\mu_i^0$ refers to the reference state of pure $i$. The subscripts $i$ and $j$ refer to molecules and the subscripts $x$ and $y$ refer to segment types. A certain segment type may be present in different molecules, for instance in the present case segment A is present in the co-solvent and the solute. The chain length of the various molecules is given by $r_{i,j}$. Note that the volume fractions $\varphi$ in this case are all bulk volume fractions ($\varphi^b$), but we drop the superscript b for simplicity. The term $\varphi_{xi}^0$ is the volume fraction of segments of type $x$ belonging to molecule $i$ in the reference state, *i.e.*, pure bulk of $i$. For $A_5W$ these values are 5/6 and 1/6 for segments A and W, respectively.

In Fig. 5b, the results for the retention of $A_5W$ in W–AW and W–$A_2W$ mixtures are replotted as a function of the shift in chemical potential of $A_5W$ in the given solvent mixture using the above equation. The curves of $A_5W$ in AW and $A_2W$ fall on the same and almost straight line. This plot shows that indeed it is the chemical potential of the solute in the solution that essentially determines the retention. Thus, a simple relationship between the composition of the solution and retention exists, in which changes in the structure of the grafted layer are relatively unimportant, common knowledge in the practice of RPLC.

Dill [9] used a plot of $(1/\varphi_m)$ ln $k'$ as a function of the volume fraction of modifier ($m$) for the case that the $\chi$ parameter between the main solvent ($s$) and the modifier is high, and at not too low $\varphi_m$ a linear plot could then be obtained. This is in accordance with the present view because in the relationship for the chemical potential the term $\varphi_s \chi_{sm} \varphi_m$ appears. Since $\varphi_s$ can be written as $1 - \varphi_m$ if the volume fraction of solute is sufficiently low, a "quadratic" term can be defined [9]. Division of ln $k'$ by $\varphi_m$ makes the linear terms in $\varphi$ constant. Therefore, if the quadratic term dominates the retention behaviour, the relationship between $(1/\varphi_m)$ ln $k'$ and $\varphi_m$ is linear.

Results in these terms are given in Fig. 5c and a reasonably linear plot is obtained for both AW and $A_2W$ at not too low $\varphi_m$. This illustrates the importance of the quadratic term (see also Schoenmakers and co-workers [3–6]). As we

have the equation of the chemical potential of the solute in a solvent mixture available, however, we prefer to plot the chemical potential as a function of ln $k'$, but in practice the linearity as demonstrated in Fig. 5c may be useful.

From the fact that the W–AW mixture leads to a curved ln $k'(\varphi_m)$ plot, we have to conclude that the W–AW mixture does not represent a water–methanol mixture, which would certainly give a straight line for this plot. The present W–AW mixture is more representative of a water–acetonitrile mixture. This complication arises because our way of modelling of water and alcohol is too simple (monomers without preferential orientation, with every hydrophobic group represented by the same A segment and every hydrophilic group by W).

Using monomeric B as the modifier with $\chi_{WB} = 0$ and $\chi_{AB} = 1$, a system resembling the water–methanol system more closely can be simulated. The results are shown in Fig. 6. In this instance an almost linear relation between ln $k_i$ and the volume fraction of modifier exists, as already anticipated above. Note that the structure of the grafted layer changes with the volume fraction of modifier because of the difference between $\chi_{AW}$ and $\chi_{AB}$ (see above). However, the change is always small and it does not affect the linearity of this logarithmic plot.

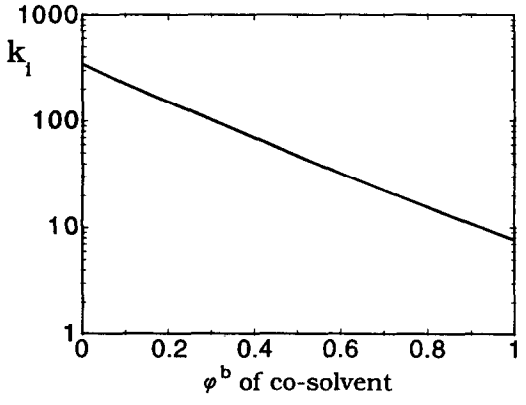


Fig. 6. Retention of $A_5W$ as a function of mobile phase composition; solvent W, modifier M. $A_{18}$ with $\sigma = 0.3$, $U^{gt} = 1$, bulk volume fraction of $A_5W$ is $1 \cdot 10^{-8}$. $\chi_{AW} = 2$, $\chi_{AM} = 1$, $\chi_{MW} = 0$. All interaction parameters with the surface are set to zero.

*7.9.3. Solutes with different shapes*

In the above the resemblance between retention in RPLC and liquid–liquid partitioning and the disorder of the grafted layer has been emphasized. However, in some instances, molecules with an identical liquid–liquid partition coefficient can be separated by RPLC. In this section we shall investigate the retention of $A_n$ isomers. As the isomers we modelled fully flexible linear $A_n$ molecules (*gauche–trans* energy, $U^{gt} = 0$), branched (star shaped) $A_n$ molecules with $U^{gt} = 0$, and $A_n$ rods, forced in an all-*trans* conformation by putting $U^{gt}$ to infinity. These solutes have identical liquid–liquid partitioning coefficients because, if calculated with the Flory equations, the shape of the molecules is irrelevant. For the RPLC calculations we used a surface modified with $A_8$ ($U^{gt} = 1$) and varied the surface coverage, $\sigma$. The interaction parameter $\chi_{AW} = 1.5$. The bulk volume fraction of $A_n$ is $1 \cdot 10^{-12}$, again a lower value than in the previous calculations, because we shall investigate the effect of chain length while phase separation should be prevented. For the same reason we reduced the $\chi$ parameter with respect to the previous calculations. The results for $n = 4$ are given in Fig. 7a. For all isomers retention shows a maximum as a function of surface coverage, as discussed above (*cf.* ref. 16). Hardly any difference can be detected between rods, branched and flexible $A_4$. For longer molecules, such as $A_7$, Fig. 7b shows that the retention of the rods is lower. The reason for this is that in contrast to flexible molecules, rod-like molecules cannot adjust their conformation on sorption into the grafted layer.

If we apply the SCAF (self-consistent anisotropic field) theory, bond cooperativity or alignment can be taken into account [28,137,139]. Leermakers and Scheutjens used the SCAF theory to predict the gel–liquid transition in membranes. SCAF should not be looked upon as an extension of the SCFA used so far, because it has a different scheme for the calculation of the entropy. SCFA is an extension of the Flory solution theory to systems which are inhomogeneous in one dimension. Far from the interface the composition of the system will be the same as calculated with the Flory equations. For SCAF this is not the case. As a result, the $\chi$-parameters

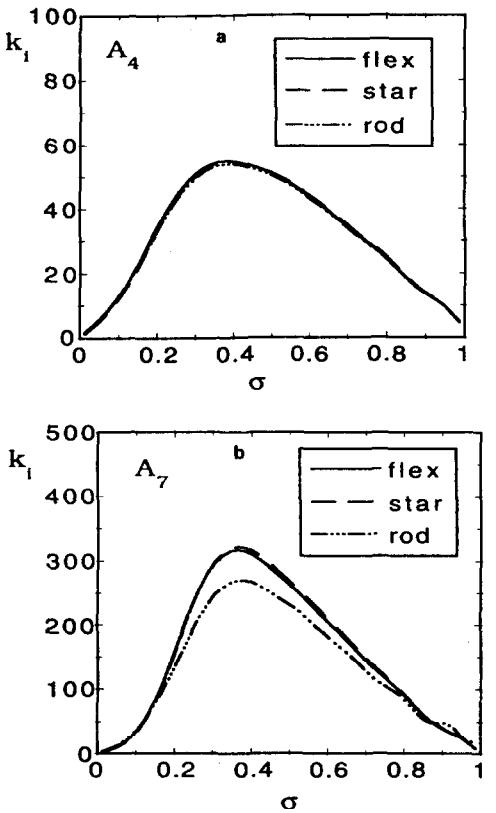


Fig. 7. Retention of $A_n$ isomers, rods, stars and flexible chains in $A_8$ ($U^{gt} = 1$) grafted layers as a function of the surface coverage. $\chi_{AW} = 1.5$. (a) $A_4$; (b) $A_7$.

chosen in SCAF cannot be compared with those in SCFA directly.

In the calculated retention coefficients of $A_4$ and $A_7$ isomers with SCAF we now find that at high coverages the rods reach higher $k$ values than the flexible molecules and the branched molecules. The rods and the chains of the grafted layer can align, which does not have much consequence for the entropy of the rods. Flexible chains will lose more entropy on alignment and therefore their retention stays lower at high coverages. Theoretically, we find alignment only at very high coverages, because alignment in the system can only occur perpendicular to the lattice layers. This might be an overestimation because a collective "tilt" or a local alignment of anchored chains is theoretically not allowed. Such alignment effects have been noted frequently in the literature [28,137,139]. The behaviour of the branched molecules, which have one bond that cannot align with respect to the fully flexible chains, is more complicated and a chain length dependence is found: for $A_4$ the retention of branched (*i.e.*, star-shaped) chains is below that for the rods and the flexible chains (see Fig. 8a), but for $A_7$ the retention of the star molecules is between that for the rods and the flexible chains (see Fig. 8b). Branching introduces more stiffness in the isomers, which for short molecules leads to a decrease in the probability of aligning and for longer chains to an increase in the probability of aligning with respect to the flexible chains. If we put $U^{gt}$ equal to infinity instead of to zero, the number of bonds that cannot align with the grafted chains increases as a function of solute chain length,

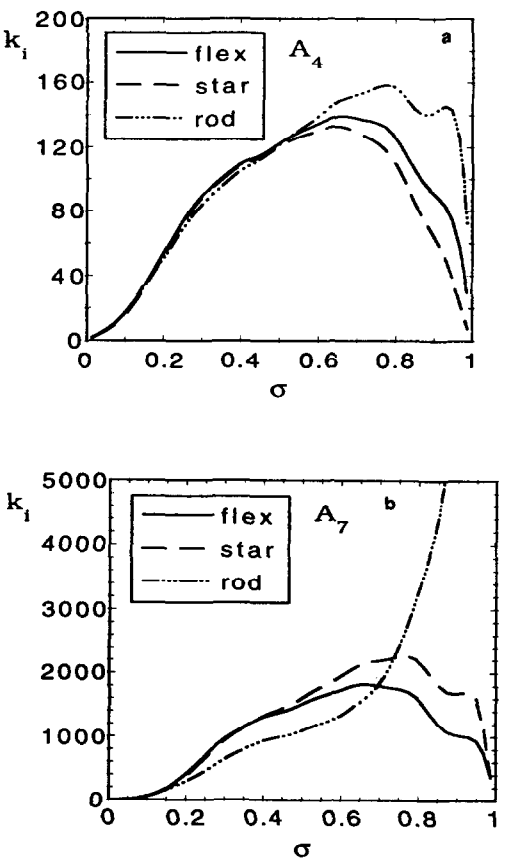


Fig. 8. Retention of $A_n$ isomers, rods, stars and flexible chains in $A_8$ ($U^{gt} = 1$) grafted layers as a function of the surface coverage. $\chi_{AW} = 1.5$, SCAF theory. (a) $A_4$; (b) $A_7$.

and lower retention of the branched isomers is expected.

It is interesting to look at the chain length effect. For instance, Tchapla *et al.* [169] stated that alignment stops when the chain length of the solute exceeds the length of the grafted chains. That this is not necessarily the case is shown in Fig. 9, where even $A_{10}$ rods have in a high coverage $A_8$ layer a much higher retention than the flexible chains. However, it is important to note that alignment starts only at the higher coverages. For even longer chains some alignment is still found (see Fig. 10). The chain length effect of flexible chains is very pronounced, as shown in Fig. 11a and in agreement with the earlier results above and in ref. 16. For rods the chain length effect at high coverage is much less (see Fig. 11b). Especially between $A_{10}$, $A_{12}$ and $A_{15}$ hardly any difference can be found at very high $\sigma$. The number of segments of these solutes, which can align with $A_8$-grafted chains, is the same for these chain lengths and therefore the number of contacts with the grafted phase does not depend on the chain length. The number of contacts with the solvent does depend on the chain length, but for unknown reasons this seems to be not very important in this instance. Interpretation of these results for rods at unrealistically high coverages for RPLC should be done with some reserve.

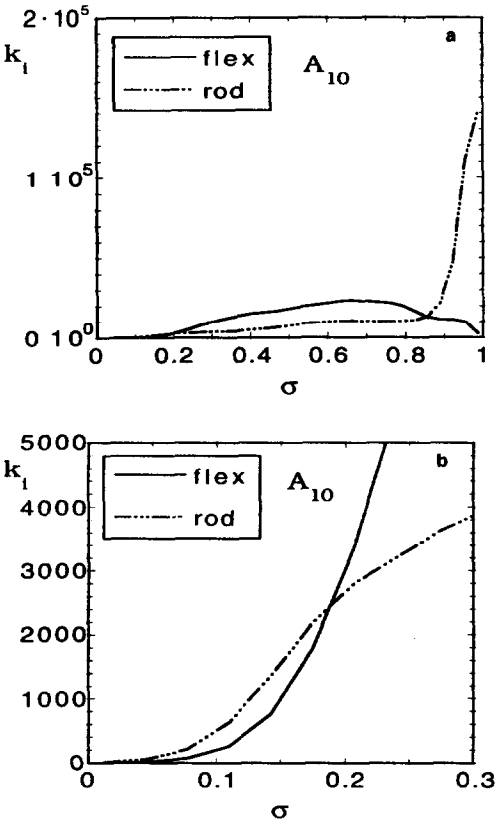


Fig. 9. Retention of $A_{10}$ rods and flexible chains in $A_8$ ($U^{gl} = 1$) grafted layers as a function of the surface coverage. $\chi_{AW} = 1.5$, SCAF theory. (b) Enlargement of part of (a).

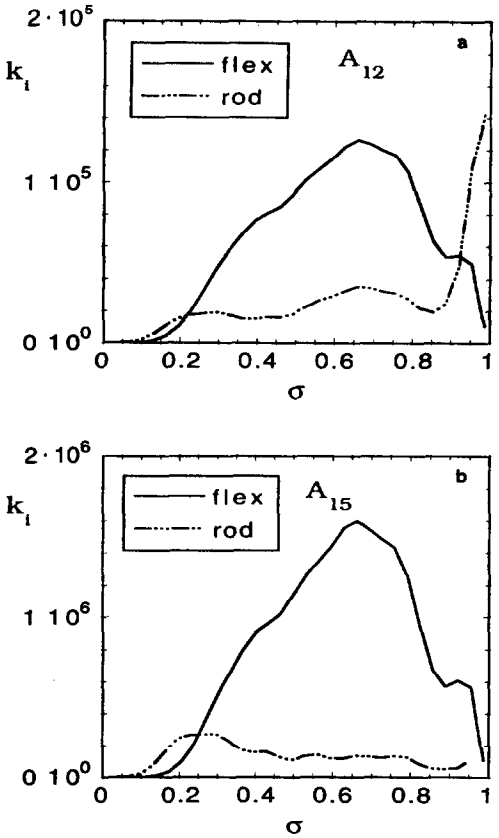


Fig. 10. Retention of (a) $A_{12}$ and (b) $A_{15}$ rods and flexible chains in $A_8$ ($U^{gl} = 1$) grafted layers as a function of the surface coverage. $\chi_{AW} = 1.5$, SCAF theory.

Another interesting effect is that the partition coefficient of long rods ($>A_7$) at low coverages is higher than those of flexible molecules. Rods do not lose much entropy on uptake in the grafted layer and therefore their retention at low coverage is considerably higher (see Figs. 9–11). We can distinguish three regions in the retention

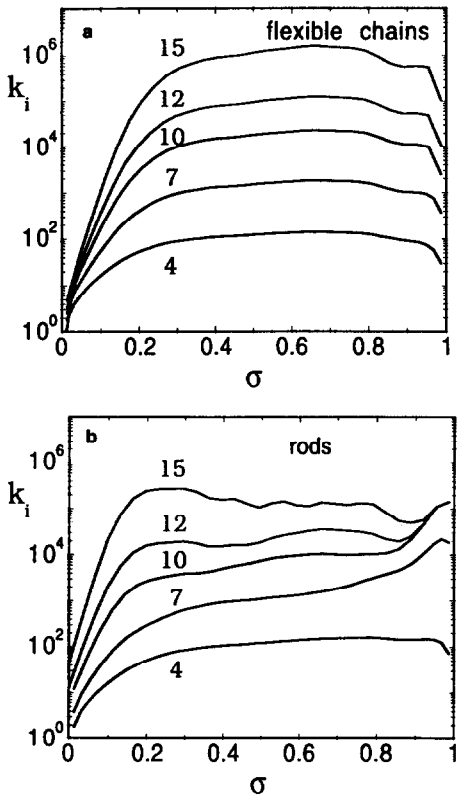


Fig. 11. Retention of $A_n$ (a) flexible chains and (b) rods in $A_8$ ($U^{s\prime} = 1$) grafted layers as a function of the surface coverage. $\chi_{AW} = 1.5$, SCAF theory.

of rods as a function of the coverage with grafted chains. At very low $\sigma$ the rods adhere preferentially because they lose less entropy on binding than flexible chains. At intermediate coverages the flexible chains adhere more because they can adjust their conformation and "fit in" the grafted layer in many different ways. At high coverages the rods can align (vertically) with the grafted chains, again without the loss of much conformational entropy, and therefore they are preferentially adhered as compared with the flexible chains.

## 8. CONCLUSIONS

The extended solubility parameter (ESP) model as reviewed in this paper, is based on an extension of the Hildebrand–Scatchard mixing rule for enthalpic interactions. Using the internal pressure concept, we developed a four-parameter ESP model, which consists of classical symmetric interactions (dispersion and orientation) and asymmetric electron- or proton (acid–base) transfer interactions. The entropic contribution to the free energy of mixing is accounted for by the (Staverman–)Flory–Huggins pseudo-lattice model.

It is shown that, using reliable estimation procedures for the partial solubility parameters based on generalized thermodynamic functions and using modern equations of state, liquid–liquid distribution data can be predicted within 20% from experimental data, also for polar systems as used in RPLC, FIA and engineering applications. This result is comparable to the predictions based on MOSCED and Hansch (octanol–water) methods. Improved predictions, within 10%, can be obtained by characterizing the system with well defined standard compounds analogous to the Rohrschneider approach in GC. Again four main factors seem to contribute to the partitioning mechanism, proving that no important interactions (such as induction forces) are left out. The latter procedure can also be applied to chemically bonded stationary phases used in RPLC, for which no reliable equations of state are available.

To model these surfaces with grafted chain molecules in contact with a solution, the self-consistent field theory for adsorption (SCFA) of chain molecules has been extended, yielding a much more detailed picture of the behaviour of reversed-phase systems. If the solvent quality is poor for the anchored chains, the case most relevant to RPLC, the chains tend to form a separate phase with a thin interphase with the solution. Neither aliphatic nor amphiphilic solute molecules are distributed uniformly in the grafted layer, not even aliphatic chains in an aliphatic layer. Especially if the solutes are chain molecules they are predominantly enriched in the boundary region between grafted chains and solvent. For homologous series the distribution coefficient increases nearly linearly with increasing aliphatic chain length of the solute, with a slope depending on the solute–solvent interactions and, for small grafted chains, on the

grafted chain length. The small non-linearity is caused by entropic factors. The slope shows that retention in RPLC cannot be modelled as adsorption on a rigid solid phase, but it resembles liquid–liquid partitioning.

Further, it appears that retention shows a maximum as a function of the surface coverage. With an increase in the surface coverage two opposing effects occur: the hydrodynamic volume of the stationary phase increases and the effect of the presence of the surface becomes smaller, both effects leading to more retention. On the other hand, the ordering in the grafted layer increases, which leads to less retention. At grafting densities common in RPLC, retention is close to its maximum and contact interactions dominate the retention behaviour. On uptake of solute in or on a grafted layer, relatively unfavourable solute–solvent and grafted chain–solvent contacts are replaced by more favourable grafted chain–solute contacts and solvent is liberated. Consequently, we conclude that, at the usual coverages in RPLC, the capacity factor of a solute is strongly related to the liquid–liquid partition coefficient. The deviations from this correlation are most pronounced at low and high grafting densities. On adherence of solutes, the boundary between hydrophilic segments (solvent + hydrophilic solute segments) and hydrophobic segments (grafted layer + hydrophobic solute segments) is hardly altered but it is shifted towards the solution by enrichment of the hydrophobic segments near the outer region of the grafted layer.

To describe specific effects on partitioning and retention in RPLC, the SCFA theory can easily be adjusted. In this paper three systems to which these theories can be applied have been discussed. The calculated effects of specific affinity for the bare solid surface and that of mixed solvents are in qualitative agreement with experiment. In order to describe shape selectivity, a different, but related theory, SCAF, must be applied. Calculated results indicate that shape selectivity depends mainly on the size of the molecules (*i.e.*, chain length) and the grafting density. Whether or not alignment of the solute molecules with the grafted chains can occur is another important factor.

## 9. SYMBOLS

| | |
|---|---|
| $a$ | length of segment |
| $a_{in}$ | term in binomial function, eqn. 43 |
| A | segment type A, usually a hydrophobic segment |
| $A$ | constant in equations (*e.g.*, eqn. 6) |
| $\|A\|$ | matrix of $a_{in}$ |
| $A_n$ | chain of $n$ segments of type A |
| $B$ | constant in equations (*e.g.*, eqn. 6) |
| c | conformation of a chain molecule expressed in layer numbers $z$ where segments are present |
| $\tilde{c}$ | $= n/V$ average molar concentration |
| $c$ or CED | $= -u/v$, cohesive energy density |
| $c_h$ | constant after Mijnlieff and Jaspers [154] |
| $C$ | constant in equations (*e.g.*, eqn. 6) |
| $C_i$ | normalization constant for molecules $i$ |
| $D$ | diameter |
| D | $= a^2/6\tau$, diffusion coefficient [113] |
| ESP | Extended solubility parameter model |
| $f^c(z)$ | fraction of segments of conformation $c$ in layer $z$ |
| $\Delta f$ | number of degrees of freedom |
| $F$, $\mathcal{F}$ | force; potential field force |
| $\mathcal{F}_S$ | $= Hz$, entropic spring force |
| FH | Flory–Huggins |
| FIA | flow-injection analysis |
| $g$ | number of segments in blob; free energy per segment; *gauche* |
| $g^+$, $g^-$ | *gauche* conformations |
| $G$ | $= {}_i\Sigma\, n_i\mu_i = H - TS$, Gibbs free energy |
| $G_x(z)$ | $= \exp[-u_x(z)/kT]$, weighting factor (probability) for segment $x$ in layer $z$ |
| $G_{x,i}(z)$ | $= \exp\{-[u_{x,i}(z)/kT]\}$, statistical weight for segments $x$ of molecule $i$ in layer $z$ |
| $G_i(z,s)$ | segment weighting factor for segment $s$ of molecule $i$ in layer $z$ |
| $G_i(z,s_1)$ | end segment distribution function in layer $z$ of molecules $i$ ($s$ segments long) with segment 1 in an arbitrary layer |
| $G_n$ | grafted chain of $n$ segments of type G |

| | |
|---|---|
| $h$ | partial molar enthalpy |
| $\Delta h^v$ | latent heat of vaporization |
| H | segment type H, used for the hydrophilic headgroup of the solute |
| $H$ | $= U + pV$, enthalpy; spring force constant (Hooke) |
| HDC | hydrodynamic chromatography |
| $k^2$ | permeability factor |
| $k_1$ | Henry's Law constant |
| $k_i$ | alternative capacity factor |
| $k'_i$ | $= (t_i - t_0)/t_0$, capacity factor of solute $i$ |
| $K_i^c$ | $= \bar{c}_{is}/\bar{c}_{im} = K_i^x(v_m/v_s)$, partition coefficient based on concentrations |
| $K_i^x$ | $= \bar{x}_{is}/\bar{x}_{im}$, mole fraction-based partition coefficient |
| $K_{i(LL)}$ | liquid–liquid partition coefficient of solute $i$ |
| $l$ | $= \langle r^2 \rangle^{1/2}$ average end-to-end distance in chain |
| $L$; L | $= Na$, Kuhn length of chain molecule; number of lattice sites per layer |
| $\mathscr{L}$ | length of a cigar-like grafted chain consisting of blobs |
| $m$ | mass; count number (of interactions), power, monomer |
| M; $M$ | number of lattice layers; molecular mass |
| $M_0$ | molecular mass of monomer segment |
| $n$ | number (of segments, segment type in a chain, moles, molecules, sites) |
| $N$ | total number (of segments, sites, etc.) |
| O | segment type O, used for the monomeric solvent |
| $p$ | pressure |
| $P$ | Langmuir partition ratio |
| $\mathscr{P}$ | $= (\partial u/\partial v)_T$, the internal pressure |
| $q_i$ | segment weighting factor for layer $i$ in Dill's theory |
| $q^c$ | number of parallel bonds of $r$-mer in conformation $c$ |
| $Q$ | mass flow-rate |
| $Q^0$ | mass flow in the absence of polymer |
| $r$ | chain length in number of chain segments |
| $r^c$ | number of segments of $r$-mer in conformation c |
| $\langle r^2 \rangle$ | $= Na^2$ mean square end-to-end distance in chain |
| $R$ | gas constant; radius |
| $R_F = aN^{3/5}$ | Flory radius of chain molecules in solution |
| RST | regular solution theory |
| RIS | rotational isomeric state approximation |
| $s$ | solvent; $= 1, \ldots, r$, segment ranking number in a chain; partial molar entropy |
| $s'$ | segment ranking number of segment $s'$, next to segment $s$, see eqn. 56 |
| S | solid; surface |
| $S$ | entropy |
| $S^{(un)mix}$ | entropy of a (un)mixed system |
| SEC | size-exclusion chromatography |
| SCAF | self-consistent anisotropic field |
| SCF(A) | self-consistent field (for adsorption) |
| $t$ | *trans* conformation; time |
| $t_i$ | residence (retention) time of solute $i$ |
| $t_0$ | mobile phase residence (dead) time |
| $T$ | temperature |
| $u$ | internal potential energy per mole |
| $u'(z)$ | hard core potential in layer $z$ |
| $u_x(z)$ | potential for segments of type $x$ in layer $z$ |
| $u_x^{int}(z)$ | $= {}_y\Sigma\, \chi_{xy}[\langle \varphi_y(z) \rangle - \varphi_y^b]kT$, total interaction potential for segments $x$, $y$, including S |
| $\Delta u^v$ | molar heat of vaporization |
| $U$ | internal energy |
| $U^{gt}$ | energy difference between a *trans* and a *gauche* conformation |
| $v$ | velocity |
| $v'$ | $= dv/dz$, velocity gradient |
| $v_p$ | $= (M_p/\rho_p)$, molar volume of phase $p$ |
| $v_{liq}$ | molar volume of pure liquid |
| $v_{gas}$ | molar volume of pure gas |
| $V$ | (phase) volume |
| $V_L$ | volume of lattice site |
| $V_m$ | volume of the mobile phase |
| $V_s$ | volume of the stationary phase |
| $w_i$ | $= n_i m_i/W$, mass fraction of $i$ |
| $W$ | total mass |
| $x$ | coordinate, segment |
| $\bar{x}_i$ | (average) mole fraction of solute $i$ in phase $p$ |
| $z$ | layer number, coordinate axis |

$z_{pn}$ term in binomial function eqn. 43
$Z$ number of neighbouring lattice sites
Z $= pv/RT$ compressibility factor

*Greek letters*

$\gamma_{ip}$ activity coefficient of $i$ in $p$
$\delta_i$ solubility parameter of $i$, square root of CED
$\delta_s$ $= V_s/V_L$, the thickness of the stationary phase, expressed in number of layers
$\delta_h$ hydrodynamic layer thickness
$\delta_H$ solubility parameter for hydrogen bonding
$\Delta$ difference between two quantities
$\zeta$ perpendicular coordinate to the wall; number of allowed bond angles
$\eta$ viscosity
$\theta_{is}$ amount of $i$ retained in/at the stationary phase per surface site
$\theta_i$ $= n_i r_i/L$, amount of $i$, with $r_i$ segments, expressed in equivalent number of layers
$\lambda_{-1}$ fraction of neighbouring lattice sites in the previous layer
$\lambda_0$ fraction of neighbouring lattice sites in the same layer
$\lambda_1$ fraction of neighbouring lattice sites in the next layer
$\mu$ chemical potential (partial molar free energy): $\mu_i = (\partial G/\partial n_i)_{p,T,n_j}$
$\prod_i$ product of terms in $i$
$\rho$ density of the (liquid) phase
$\sigma$ $= n_{chains}/N_{sites}$, surface coverage, grafting density
$\sigma_{sep}$ $\sim N^{-6/5}$, maximum surface coverage for separated chains
$_i\Sigma, \sum_i$ summation of terms in $i$
$\tau$ step time in random walk [113]
$\varphi_i$ $= n_i v_i/V$, volume fraction of $i$
$\varphi_m$ volume fraction of modifier in mobile phase
$\bar{\varphi}_{ip}$ average volume fraction of $i$ in $p$ ($p$ = m, s)
$\varphi_i(z)$ volume fraction of molecules $i$ in layer $z$
$\varphi_x(z)$ volume fraction of segments $x$ in layer $z$
$\varphi_{xi}(z)$ volume fraction of segments $x$, belonging to molecules $i$, in layer $z$
$\varphi_i(z,s)$ volume fraction of segments $s$ of molecule $i$ in layer $z$
$\varphi_{xi}(z,s)$ volume fraction of segments $s$ of molecule $i$ in layer $z$, where segments $s$ must be of type $x$
$\langle\varphi_x(z)\rangle$ average fraction of contacts (segments $x$) around a site in layer $z$
$\varphi_i^b$, $\bar{\varphi}_i^b$ $= \varphi_i(z \rightarrow \infty)$, bulk volume fraction of molecules $i$
$\varphi_s$ solvent volume fraction
$\varphi^g(z)$ grafted chain volume fraction in layer $z$
$\chi_{ip}$ Flory–Huggins interaction parameter for solute $i$ in phase $p$: standard free energy $\Delta\mu_{ip}/RT$ for transfer solute $i$ from pure $i$ to $p$
$\omega^c$ degeneracy of $r$-mer in conformation c
$\Omega$ probability

*Subscripts and superscripts*

a acidic interaction
b basic interaction; blob; bulk
c concentration based
c conformation of a chain molecule expressed in layer numbers $z$, where segments are present
d dispersion interaction
D diameter
e excess contribution
ex exchange interaction
ext external field
H hydrogen bonding (acid–base) interaction
h enthalpic contribution
$i$ index for molecule $i$
ind induction contribution
int internal; interaction
kin kinetic interactions
L lattice based
m mobile phase
$m$ modifier
mix under mixed conditions
np non-polar interactions
o orientation interaction
O octanol; solvent
p particle; polymer

| | |
|---|---|
| $p$ | phase |
| s | entropic contribution; stationary phase; solid |
| $s$ | solvent |
| S | solid |
| T | total |
| v | vaporization interactions |
| $x$ | mole fraction based |
| $x$, $y$ | indices for segment types |
| 0 | standard condition |
| $\theta$ | overall |

## REFERENCES


1 K.K. Unger, *Porous Silica*, Elsevier, Amsterdam, 1979.
2 R. Tijssen, H.A.H. Billiet and P.J. Schoenmakers, *J. Chromatogr.*, 122 (1976) 185.
3 P.J. Schoenmakers, H.A.H. Billiet, R. Tijssen and L. de Galan, *J. Chromatogr.*, 149 (1978) 519.
4 P.J. Schoenmakers, H.A.H. Billiet and L. de Galan, *J. Chromatogr.*, 185 (1982) 179; 218 (1981) 261; 282 (1983) 107.
5 P.J. Schoenmakers, H.A.H. Billiet and L. de Galan, *Chromatographia*, 15 (1982) 205.
6 P.J. Schoenmakers, *Optimization of Chromatographic Selectivity, a Guide to Method Development* (*Journal of Chromatography Library*, Vol. 35), Elsevier, Amsterdam, 1986.
7 P. Jandera, H. Colin and G. Guiochon, *Anal. Chem.*, 54 (1982) 453.
8 J.A. Marqusee and K.A. Dill, *J. Chem. Phys.*, 85 (1986) 434.
9 K.A. Dill, *J. Phys. Chem.*, 91 (1987) 1980.
10 K.A. Dill, J. Naghizadeh and J.A. Marqusee, *Annu. Rep. Phys. Chem.*, 39 (1988) 425.
11 J.G. Dorsey and K.A. Dill, *Chem. Rev.*, 89 (1989) 331.
12 P.T. Ying, J.G. Dorsey and K.A. Dill, *Anal. Chem.*, 61 (1989) 540.
13 Cs. Horváth, W.R. Melander and I. Molnar, *J. Chromatogr.*, 125 (1976) 129; *Anal. Chem.*, 49 (1977) 142.
14 W.R. Melander and Cs. Horváth, in Cs. Horváth (Editor), *HPLC, Advances and Perspectives*, Vol. 2, Academic Press, New York, 1980, p. 113.
15 M. Jaroniec and D.E. Martire, *J. Chromatogr.*, 351 (1986) 1; 387 (1987) 55.
16 M.R. Böhmer, L.K. Koopal and R. Tijssen, *J. Phys. Chem.*, 95 (1991) 6285.
17 D.E. Martire and R.E. Boehm, *J. Phys. Chem.*, 87 (1983) 1045.
18 D.E. Martire and R.E. Boehm, *J. Phys. Chem.*, 84 (1980) 3620.
19 A.T. Clark and M. Lal, *J. Chem. Soc., Faraday Trans. 2*, 74 (1978) 1857.
20 T. Cosgrove, T. Heath, B. van Lent, F.A.M. Leermakers and J.M.H.M. Scheutjens, *Macromolecules*, 20 (1987) 1692.
21 A. Chakrabarti and R. Toral, *Macromolecules*, 23 (1990) 2016.
22 Th.D. Hahn and J. Kovac, *Macromolecules*, 23 (1990) 5153.
23 P.G. de Gennes, *Scaling Concepts in Polymer Physics*, Cornell University Press, Ithaca, NY, 1979, 1985; *Adv. Colloid Interface Sci.*, 27 (1987) 189.
24 P.G. De Gennes, *Macromolecules*, 13 (1980) 1069.
25 J.M.H.M. Scheutjens and G.J. Fleer, *J. Phys. Chem.*, 83 (1979) 1619; 84 (1980) 178; *Macromolecules*, 18 (1985) 1882.
26 O.A. Evers, J.M.H.M. Scheutjens and G.J. Fleer, *Macromolecules*, 23 (1990) 5221; O.A. Evers, *Ph.D. Thesis*, Wageningen Agricultural University, Wageningen, 1990.
27 B. van Lent and J.M.H.M. Scheutjens, *Macromolecules*, 22 (1989) 1931; B. van Lent, *Ph.D. Thesis*, Wageningen Agricultural University, Wageningen, 1989.
28 F.A.M. Leermakers and J.M.H.M. Scheutjens, *J. Chem. Phys.*, 89 (1988) 3264; F.A.M. Leermakers, *Ph.D. Thesis*, Wageningen Agricultural University, Wageningen, 1988.
29 H.J. Ploehn, W.B. Russel, B. William and C.K. Hall, *Macromolecules*, 21 (1988) 1075; 22 (1989) 266.
30 M. Björling, *Macromolecules*, 25 (1992) 3956.
31 M. Muthukumar and J.-S. Ho, *Macromolecules*, 22 (1989) 965.
32 S.T. Milner, T.A. Witten and M.E. Cates, *Macromolecules*, 21 (1988) 2610; 22 (1989) 853; *Europhys. Lett.*, 5 (1988) 413.
33 E.B. Zhulina, O.V. Borisov and V.A. Priamitsyn, *J. Colloid Interface Sci.*, 137 (1990) 495; E.B. Zhulina, O.V. Borisov and L. Brombacher, *Macromolecules*, 24 (1991) 4679; E.B. Zhulina, O.V. Borisov, V.A. Priamitsyn and T.M. Birshtein, *Macromolecules*, 24 (1991) 140; see also ref. 133.
34 A.N. Semenov, *Sov. Phys. JETP*, 61 (1975) 733.
35 J.H. Hildebrand, J.M. Prausnitz and R.L. Scott, *Regular and Related Solutions*, Van Nostrand Reinhold, New York, 1970.
36 J.M. Prausnitz, *The Molecular Thermodynamics of Fluid-Phase Equilibria*, Prentice Hall, Englewood Cliffs, NJ, 1969 (2nd ed. with R.N. Lichtenthaler and E.G. de Azevedo, 1986).
37 P.J. Flory, *Principles of Polymer Chemistry*, Cornell University Press, Ithaca, NY, 1st ed., 1953; 2nd ed., 1971.
38 B.L. Karger, L.R. Snyder and C. Eon, *J. Chromatogr.*, 125 (1976) 71; *Anal. Chem.*, 50 (1978) 2126.
39 B.L. Karger, L.R. Snyder and Cs. Horváth, *An Introduction to Separation Science*, Wiley, New York, 1973.
40 R. Kaliszan, *Quantitative Structure–Chromatographic Retention Relationships* (*Chemical Analysis Series*, Vol. 93), Wiley, New York, 1987.
41 J. Wieling, *Ph.D. Thesis*, University Groningen, Groningen, 1993.
42 L. Rohrschneider, *J. Gas Chromatogr.*, 6 (1968) 5.
43 L. Rohrschneider, *Fortschr. Chem. Forsch.*, 11 (1968) 146.

44 A. Leo, C. Hansch and D. Elkins, *Chem. Rev.*, 71 (1971) 525.
45 C. Hansch and A. Leo, *Substituent Constants for Correlation Analysis in Chemistry and Biology*, Wiley, New York, 1979, Appendix II, pp. 171–330.
46 J. Wisniak and A. Tamir, *Liquid–Liquid Equilibrium and Extraction*, Elsevier, Amsterdam, 1980.
47 J.M. Sørensen and W. Arlt, *Liquid–Liquid Equilibrium Data Collection. Ternary Systems (Dechema Chemistry Data Series)*, Vol. V, Parts 2 and 3, Dechema, Frankfurt a/M, 1980.
48 (a) A.F.M. Barton, *Chem. Rev.*, 75 (1975) 731; *J. Chem. Educ.*, 48 (1971) 731; *Handbook of Solubility Parameters and Other Cohesion Parameters*, CRC Press, Boca Raton, FL, 2nd ed., 1991; (b) J. Růžička and E.O. Hansen, *Flow Injection Analysis*, Wiley-Interscience, New York, 2nd ed., 1988; (c) W.A.I. Knaepen, R. Tijssen and E.A. van den Bergen, *SPE J., Res. Eng.*, May (1990) 239.
49 P.L. Smith and W.T. Cooper, *Chromatographia*, 25 (1988) 55.
50 J. Szanto and T. Veress, *Chromatographia*, 20 (1985) 205.
51 J.H. Park and P.W. Carr, *Anal. Chem.*, 59 (1987) 2596.
52 C.M. Hansen, *J. Paint Technol.*, 39 (1967) 104, 505 and 511; 42 (1970) 660; C.M. Hansen and A. Beerbower, in H.F. Mark, J.J. McKetta, Jr. and D.F. Othmer (Editors), *Kirk–Othmer Encyclopedia of Chemical Technology*, Suppl. Vol., Wiley Interscience, New York, 2nd ed., 1971, pp. 889–910.
53 K.L. Hoy, *J. Paint Technol.*, 42 (1970) 76.
54 E.R. Thomas and C.A. Eckert, *Ind. Eng. Chem. Process Des. Dev.*, 23 (1984) 194.
55 K.S. Pitzer and L. Brewer, *Thermodynamics* (revision of Lewis and Randall), McGraw-Hill, New York, 2nd ed., 1961.
56 R.C. Reid, J.M. Prausnitz and T.K. Sherwood, *The Properties of Gases and Liquids*, McGraw-Hill, New York, 3rd ed., 1977.
57 P.J. Schoenmakers, *J. Chromatogr.*, 315 (1984) 1; see also ref. 6.
58 A.J. Staverman, *Recl. Trav. Chim. Pays-Bas*, 56 (1937) 885; 69 (1950) 163; *Ph.D. Thesis*, Leiden, 1938; *cf.*, review in *Encyclopedia of Physics*, Vol. XIII, Springer Verlag, Berlin, 1962, p. 399.
59 J.H. Hildebrand, *J. Chem. Phys.*, 15 (1947) 225.
60 H. Tompa, *Trans. Faraday Soc.*, 48 (1952) 363.
61 R.N. Lichtenthaler, D.S. Abrams and J.M. Prausnitz, *Can. J. Chem.*, 51 (1973) 3071.
62 R.N. Lichtenthaler, D.D. Liu and J.M. Prausnitz, *Ber. Bunsenges. Phys. Chem.*, 78 (1974) 470.
63 M.D. Donohue and J.M. Prausnitz, *Can. J. Chem.*, 53 (1975) 1586.
64 D.S. Abrams and J.M. Prausnitz, *AIChE J.*, 21 (1975) 116.
65 A. Fredenslund, R.L. Jones and J.M. Prausnitz, *AIChE J.*, 21 (1975) 1086.
66 J. Gmehling, P. Rasmussen and A. Fredenslund, *Ind. Eng. Chem., Process Des. Dev.*, 21 (1982) 118.
67 A. Fredenslund, J. Gmehling and P. Rasmussen, *Vapor–Liquid Equilibria Using UNIFAC*, Elsevier, Amsterdam, 1977.
68 Y. Moroi, N. Nishikido, H. Uehara and R. Matuura, *J. Colloid Interface Sci.*, 50 (1975) 254.
69 R.J. Conder and C.L. Young, *Physicochemical Measurement by Gas Chromatography*, Wiley, Chichester, 1979.
70 R. Koningsveld and L.A. Kleintjens, *Macromolecules*, 4 (1971) 637.
71 A. Bondi, *Physical Properties of Molecular Crystals, Liquids and Glasses*, Wiley, New York, 1968; *J. Phys. Chem.*, 68 (1964) 441.
72 E.A. Guggenheim, *Mixtures*, Clarendon Press, Oxford, 1952.
73 A. Fredenslund and P. Rasmussen, *Fluid Phase Equilib.*, 27 (1986) 347.
74 G.J. Price and M.R. Dent, *J. Chromatogr.*, 483 (1989) 1.
75 G.M. Wilson, *AIChE Symp. Ser.*, 140(70) (1974) 120.
76 E.B. Bagley, T.P. Nelson and J.M. Scigliano, *J. Paint Technol.*, 43, No. 555 (1971) 35; *J. Phys. Chem.*, 77 (1973) 2794.
77 E.B. Bagley and J.M. Scigliano, *Polym. Eng. Sci.*, 11 (1971) 177.
78 E.B. Bagley, T.P. Nelson, J.W. Barlow and S.A. Chen, *Ind. Eng. Chem., Fundam.*, 10 (1971) 27; 9 (1970) 93.
79 I.A. Wiehe and E.B. Bagley, *AIChE J.*, 13 (1967) 836.
80 M.R.J. Dack, *Chem. Soc. Rev.*, 4 (1975) 211; *Aust. J. Chem.*, 28 (1975) 1643; 29 (1976) 771 and 779.
81 M.R.J. Dack, *Solutions and Solubilities, Parts I and II (Techniques of Chemistry Series*, Vol. VIII), Wiley, New York, 1975.
82 G. Allen, G. Gee and G.J. Wilson, *Polymer*, 14 (1960) 456.
83 G. Allen, G. Gee, D. Mangaraj, D. Sims and G.J. Wilson, *Polymer*, 14 (1960) 467.
84 R.S. Drago and B.B. Wayland, *J. Am. Chem. Soc.*, 87 (1965) 3571.
85 R.S. Drago, G.C. Vogel and T.E. Needham, *J. Am. Chem. Soc.*, 93 (1971) 6014.
86 C.S. Chamberlain and R.S. Drago, *J. Am. Chem. Soc.*, 98 (1976) 6142.
87 R.S. Drago, *J. Chem. Educ.*, 51 (1974) 300.
88 P.A. Small, *J. Appl. Chem.*, 3 (1953) 71.
89 B.J. Lee and M.G. Kesler, *AIChE J.*, 21 (1975) 510.
90 P. Choi, T.A. Kavassalis and A. Rudin, *J. Colloid Interface Sci.*, 150 (1992) 386.
91 R. Tijssen, P.J. Schoenmakers, M.R. Böhmer, L.K. Koopal and H.A.H. Billiet, unpublished work (tables are available from the authors).
92 G.J. Pierotti, C.H. Deal and E.L. Derr, *Ind. Eng. Chem., Fundam.*, 1 (1962) 17.
93 R.K. Gilpin, *J. Chromatogr. Sci.*, 22 (1984) 371.
94 L.C. Sander, J.B. Callis and L.R. Field, *Anal. Chem.*, 55 (1983) 1068.
95 P. Munk, *Introduction to Macromolecular Science*, Wiley, New York, 1989.
96 P.J. Flory, *Statistical Mechanics of Chain Molecules*, Wiley-Interscience, New York, 1969.

97 C. Williams, F. Brochard and H.L. Frisch, *Annu. Rev. Phys. Chem.*, 32 (1981) 433.
98 R.J. Young, *Introduction to Polymers*, Chapman and Hall, London, 1989.
99 H. Yamakawa, *Modern Theory of Polymer Solutions*, Harper and Row, New York, 1971.
100 P.J. Flory, *Br. Polym. J.*, March (1976) 1.
101 M.V. Volkenstein, *Configurational Statistics of Polymeric Chains* (*High Polymers Series*, Vol. XVII), Wiley-Interscience, New York, 1963.
102 T.M. Birshtein and O.B. Ptitsyn, *Conformations of Macromolecules* (*High Polymers Series*, Vol. XXII), Wiley-Interscience, New York, 1966.
103 H. Morawetz, *Macromolecules in Solution* (*High Polymers Series*, Vol. XXI), Wiley-Interscience, New York, 1965.
104 W.C. Forsman (Editor), *Polymers in Solution, Theoretical Considerations and Newer Methods of Characterisation*, Plenum Press, New York, 1986.
105 R. Tijssen and J. Bos, in F. Dondi and G. Guiochon (Editors), *Theoretical Advancement in Chromatography and Related Separation Techniques* (*NATO–ASI Proceedings*, Vol. C383), Kluwer, Dordrecht, 1992, pp. 397–441.
106 R.B. Bird, C.F. Curtiss, R.C. Armstrong and O. Hassager, *Dynamics of Polymer Liquids*, Wiley-Interscience, New York, 2nd ed., 1987.
107 M.C. Williams, *AIChE J.*, 21 (1975) 1.
108 J. Brandrup and E.H. Immergut (Editors), *Polymer Handbook*, Wiley-Interscience, New York, 3rd ed., 1989.
109 M. Daoud and P.G. de Gennes, *J. Phys. (Paris)*, 38 (1977) 85.
110 F. Brochard and P.G. de Gennes, *J. Chem. Phys.*, 67 (1977) 52.
111 S. Daoudi and F. Brochard, *Macromolecules*, 11 (1978) 751.
112 F. Brochard-Wyart and E. Raphael, *Macromolecules*, 23 (1990) 2276.
113 A. Halperin, *J. Phys. (Paris)*, 49 (1988) 547.
114 P. Auroy, L. Auvray and L. Léger, *Macromolecules*, 24 (1991) 5158.
115 P. Auroy, L. Auvray and L. Léger, *Phys. Rev. Lett.*, 66 (1991) 719.
116 P. Auroy and L. Auvray, *Macromolecules*, 25 (1992) 4134.
117 J.J. Magda, G.H. Frederickson, R.G. Larson and E. Helfland, *Macromolecules*, 21 (1988) 726.
118 T. Ohta and K. Kawasaki, *Macromolecules*, 19 (1986) 2621.
119 S. Hirz, *Thesis*, University of Minnesota, Minneapolis, MN, 1987.
120 S. Alexander, *J. Phys. (Paris)*, 38 (1977) 977, 983.
121 M. Murat and G.S. Crest, *Phys. Rev. Lett.*, 63 (1989) 1074; *Macromolecules*, 22 (1989) 4054.
122 L.I. Klushin and A.M. Skvortsov, *Macromolecules*, 24 (1991) 1549.
123 E.A. Guggenheim, *Thermodynamics*, North-Holland, Amsterdam, 6th ed., 1977.
124 J.C. Giddings, *Unified Separation Science*, Wiley-Interscience, New York, 1991.
125 C. Ligoure and L. Leibler, *J. Phys. (Paris)*, 51 (1990) 1313.
126 E.F. Casassa, *J. Polym. Sci., Part B*, 5 (1967) 773.
127 E.F. Casassa and Y. Tagami, *Macromolecules*, 2 (1969) 14.
128 E.F. Casassa, *Macromolecules*, 9 (1976) 182.
129 E.F. Casassa, *J. Phys. Chem.*, 75 (1971) 3929.
130 E.F. Casassa, *Sep. Sci.*, 6 (1971) 305–319.
131 M. Doi and S.F. Edwards, *The Theory of Polymer Dynamics* (*International Series of Monographs on Physics*, Vol. 73), Clarendon Press, Oxford, 1986.
132 M. Doi, *J. Chem. Soc., Faraday Trans. 2*, 71 (1975) 1720.
133 C.M. Wijmans, J.M.H.M. Scheutjens and E.B. Zhulina, *Macromolecules*, 25 (1992) 2657.
134 A. Silberberg, *J. Chem. Phys.*, 46 (1967) 1105.
135 A.P. Gast and L.J. Leibler, *J. Phys. Chem.*, 89 (1986) 3947.
136 E.A. DiMarzio and R.J. Rubin, *J. Chem. Phys.*, 55 (1971) 4318.
137 J.M.H.M. Scheutjens, F.A.M. Leermakers, N.A.M. Besseling and J. Lyklema, in K.L. Mittal (Editor), *Surfactants in Solution*, Vol. 7, Plenum Press, New York, 1989, p. 25.
138 D. Morel, K. Tabar, J. Serpinet, P. Claudy and J.M. Letoffe, *J. Chromatogr.*, 395 (1987) 73.
139 F.A.M. Leermakers and J.M.H.M. Scheutjens, *J. Chem. Phys.*, 89 (1988) 6912.
140 M.R. Schure, presented at *19th International Symposium on Chromatography, Aix-en-Provence, September 1992.*
141 D.E. Martire, in F. Dondi and G. Guiochon (Editors), *Theoretical Advancement in Chromatography and Related Separation Techniques* (*NATO–ASI Proceedings*, Vol. C383), Kluwer, Dordrecht, 1992, pp. 261–288.
142 E. Helfland and Y. Tagami, *J. Chem. Phys.*, 56 (1972) 3592.
143 K.M. Hong and J. Noolandi, *Macromolecules*, 13 (1980) 964.
144 D.W.R. Gruen and E.H.B. de Lacey, in K.L. Mittal and B. Lindman (Editors), *Surfactants in Solution*, Vol. 1, Plenum Press, New York, 1984, p. 279.
145 D.N. Theodorou, *Macromolecules*, 21 (1988) 1391 and 1400.
146 K.A. Dill and R.S. Cantor, *Macromolecules*, 17 (1983) 380.
147 J. Lyklema, *Fundamentals of Interface and Colloid Science, Vol. I: Fundamentals*, Academic Press, London, 1991, Ch. 2.
148 J.M.H.M. Scheutjens, *Ph.D. Thesis*, Wageningen Agricultural University, Wageningen, 1985.
149 J.M.H.M. Scheutjens, G.J. Fleer and M.A. Cohen Stuart, *Colloids Surf.*, 21 (1986) 285.
150 R.S.P. Parnas and Y.C. Cohen, *Macromolecules*, 24 (1991) 4646.
151 H.C. Brinkman, *Appl. Sci. Res.*, A1 (1949), 27, 81 and 333.
152 S.T. Milner, *Macromolecules*, 24 (1991) 3704.

153 M.A. Cohen Stuart, F.H.W.H. Waajen, T. Cosgrove, B. Vincent and T.L. Crowley, *Macromolecules*, 17 (1984) 1825.
154 P.F. Mijnlieff and W.J. Jaspers, *Trans. Faraday Soc.*, 67 (1971) 1837.
155 M.A. Cohen Stuart, *Adv. Colloid Interface Sci.*, 24 (1986) 143.
156 M.R. Böhmer and L.K. Koopal, *Langmuir*, 6 (1990) 1478.
157 C. Tanford, *The Hydrophobic Effect*, Wiley-Interscience, New York, 2nd ed., 1980.
158 T. Cosgrove, T.G. Heath, K. Ryan and B. van Lent, *Polymer Commun.*, 28 (1987) 64.
159 H.J. Möckel and T. Freyboldt, *Chromatographia*, 17 (1983) 215.
160 H.J. Möckel, poster presented at the *19th International Symposium on Chromatography, Aix-en-Provence, September 1992.*
161 K. Karch, I. Sebastian and I. Halasz, *J. Chromatogr.*, 122 (1976) 3.
162 G.E. Berendsen and L. de Galan, *J. Chromatogr.*, 196 (1980) 21.
163 C.H. Lochmüller and D.R. Wilder, *J. Chromatogr. Sci.*, 17 (1979) 574.
164 F. Morishita, H. Kalihana and T. Kojima, *Anal. Lett.*, 17 (1984) 2385.
165 E. Grushka, H. Colin and G. Guiochon, *J. Chromatogr.*, 248 (1982) 325.
166 R.J. Smith, C.S. Nieass and M.S. Wainwright, *J. Liq. Chromatogr.*, 9 (1986) 1387.
167 P. Jandera, *Chromatographia*, 19 (1984) 101.
168 S.I. Andersen and K.S. Birdi, *Prog. Colloid Polym. Sci.*, 82 (1990) 52.
169 A. Tchapla, H. Colin and G. Guiochon, *Anal. Chem.*, 56 (1984) 621; S. Héron and A. Tchapla, presented at *19th International Symposium on Chromatography, Aix-en-Provence, September 1992*; *Chromatographia*, 36 (1993) 11.
170 G.E. Berendsen, P.J. Schoenmakers, L. de Galan, G. Vigh, Z. Varga-Puchony and J. Inczedy, *J. Liq. Chromatogr.*, 3 (1980) 1669.
171 H. Engelhardt and G. Ahr, *Chromatographia*, 14 (1981) 227.
172 M.L. Miller, R.W. Linton, S.G. Bush and J.W. Jorgenson, *Anal. Chem.*, 56 (1984) 2204.
173 M.C. Hennion, C. Picard and M. Caude, *J. Chromatogr.*, 166 (1978) 21.
174 K.B. Sentell and J.G. Dorsey, *Anal. Chem.*, 61 (1989) 930.
175 P. Claudy, J.M. Letoffe, C. Gaget, D. Morel and J. Serpinet, *J. Chromatogr.*, 329 (1985) 331; D. Morel, J. Serpinet, J.M. Letoffe and P. Claudy, *Chromatographia*, 22 (1986) 103.